THREE DIMENSIONAL RECONSTRUCTION
OF
THE MUSCLES OF MASTICATION

by

Marcio Lima Grossi

A thesis submitted in partial fulfillment of the requirements for the degree of
Master of Science in Restorative Dentistry - Occlusion
Horace H. Rackham School of Graduate Studies
The University of Michigan, Ann Arbor, Michigan
July 1991

Thesis Committee:

Dr. Christian S. Stohler, Chairman
Dr. David S. Carlson
Dr. John H. Lillie

To my wife Patricia for her unlimited
love and support.

ACKNOWLEDGEMENTS

I would like to offer my sincerest thanks to my thesis committee members:

Dr. Christian S. Stohler, Chairman

Dr. David S. Carlson

Dr. John H. Lillie

Special thanks are also extended to Dr. Carlos W. de A. Wagner, Dr. Daniel Chiego, Jr., Doris Milton, Dr. Holly Smith, Dr. James C. Ragain, Jr., Dr. John Swales, Dr. Sian Kwa, Dr. Walter A. Bretz, Dr. Weber Ursi and Xin Zhang and for their valuable advice. I would also like to offer my gratitude to the American people for the positive cultural exchange.

TABLE OF CONTENTS

LIST OF FIGURES

LIST OF TABLES

INTRODUCTION

The calculation of forces transmitted through the human temporomandibular joint has been the object of interest to researchers and clinicians for significant amount of time. Just as an example, the hypothesis that abnormal loading of the temporomandibular joint (TMJ) can lead to degenerative disease processes (Roberts, 1974) remains unproven, because it has not been possible to determine whether patients with TMD have abnormal joint loading. The correct measurement of TMJ loading would also be helpful in designing total joint prostheses (Hohl and Tucek, 1982). Direct measurement of forces within the temporomandibular joint has proven to be troublesome (Brehnan et al., 1981; Hohl and Tucek, 1982; Hylander, 1979) and involves invasive techniques that are not necessarily applicable to human subjects.

The calculation of the TMJ forces from mathematical models has a long history, but it has lead to contradictory results. The greatest discussion has been over whether the TMJ is even a load bearing joint (Gysi, 1921; Barbenel, 1972, 1974; Hylander, 1978; Smith, 1978) or not (Roberts, 1974). There has also been controversy about which condyle is more heavily loaded during a unilateral bite: the working or nonworking (balancing) condyle (Gysi, 1921; Hylander, 1978; Smith, 1978). After much disagreement and some scientific data (Hylander, 1975, 1979; Brehnan et al., 1981), it is now generally recognized that the TMJ is a load bearing structure under most normal situation, and that the balancing side condyle is more heavily loaded during a unilateral bite. Nevertheless, exact values for human temporomandibular joint loads are still unknown.

The correct determination of the total reaction force requires the following information: (1) the magnitude and direction of the bite force, (2) the magnitude and direction of each muscle force, and (3) the lengths of the moment arms of the bite force and of each muscle force. The magnitude and direction of the bite force can be measured with force transducers with no major difficulties (e.g. Hylander, 1978). The analysis performed in one study (Throckmorton and Throckmorton, 1985) determined that the magnitude of the TMJ reaction force is most sensitive to the relative lengths of the moment arms for the bite force and the muscle forces. Errors in estimation of the relative magnitudes of the muscle forces had little effect upon the magnitude of the resulting joint reaction force. The joint force direction is most sensitive to the ratio of the bite force and muscle force moment arms and to a lesser degree to the relative magnitude of the muscle forces.

The muscle force direction influences the calculation of joint load by determining two aspects of the moment produced by the muscle force. First, the total muscle force is determined by the direction of the muscle force. Second, the direction of the muscle force determines the length of the muscle force moment arm. Until this very moment, no work has been done to precisely determine directions of force for the masticatory muscles; in fact, there have been no experimental studies to precisely measure the directions of the masticatory muscle forces. A number of studies empirically selected directions for the elevator forces of the mandible which were consistent with previous topographic anatomical studies but without any supporting scientifically determined measurements (Roberts, 1974; Smith, 1978).

A comprehensive model containing all forces contributing to the TMJ reaction force would be highly complex, including at least ten muscle force vectors in one hemiface, the bite force vector, the connective tissue force vectors, and with all these vectors determined in three dimensional space. Such a comprehensive model has not yet been developed, nor is it known whether all of the variables mentioned above are required for a reliable calculation of the TMJ reaction force. A reliable calculation should be one in which the

error of the calculated value is hypothetically no less than the measurement error of the measured parameters (Throckmorton, 1990).

The purpose of this study was to develop a three-dimensional 10 muscle model in representing the muscle force direction of the masticatory and suprahyoid muscles. The above mentioned model was developed in the left left hemiface of an adult male caucasian cadaver.

LITERATURE REVIEW

JOINT FORCE MAGNITUDE

Animal Experiments

Exact values of forces occuring within the temporomandibular joint in humans during normal function are not know yet. Most of the direct measurements of these forces have been made only in animal models.

Hylander (1979) analyzed the mandibular bone strain in the region immediately below the temporomandibular ligament in adult and sub-adult *Macaca fascicularis* and *Macaca mulatta*. Monkeys were provided with either food objects, a wooden rod, or a specially designed bite-force transducer. Registration of bone strain was made during incisal biting and mastication, and also during isometric biting task on the rod and/or the bite force transducer. The data obtained from the measurements of bone strain indicated that the temporomandibular joint is loaded by a reaction force during the power stroke of mastication and incision of food, and during isometric molar and incisor biting. The author observed that the temporomandibular joint is loaded more on the contralateral side during both mastication and isometric molar biting. Patterns of ipsilateral TMJ reaction force in monkeys during isometric biting changed according to the bite point position. If the bite is positioned along the premolars or the first two molars, a compressive reaction force is exerted about the TMJ on the same side. On the other hand, if it is located along the third

4

molar; the stress on the TMJ on the same side is very little, absent, or it is loaded in tension.

Hylander and Bays (1979) used rectangular rosette or single-element strain gauges bonded to surgically-exposed mandibular cortical bone in the region immediately below the temporomandibular ligament in adult and sub-adult macaques. After that, bone strain was registered during incision and mastication of apples. Their findings showed that the joint is loaded proportional to the position of the bite point. Bone strain measurements were greater on the contralateral side than on ipsilaterally during mastication, indicating that the net compressive reaction force along the contralateral joint possibly exceeds the net compressive reaction force along the ipsilateral joint during these moments. The largest bone strain measurements were recorded during apple incision, indicating that the temporomandibular joint is also loaded during incisal biting.

Brehnan *et al* . (1981) made a description of a novel technique of directly measuring loads at the articulating surface of the head of the condyle in one male *Macaca arctoides*. The monkey was given hard and soft foods to chew after surgical implantation of a pressure-sensitive foil in the temporomandibular joint. Loads were recorded during incisal biting and molar chewing. The bite data generated by the authors suggested that the condylar head was loaded during molar chewing with a maximum load of 1-3 lb. During incisal biting, the condylar head was loaded with a larger load of 3-4 lb. Additionally, it was observed that during the calibration of the transducer as the condyle translates forward over the articulating eminence during opening, loading as large as during incisal biting was noted. Their findings are in agreement with data provided by Hylander *et al.* (1979).

Roth *et al.* (1984) studied the synovial fluid hydrostatic pressure within the temporomandibular joint of the pig, *Sus scrofa domesticus*, using the "wick method" for fluid pressure determination. They registered acute hydrostatic pressure levels in seven surgically exposed temporomandibular joint capsules of five pigs. The synovial fluid hydrostatic pressure was in subatmospheric state with the mandible in the resting position

(mean = - 3.8 mm of mercury) in six out of seven of the surgically exposed TMJ capsules. The fluid pressure elevated as a consequence to operator-manipulated jaw position and went back to baseline levels after release of the mandible. Additionally, the authors made an attempt to study the fluid pressure in the TMJ cavity of a functioning experimental animal by means of a chronically implanted catheter in the joint space. After successful implantation in two animals, the fluid pressure was registered at 10- and 14-day intervals. Similar, and again less negative mean "resting values" were observed; in addition, it was found that fluid pressures were greatly elevated during mastication.

Boyd *et al.* (1990) determined the forces at the articular surface of the temporomandibular joint condyle in two stump-tail monkeys *(Macaca arctoids)* during chewing, incisal biting, drinking and also during aggressive behaviors. They measured the force with a thin piezoelectric foil transducer, which was cemented over the anterior and superior surfaces of the condyle. The force applied across the foil was transmitted by a telemetry unit and transmitted to an FM radio receiver. FM signals were demodulated, and a signal proportional to the force applied between the condyle and the TMJ fossa was displayed on a chart recorder. Data were collected over an 8-day period. They found the TMJ as being a load bearing joint with the greatest force of 39.0 lb (17.7 kg) measured during feisty vocal aggression. Forces ranged as high as 34.5 lb (15.7 kg) during chewing and 28.5 lb (13.0 kg) during incisal biting. Forces were greater on the working (food) side than on the nonworking (balancing) side by average ratios of 1.4 to 2.6. A large unilateral interference at the most distal molar greatly disturbed chewing. It reduced TMJ forces by 50% or more, and the monkey refused to chew on the side opposite the interference.

Oyen and Tsay (1991) obtained in vivo measurements of bite force and bone strain obtained in growing African green monkeys. These measurements were used to study skull biology and geometry. Strain values and distributional patterns seen in association with forceful jaw elevation were not consistent with most traditional explanations that connect upper facial morphology with masticatory function and use beam models of craniofacial

architecture. The results suggested careful use of concepts about skeletal geometry based on static analysis that have not been experimentally analysed with *in vivo* procedures. In particular, a reassessment of conventional ideas about the generation and dissipation of forces during contraction of the jaw elevator muscles seems called for.

All the studies mentioned above strongly support the hypothesis of the temporomandibular joint as being a stress-bearing joint. Methods and findings can be considered fairly reproducible and reliable. Unfortunately, the major problem with all these experiments is the fact that they require invasive techniques; therefore, they cannot be applied to human subjects.

Mathematical Models

From a hypothetical standpoint, the temporomandibular joint forces of humans can be modeled with non-invasive measures if we know: (1) the magnitude and direction of the bite force, (2) the magnitude and direction of each muscle force, and (3) the lengths of the moment arms of the bite force and of each muscle force . Many different mathematical model studies have been carried out in order to measure all the effect of various variables.

Throckmorton (1985) tried to determine the effect of error of muscle force direction on quantitative calculation of the temporomandibular joint reaction force in a two-dimensional, two-muscle model. The direction of the temporalis and masseter muscle force vectors were augmented by a computer program using the model. The program also provided a set of curves displaying the relationship between muscle force direction and the direction and magnitude of the temporomandibular joint reaction force. The major effect of muscle force direction was its influence on the length of the muscle force moment arm. Their data showed that calculation of the joint reaction force is much more sensitive to errors in muscle force direction than to muscle force magnitude. They also found that calculation of the magnitude of the joint reaction force is less sensitive to error than the

calculation of joint reaction force direction. An error of 1° in muscle force direction could produce a 2° error in joint force direction. Vector positions that enhanced calculation of joint force magnitude increased the sensitivity to errors when calculating joint force direction. He concluded that a two-muscle model requires very precise determination of muscle force directions to reliably calculate the temporomandibular joint reaction forces.

Throckmorton and Throckmorton (1985) investigated a two-dimensional, two muscle model in order to evaluate the effect of measurement errors on quantitative calculation of temporomandibular joint reaction force. The magnitude of the bite force and muscle forces and the lengths of their moment arms were augmented by a computer program. The program also calculated the joint reaction force at each increment, using the two-dimensional model. The authors found that the computation of the joint reaction force is most sensitive to the relative lengths of the bite force and muscle forces moment arms. Absolute values for each muscle force were not necessary and errors in the magnitudes of the muscle forces had a little effect on calculation of the total reaction force.

Kang *et al.* (1990) presented a mathematical model in order to determine the contribution of each muscle acting on the mandible in the development of a given bite force. They gave special attention to the representation of the widely radiated temporalis and accounted for the attachment of the external pterygoid to the capsular ligament. They used an optimization technique based on minimizing the maximum stress occurring in the muscles in order to resolve the statically indeterminate nature of the problem formulated. They compared the theoretically predicted values of the muscle forces to experimental results taken from the literature.

Koolstra *et al.* (1990) estimated the orientation of muscle action lines in 9 healthy subjects, by reconstructing the muscle shape from a series of parallel sections obtained by MRI in both frontal and sagittal planes. In order to gain more knowledge into sources of error, the lines of action of the masseter and medial pterygoid were estimated from two mutually perpendicular series of sectional images. Sectional images were made with a 0.6

Tesla system (Technicare Teslacon, USA) equipped with a 20 cm head coil. From each sectional image the outlines of the following structures were traced: mandible, masseter, medial pterygoid, lateral pterygoid and temporalis muscles. Results indicated that the accuracy of the estimate was mainly dependent on the reliability of the reconstructions; the average accuracy of the estimated orientations was about 5 degrees. Inadequate reconstruction of muscle shape caused by tracing errors due to MRI poor resolution, minor movements of the subjects head, and the thickness of the imaged slice were considered the main causes of error in method. No dramatic asymmetries were found between the left and the right sides; however, individual asymmetries were found large in some cases.

Korioth and Hannam (1990) used a 3-D computer model to calculate the magnitude and direction of temporomandibular reaction forces during simulated clenching on interocclusal acrylic resin shims and between natural teeth. Muscle tensions were proportioned according to the task provided. They included as working-side tooth contacts the canine alone, as well as group function. The occlusal loads were progressively shifted toward a posterior contralateral simple balancing contact. In the acrylic resin shim experiments, group function with simple balancing contact provided the highest forces at the load point and at both temporomandibular joints. They found that the movement of the occlusal load toward the balancing side produced greater, anteriorly oriented forces on the working condyle. For natural teeth, changes in the angle of resultant tooth force (simulating facet angulation) greatly influenced condylar forces. As the occlusal load moved toward the balancing side, greater and more laterally oriented forces were produced on the balancing condyle. Unilateral clenching on the canine produced the least condylar and bite forces. The simulation involving natural teeth offered a possible explanation for deviations in form and osteoarthrosis at the temporomandibular joints.

At the present time, there is a great doubtful concerning the calculation of all these variables, with the exception of the bite force magnitude and position. This is due to the

fact that a complete study containing all necessary information to calculate the TMJ reaction forces is missing.

BITE FORCE MEASUREMENTS

Different Methods for Measurement of Bite Force

A modern apparatus usually used for bite force measurements is constructed as a strain gauge dynamometer (Carlsson, 1974; Linderholm and Wennstrom, 1970; Devlin and Wastell, 1985). One such representative strain gauge construction was described by Linderholm and Wennstrom (1970). The device consisted of steel bars that were supplied with strain gauges connected in a Wheatstone bridge and a potentiometer writer. One bar was formed into two bite plates 15 X 15 X 2 mm with rifled bite areas. Floystrand, Kleven and Oilo (1982) constructed a miniature bite fork 3.4 mm thick. The sensory unit was semiconductor with planar resistors diffused on both sides mounted in a metal housing formed in the shape of a fork. Devlin and Wastell (1985) described a semiconductor strain construction where the transducer was positioned over the palate midline, opposite the premolar teeth. It was compressed between two cast metal platforms the purpose of which was to distribute the biting load over the posterior teeth of both sides while preventing the teeth from coming into contact.

The change in electric potential or voltage that follows from the loading of the bite force transducer can be registered as a DC-signal on a milivoltmeter. However, for clinical purposes it is advantageous if a transformation can be made to the force variables Newton, pounds, or kilograms (1kg = 2.21 lb = 9.8N). Therefore, the loading registered is usually transformed into one of these variables, which is presented on a graph or a digital display unit connected with a printer.

The bite force transducers described above have been used either for the measurement of bite force between single pairs of antagonizing teeth (Carlsson, 1974; Linderholm and Wennstrom, 1970; Hagberg et al., 1986) or for estimations of bilateral forces or total forces (Devlin and Wastell, 1985; Gibbs et al., 1986; Pruim et al., 1978). The bite opening between the jaws that is caused by the intraoral insertion of the fork can affect the bite force values (Manns et al., 1979).

Another method for using strain gauges is to incorporate the apparatus within a tooth or under artificial teeth in a completer denture (Brudevold, 1951; Atkinson and Shepherd, 1967; De Boever et al., 1978). One drawback with this method is that bite forces for healthy natural teeth cannot be measured and the application of the transducer is too complicated for general clinical usage. On the other hand, this method makes it possible to measure forces during functions such as mastication.

Gibbs et al. (1981a, 1981b) developed a method that enabled total biting forces and masticatory forces to be measured without intraoral instrumentation: "the sound transmission system." Sinusoidal sound vibration at a specific frequency from a piezoelectric crystal transducer was introduced on the forehead. The sound vibration transmitted to the chin through craniomandibular pathways was received by an accelerometer placed on the chin. The greater the force between the mandible and the maxillae, the greater the vibration received by the accelerometer. The amplitude of vibration was individually calibrated and transformed into force by the use of an intraoral strain gauge dynamometer and an integrated surface EMG recorded from the masseter muscles (Gibbs et al., 1981a).

Apart from the interest in the capacity to produce maximal bite force values, submaximal force levels when biting on a bite fork have been analyzed (Haraldson et al., 1979; Wennstrom, 1971; Wennstrom, 1972). Wennstrom et al. (1972) using a rating scale with five force levels showed that subjects with a full maxillary denture and partial mandibular dentures were able to perform bites at verbally and numerically specified force

levels with great accuracy. This ability has been used to estimate the bite force during chewing among subjects with natural teeth by reproduction of chewing forces on a bite fork with the instruction "bite as when chewing" (Haraldson et al., 1979; Helkimo and Ingervall, 1978). Discrimination of bite force at very low levels has also been investigated (Williams *et al.*, 1985).

The combinations of EMG registration and bite force measurements can be used for estimations of masticatory forces (Hagberg, 1986a; Hagberg, 1986b; Hagberg, 1987). Amplitude probability distribution analysis of EMG activity registered from mandibular elevators during chewing was performed. A calculation of rough estimates of masticatory forces in Newtons could be made by a transformation of EMG voltage measurements, registered during chewing, to Newtons, using a reference contraction of gradually increased biting force while biting down on a bite force sensor.

Masticatory Forces

Masticatory forces (chewing) have commonly been measured with built in force transducers in the teeth (Brudevold, 1951; Laurell, 1985; De Boever *et al.*, 1978) or by an indirect estimation of the force used during chewing reproduced on a bite fork (Haraldson *et al.*, 1979; Helkimo and Ingervall, 1978). The masticatory forces are generally at their highest when the food is initially crushed between the teeth (Carlsson, 1974). Generally forces used during chewing are lower than the maximal bite force values registered. The masticatory forces are reported to be significantly higher for hard foods (i.e., peanuts or almonds) than for soft foods (i.e., cheeses or chewing gum). Higher masticatory force values are reported for subjects with complete dentitions and no signs of periodontal disease (Gibbs *et al.*, 1981; Hagberg, 1986; Hagberg, 1987) than for those subjects with a reduced amount of periodontal support after treatment for a periodontal disease (Laurell, 1985) or for denture wearers (Brudevold, 1951; Yurkstas and Curby, 1953). Haraldson,

Carlsson, and Ingervall (1979) found no significant differences in masticatory forces between patients with osseointegrated implant bridges and matched controls.

The type of muscular contraction used for maximal biting and for chewing differs in that the first is isometric and the latter dynamic. The EMG pattern found for the mandibular elevators of patients with disturbances of the stomatognathic system in comparison with controls shows that these patients chew with greater relative strength, longer relative contraction times, and stronger intermediary activity between strokes (Moller *et al.*, 1984). Hagberg (1986) also found by a combined method of bite force registration and EMG analysis, that the chewing of hard food (almonds) produced a clear difference in chewing patterns between patients and controls. Patients with painful masseter muscles used higher relative masticatory forces for force levels below maximal loading than the controls (Hagberg, 1986; Hagberg, 1987). Generally an increase in EMG amplitudes during nonfatiguing contractions corresponds to increased exerted force (Bigland and Lippold, 1954). The EMG muscle activity of masticatory muscles has also been shown to increase with increasing bite force (Manns *et al.*, 1979; Haraldson *et al.*, 1985). Therefore, the EMG findings suggest a difference in the distribution of actual bite force values within the chewing cycle for patients and controls.

MUSCLE FORCE MAGNITUDES

Cross-sectional Area Studies

A great number of the studies assessing muscle force magnitude have measured the forces based on the cross-sectional area of each muscle mass.

Weber (1851) computed the physiological cross-section according to the formula P/pL in which P represents the weight of the muscle in grams, L the average length of the muscle fibers in cm and p the specific gravity of the muscular substance. To the latter,

Weber gives a value of 1.0583. In one and the same cadaver he, accordingly, calculated the physiological cross-section of the temporal muscle at 8.008 cm^2, that of the masseter muscle at 7.458 cm^2 and that of the medial pterygoid muscle at 3.901 cm^2.

Gysi (1921) traced on squared paper outlines of cross-sections of the muscles of occlusion from two heads, obtaining the following average results: masseter, 3.87 sq. cm; internal pterygoid, 2.3 sq. cm; temporal, 4.3 sq. cm. It is not stated whether these are averages for muscles from both sides, nor is any indication of variation given.

Freisfeld (1927) calculated the physiological cross-section of the cadaver of a stillborn by making an incision perpendicular to the longitudinal line of the muscle through the thickest part of the muscle. The circumference of the incision surface was then delineated on a piece of pasteboard. The drawn figure was cut out, weighed and compared in weight to that of a piece of known area, cut from the same pasteboard. Freisfeld found the cross-section of the temporal muscle to be 1.2 sq. cm, that of the masseter muscle 1.37 sq. cm and that of the medial pterygoid muscle 0.72 sq. cm.

Using these calculations of the physiological cross-sections of the masticatory muscles, Schnabel (1933) likewise made an incision perpendicularly through the thickest part of a muscle. He then pressed the surface of the transverse section together with a special measuring instrument, to an elliptic shape. Thereafter, he calculated the size of the cross-section from the formula for the elliptic area. Schnabel performed in that manner calculations of the cross-section surfaces of the masticatory muscles on seven preparations, obtaining the following limit values: for the temporal muscle 4.4588-11.8064 sq. cm, for the masseter muscle 7.4732-15.072 sq. cm and for the medial pterygoid muscle 3.9564-10.205 sq. cm.

Mainland and Hiltz (1934) tried to measure directions, relative amounts, and approximately absolute amounts (possible variations, rather than averages) of forces exerted by the masseter (superficial and deep parts), internal pterygoid, and temporal (anterior and posterior parts). They examined both sides of twelve heads of dissecting-

room subjects, ages ranging from 22 to 87 years, being five specimens females and seven males. Their method included determination of cross-sectional area, perpendicular to all muscle fibers, by inking cut surfaces, imprinting on paper, tracing on kodaloid, cutting out and weighing; estimation of absolute force on a basis of 10kg. per sq. cm; resolution of forces into components acting upward, forward or backward, laterally or medially. Total forces (both sides) in three heads completely examined were approximately 308 kg, 273 kg, and 283 kg.

Ebert (1939) calculated the physiological cross-section of the masseter muscle in six human cadavers. He divided the muscle into isolated muscle fibers. The fibers were pressed together in a rectangular indentation in the edge of a wooden slab. It was, therefore, possible to state at once the area covered by the fibers. This area, viz, the physiological cross-section of the muscle, varied between 7 and 15 sq. cm with a mean value of 11 sq. cm. From those figures he assessed the strength of the muscle at 10 X 11, equalling 110 kg.

Since the physiological cross-section of a muscle constitutes the sum of the transverse areas of the muscle fibers, it should be pointed out that in these methods it is by no means certain that all muscular fibers are included in the calculation of muscle force. Based on that, their results should be considered just an estimation of the actual muscle force.

Electromyographic Studies

Other studies have utilized integrated electromyography in order to estimate the force magnitudes of the muscles

Barbenel (1974) presented a hypothetical analysis, which utilizes experimentally determined line of muscle action, allowing some estimate of the temporomandibular joint force existent during biting. This analysis permitted an evaluation of the effect of occlusal

load variations to be performed, but in the absence of data on muscle activity the results of the analysis could suggest only the lowest magnitude of the joint load. The equations of equilibrium of the mandible under a static load were determined and the solutions providing the minimum joint force were analysed. He used integrated electromyography to calculate the forces at the TMJ with the mandible supporting a static load on the incisor and canine teeth. The author concluded that the temporomandibular joint is load-bearing during function under the occlusal loading conditions studied, and the joint force detected during the electromyographic analysis was at least 2-7 times greater than the occlusal load.

Pruim *et al.* (1978) introduced a novel method to relate jaw muscle EMG-activity to static bite forces. They measured the bite force bilaterally in many reproducible positions on the human dentition by means of small wedge opener and closer muscles. They used visual feedback methods to obtain bite recordings at various levels of bite force and muscle activity. They found a linear relationship between integrated EMG-activity and the force exerted by individual muscles in isometric conditions. The anterior and posterior parts of the temporal muscle presented a different functional behavior. The importance of the opener muscles as antagonists was such, that it would not be ignored in a muscle force analysis. They concluded that the phenomenon of linear behavior of both the agonistic and antagonistic muscles is an indication that physiological maximum forces were at least approached in the agonists.

Pruim *et al.* (1980) introduced a mathematical model based on a supposed linear relationship between the forces exerted by a muscle and its integrated electromyogram for calculating muscle forces and joint forces acting on the human mandible during static bite situation. They included the complete data from one of 7 male subjects as an example of the approach and to illustrate the relevance of the mechanical model for calculating these forces. Based on the assumption that the maximum muscle tension (T), expressed in N/m^2 (kg/cm^2) is equal for all muscles, a value of this quantity could be calculated for any bite in any of three bite positions. It seemed to be dependent upon the test person only. Forces in

the lateral pterygoid muscles and in the temporomandibular joints increased almost linearly with increasing bite forces. Highest bite forces and muscle forces were exerted most often when biting occured in the region of the first molar. The loading of the temporomandibular joint was highest when biting in the area of the first premolar. Muscle activity might be inhibited in this situation. Forces in all muscles were dependent on the position of the bite force, most clearly demonstrated in the temporal muscles. Joint forces were higher when the bite force was applied more ventrally and may initiate an inhibition when biting in position P_1. In position M_2, all forces were considerably lower than expected on the basis of the mechanical model only.

Throckmorton *et al.* (1990) measured bilateral activity in the anterior temporal, posterior temporal, and superficial masseter muscles during isometric bites or closures and chewing at five different positions along the teeth. They compared the resulting ratios of muscle activity on the working/balancing sides with ratios required to maintain equal joint forces. They also used the values of the muscle activity were to estimate the ratio of joint forces on the working/balancing side at each tooth position. Results indicated that the muscle activity patterns do not keep equal joint forces, nor are the muscles responding to joint forces exceeding critical limits. These results indicated that patterns of muscle activity are designed to control the position and magnitude of occlusal forces rather than temporomandibular joint ones. If these same patterns of activity were kept following repositioning of dental and skeletal elements, adverse temporomandibular joint forces could result.

Van Ruijven and Weijs (1990) described a muscle model that uses electromyogram (EMG), muscle length and speed of contraction to predict muscle force. Physiological parameters were the Hill constants and the shape of the twitch response to a single stimulus. They incorporated the model in a model of the rabbit jaw, and they tested it by predicting the bite force produced by the jaw muscles during mastication. The time course of the calculated force appeared to match the bite force, measured *in vivo* by a strain gauge,

applied to the bone below the teeth. The variation in peak strain amplitude from cycle to cycle correlated with the variation predicted by the model. The peak amplitude of the integrated EMGs of individual jaw muscles showed an average correlation with peak strain of 0.41. The use of the sum of the available peak amplitudes, weighted according to their effect upon the bite force, increased the correlation to 0.46; the model predicted bite forces and showed a correlation of 0.57 with the strain. The increase in correlation was statiscally significant. The muscle forces were calculated using a minimum number of easily attainable constants.

One of the major criticisms to both the mathematical and ectromyographical approach is the fact that there is no experimental correlation between these models and the actual force generated by the jaw muscles. Therefore, the results and conclusions of these studies should be carefully evaluated and further confirmed by other studies.

DIRECTION OF THE JAW MUSCLE FORCES

Up to this very moment, precise determination of the direction of the jaw muscle forces has received very little attention. The method most commonly used to estimate the jaw muscle force directions has been the use of a line connecting the midpoints of the origins and insertions of each muscle.

Van Eijden *et al.* (1988) determined the possible range of bite force directions and magnitudes and the concomitant joint force of each individual muscle by a mathematical model describing static equilibrium in the sagittal plane. They defined the range of force directions for each muscle by the action lines of the most anterior and the most posterior (for the lateral pterygoid, most superior and most inferior) muscle bundles. Calculations from the various directions of the reaction force in the temporomandibular joint demonstrated that each muscle can produce a unique variety of bite force directions. With the exception of the lateral pterygoid and posterior temporalis, the range and orientation of

possible bite forces was closely related to the orientation of the joint force. Generally, at the canine tooth the bite forces were oriented more posteriorly than at the second molar. Within a muscle, distinct portions may proportionate considerably different bite force magnitudes; the largest bite forces are produced at horizontal and vertical joint force directions. The posterior portions of the deep masseter and temporalis muscles and the lateral pterygoid muscle have the largest mechanical advantage. In the majority of muscles, the magnitude of the joint reaction force is smallest at an oblique joint force direction.

Koolstra *et al.* (1988) described a three-dimensional mathematical model of the human masticatory system, containining 16 muscle forces and two joint reaction forces. The model permitted the simulation of static bite forces and concomitant joint reaction forces for various bite point locations and mandibular positions. They determined the orientation of muscle action lines by marking the centroids of the areas of attachment of the different muscles ligaments to the mandible and skull by tiny lead markers. These markers were identified on a sagittal and frontal X-ray picture, both taken perpendicular to the FH with a film-focus distance of 4.5m. They computed the action lines of the muscle elements from the obtained sites of attachment, relative to a system of cartesian coordinates. Their model predicted that at each specific bite point, bite forces could be generated in a wide range of directions, and that the magnitude of the maximum bite force depended on its direction. The relationship between bite force direction and its maximum magnitude depended on bite point location and mandibular position. Generally, the direction of the largest possible bite force does not coincide with the direction perpendicular to the occlusal plane.

Due to the great complexity in fiber arrangement of the majority of the jaw muscles, this method would give nothing more than an average direction at best. Other authors tried to increase the accuracy of muscle force direction by dividing the muscles into several subunits, and they have also used fiber direction as well as origin an insertion.

Gaspard *et al.* (1973) published a series of three papers on the architectural organization of the masseter, temporal and pterygoid muscles. In the first paper, they compared the macroscopic structure of the masseter in man and primates. The masseter of the *Catarrhines* was composed, from outside to inside, of three partially fused portions: *the masseter superficialis, the masseter intermedius and the masseter profundus. The masseter superficialis* was divided in two musculo-tendinous sheets, *the laminae prima* and *secunda*, each reinforced by a constitutional aponeurosis. *The masseter intermedius* remained undivided. *The masseter profundus* was subdivided into two portions: the unifasciculated *pars anterior* and the bi or trifasciculated *pars posterior*. The different parts of the human masseter were homologous to those of the simian masseter. The following correspondence could be established: 1) the superficial part of the human masseter = *masseter superficialis laminae prima et secunda* + *masseter intermedius* + *masseter profundus pars anterior* of the *Catarrahine* monkeys. 2) The deep part of the human masseter = *masseter profundus pars posterior laminae prima, secunda et tertia* of the *Catarrhine* monkeys.

In the second paper, they undertook a macroscopic study of the temporal muscle in man, monkeys and prosimians. The temporal of the *Catarrhinians* showed three contractile parts: the *pars orbitalis* and the *pars temporalis laminae superficialis* and *profunda*. In the inside, it was reinforced by a powerful fan-like tendon. The temporal was flanked by two bundle: the maxillo-mandibularis and the zygomatico-mandibularis which were adjacent superficially to the masseter. This type of organization was found in all monkeys (*Platyrrhinians, Cynomorphs and Anthropomorphs*) and illustrated the *pithecoid* type originating from the primitive model found in insectivore: the *erinacoid* type. The study of prosimians (*Lemurs, Loris, Daubentonians and Tarsars*) showed intermediary morphologic types between these two muscular dispositions. Phylogenesis demonstrated that the human temporal architecture was very similar to that of the upper primates, by conserving however some archaic characters.

In the third paper, the three authors: Gaspard, Laison and Mailland, made a similar analysis of the pterygoid muscle between man and other mammals. They found that the pterygoid muscles in man was much more complex. However, the analysis of the macroscopic structure of these deep masticatory muscles allowed the demonstration of a homology between the different aponeurotic and muscular components of the human type with those of pithecoid type and correlatively with the mammalian archetype. The important muscular modifications observed in the modern man could be correlated with the craniofacial transformations following the achievement of a standing position, to the passage from plagiocephalia to orthocephalia, and to the very important and relatively fast evolution of the central nervous system (the neurological evolution having, so to speak, bypassed the evolution of the muscles).

Baron and Debussy (1979) made a biomechanical analysis using anatomical knowledge about the architecture of the masticatory muscles. The points of origin and insertion of the twelve fascicles which form part of the muscles, precisely described and situated according to three perpendicular spatial reference planes, had for point of origin the bisector of a line joining the two mandibular condylar vertices. The functional potential of the 12 fascicles was defined by analysing the projections on the three reference planes. He found that the masseter is composed of three principal parts with different orientations: the superficial portion, the deep portion and the central portion. The temporal muscle is composed by the anterior, medial and posterior portions. The medial pterygoid, which seems to be in anatomic symmetry with the masseter, has a less diversified potential. The lateral pterygoid is comprised by a superior and inferior heads. He concluded that a biomechanical study does not alone permit a definitively evaluation of the functions of each bundle and that selective electromyography and kinematic analyses were needed to confirm and refined their "rudimentary" results.

Whether these studies using more complex techniques improved the precision of the muscle force directions is still unknown. This is due to the fact that no other experimental

measurements of jaw muscle directions are available at the present time for comparison. The precise determination of the moment arm length for each muscle force depends on the direction chosen for that force and the position of the vector relative to the center of rotation. Both of these factors, force direction and vector position, are calculated by the anatomical points chosen as the origin and insertion of the muscle. In order to generate the data to calculate the resultant temporomandibular joint forces, it is necessary to measure the bite force magnitudes, bite force direction, and quantitative electromyographic recording from the greatest number of muscles or portions of muscles as possible. In addition, it is also necessary to know the precise location of the joint, bite, and muscles. Up untill now, there has been no experiment where all these variables have been measured; the study with the largest number of quantitative electromyographic recordings is five (Moller, 1966).

MATERIALS AND METHOD

Material

Fifty (50) head and neck horizontal sections of the left side of an adult male caucasian cadaver were used. Sections were spaced 5 mm apart and parallel to the Frankfort horizontal plane (Fig. 1). With the exception of the upper and lower third molar, the dentition was complete. Prior to performing the specimen with fixation, the teeth were placed in centric occlusion and the mandible ligated to the maxilla. By this means, the orientation of the section through the lower face was also maintained relative to the Frankfort horizontal plane. Each section was graphically reproduced by an illustrator in the original magnification. The sections were part of an anatomical study performed by Dr. John H. Lillie.

Digitizing of Sections

Sections were digitized by means of a graphic tablet and the appropriate support software PC3D (Jandel Scientific Co., 65 Koch Road, Corte Madera, CA 94925). Due to the software limitation in the number of polygons (maximum 15), the head and neck sections were digitized, integrated and reconstructed as two separated sets of polygons: one for the head and the other for the neck sections. The structures were generated using the program function 3D-TRACE. In order to minimize possible errors in tracing, amplified copies (140%) were taken of the original illustrations.

23

In the head sections, the following structures were digitized: 1) the skull, including the calvarium, the cranial base, the nasal maxillary process, and the zygomatic arch; 2) the superficial temporal and external carotid arteries; 3) the temporalis muscle; 4) the temporalis tendon; 5) the masseter muscle; 6) the masseter tendon; 7) the mandible, including the coronoid process, the condyle, the condylar neck, the ramus and the corpus; 8) the lateral pterygoid muscle (superior head); 9) the lateral pterygoid tendon (superior head); 10) the lateral pterygoid muscle (inferior head); 11) the lateral pterygoid tendon (inferior head); 12) the medial pterygoid muscle; 13) the medial pterygoid tendon; 14) upper teeth and 15) lower teeth.

In the neck sections, the digitized structures were: 1) the skull and spine, including the cranial base, the occipital condyles, the vertebrae from C_1 to C_4; 2) the mandible, including the coronoid process, the condyle, the condylar neck, the ramus and the corpus; 8) the lateral pterygoid muscle (superior head); 3) the hyoid bone; 4) the internal jugular vein; 5) the digastric muscle (anterior belly); 6) the digastric tendon (anterior belly); 7) the digastric muscle (posterior belly); 8) the digastric tendon (posterior belly); 9) the stylohyoid muscle; 10) the stylohyoid tendon; 11) the myolohyoid muscle; 12) the mylohyoid tendon; 13) the geniohyoid muscle; 14) the geniohyoid tendon and 15) fibrous loop.

Alignment of Sections for 3-D Reconstruction

Both set of sections (head and neck) were aligned according to "the best fit method" using the program function 3D-ALIGN. For the head sections, the calvarium and the superficial and external carotid arteries were used as fiduciaries. These two arteries were selected for two main reasons. First, both arteries are more superficially located; therefore, they avoid superimposition with other anatomical structures and allow better visualization. Second, the superfical temporal artery is a continuation of the external carotid artery following almost a straight line from the neck to the calvarium. The internal carotid artery

and the internal jugular vein were excluded because both change their direction after penetrating into the cranial base. For the neck sections, the internal jugular vein was chosen, because it follows almost a straight line through the neck up to the cranial base .

Muscle Projection

All sections, after being individually digitized, were integrated using the program function 3D-DESCRIBE which describes a set of files concerning magnification of each section, distance between sections (angstroms), and number of individual sections. Consequently, a new file containing either all head or neck sections was created. These files were displayed either in the frontal, horizontal or sagittal planes utilizing the program function 3D-DISPLAY. The program not only allows the display of all structures at the same time, but also allows selection of one or more individual structures. This ability permitted the study of all head and neck muscles in many different positions and angulations in relation to the coordinate system X,Y and Z . The angulations chosen for the study of all head and neck muscles individually were: 1) R(180X), for the view in the horizontal plane; 2) R(90X), for the view in the frontal plane; and 3) R(90X) and R(-90Y) for the view in the sagittal plane. The angulations in the frontal and sagittal planes were chosen, because they provide a perpendicular view, and the image of each muscle section is displayed as a straight line making easier the location and calculation of each muscle vector. In the horizontal plane, the view chosen was also perpendicular providing the correct representation without distortion in both size and shape of the muscle sections.

In the frontal and sagittal planes, all muscle sections of an individual muscle were displayed, but in the horizontal plane just the first and the last sections were displayed to facilitate the visualization and avoid superimposition of other sections. This allowed computation of the centroids of the first and last sections and the determination of the muscle vector in the horizontal plane. One exception was made for the masseter muscle,

because its first section does not allow the visualization of both the superficial and deep portions. The other exception was the temporalis muscle in which the first muscle section and the first section showing the coronoid process were chosen, because the final portion of the temporalis muscle is mostly comprised by a thick tendon which inserts in the coronoid process.

In the head muscles, the following muscles were individually displayed in the horizontal, frontal, and sagittal planes: 1) the temporalis muscle (anterior, medial and posterior portions), 2) the masseter muscle (superficial and deep portions), 3) the lateral pterygoid muscle (superior head), 4) the lateral pterygoid muscle (inferior head), and 5) the medial pterygoid muscle. In the neck sections, the muscles displayed were: 1) the digastric muscle (anterior belly), 2) the digastric muscle (posterior belly), 3) the stylohyoid muscle, 4) the mylohyoid muscle and 5) the geniohyoid muscle. The overall number of muscles displayed is ten, considering the inferior and superior head of the lateral pterygoid muscle and the anterior and posterior belly of the digastric muscle as separate entities. However, if all muscle portions are taken into account and considered as individual muscles, a total of 13 was studied.

Computation of the Centroid

In order to determine the origin and insertion of each vector, it was necessary to calculate first the centroid of each muscle of its first and last sections, with the exception of the masseter and temporalis as explained above. Consequently, projections of the first and last sections of each muscle in the horizontal plane were displayed for true representation and calculation of the correspondent centroids. The computer software ZIDAS (ZIDAS System - Carl Zeiss, Inc.) was used for computation of the location of the centroid of the first and last sections of each muscle. The location was given in terms of coordinates (mm)

in the X and Y axes. The X and Y axes in these case are represented by the lower and left border of the page (Fig. 2) .

Due to the fact that the computer software PC3D was displaying the muscle images in different magnification in the three different planes (autoscaling), it became necessary to calculate the different magnification in each plane and to transfer the centroid localization from the horizontal to the other two planes. This was calculated in the following manner: 1) X' and Y' axes (tangent to the lower and left border of each muscle section) were drawn for the first and last section of each muscle, being the X' axis correspondent to the frontal plane, and the Y' axis correspondent to the sagittal plane (Fig. 2); 2) lines perpendicular to the X'and Y' axes were traced from the centroid and the tangents of the right and upper border of the first and last sections of each muscle; and 3) the distance from the intersection of the X' and Y' axes to the centroid and tangent projections were then measured. The distance from the intersection of the X' and Y' axes to the perpendicular of the centroid in the X' axis corresponded to the distance of the centroid of this section (mm) from medial to lateral in the frontal plane, and the distance from the intersection to the tangent of the right border of the muscle section in the X' axis corresponded to the overall width of the muscle in the frontal plane. The distance from the intersection of the X' and Y' axes to the perpendicular of the centroid in the Y' axis corresponded to the distance of the centroid of this section (mm) from anterior to posterior in the frontal plane, and the distance from the intersection to the tangent of the upper border of the muscle section in the Y' axis corresponded to the overall length of the muscle in the sagittal plane.

Magnification Factors

In order to determine the different magnification factors of each series of projections, the following procedures were undertaken. First, the distance between the sections in the frontal plane [D sec(n,n+1) M(b)] was measured with a ruler and divided

by the original distance between sections [D sec(n,n+1) M(1)], in each case 5 mm. The result of this division gave the magnification of the frontal plane [M(b)] in relation to the original magnification [M(1)]. Second, the conversion factor from M(b) to M(1) [CF M(b->1)] was calculated by dividing M(1)/M(b). This calculation was made in order to allow the latter measurement of the vectors and section length (mm) and the subsequent conversion to their original lengths. Third, the length of either the first and last sections in the frontal plane [L sec(n) M(b)] were measured (mm) and multiplied by the conversion factor from the frontal to the original length [CF (b->1)], providing their lengths in the original magnification [L sec(n) M(1)]. Fourth, the length of either the first and last sections in the horizontal plane were then measured [L sec(n) M(a)] and divided by the corresponding length in the original magnification [L sec(n) M(a)] . This result gave the magnification of the horizontal plane [M(a)] in relation to the original magnification [M(1)]. Fifth, for the same reasons and likewise in the frontal plane, the conversion factor from the horizontal plane magnification to the original magnification [CF M(a->1)] was determined by dividing M(1)/M(a). Sixth, the distance between sections in the sagittal plane [D sec(n,n+1) M(c)] was divided by the distance between sections in the original magnification [D sec(n,n+1) M(1) = 5 mm] giving the magnification of the sagittal plane [M(c)]. Likewise in the frontal and horizontal planes , the conversion factor from the sagittal plane to original magnification was provided by dividing M(1)/M(c) (Fig. 3). The conversion factors from one plane to the other were given by the general formula: CF M(x->y) = M(y)/M(x). Finally, once all magnification factors for all projections were made, the section lengths and widths and the correct position of the centroids of all muscles could then be transferred from the horizontal to the frontal and sagittal planes .

Muscle Vectors

Once all centroids were computed in all planes for all muscles, the vectors were then determined by connecting the centroids from the last to the first section. This direction was chosen for all head and neck muscles, due to the fact that this direction is coincident with the direction of the elevator muscles, that is, from inferior to superior. Exception was made for the lateral pterygoid muscle (superior and inferior heads), because its normal muscle direction is from posterior to anterior, protruding the mandible. In this case, the vector was determined by a line parallel to the muscle sections on the midline between the centroids of the first and last sections. Its length was determine by tracing a perpendicular line from the most anterior and most posterior borders of the sections.

Once determined, the vectors were then measured in length with a professional ruler in all planes and converted to their original magnifications using the following general formula : [L vec M(1) = L vec M(x) x CF M(x->1)]. After that, they were measured in angles with a professional protractor (Fig. 4). In this case, there was no need for conversions, because the vector angles don't change with the change in magnification. Once the vectors were measured, there was still a need to localize their origin in relation to the head as a whole. In order to do that, a reference point in the head was chosen : the mesio-vestibular cusp of the lower first molar (Fig. 5).

Statistical Analysis

In order to verify the intraobserver reliability of vector measurements, both in distance (mm) and in angulation (degrees), five measurements at five different times were undertaken by the same observer. The same procedure was made to verify the interobserver reliability of vector measurements, but in this case, five different observers were chosen to perform the same amount and type of vector measurements. The test used was the

intraclass correlation coefficient of reliability at 95% of significance level for one factor ANOVA for both intra- and interobserver measurements. Reliability estimates were performed for one single measurement and for all measurements in each set of measurements.

Due to the great number of conversions made in this study, another analysis was made in order to verify if the conversion from one magnification to the other could change the measurement values (mm) to a significant degree. The conversion factor reliability was made by converting the original length of the vector to a given magnificaton and again back to original magnification and see if the original value has changed significantly. This procedure was repeated four times for each vector length measurement in the horizontal plane.
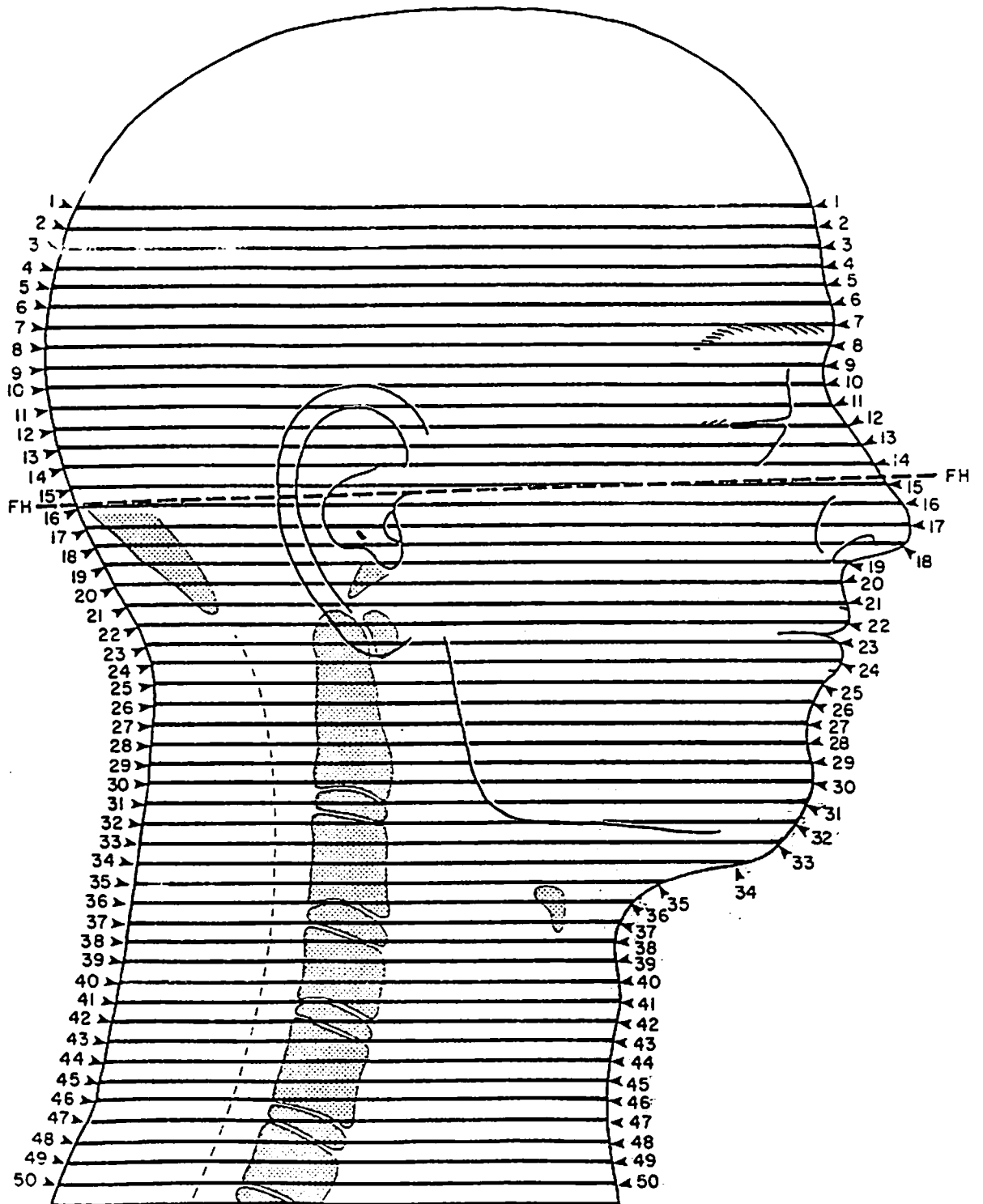
Figure 1. Schematic representation of the head and neck horizontal sections made in a cadaver (Courtesy of Prof. John Lillie).

CENTROID, MUSCLE LENGTH & WIDTH

H P
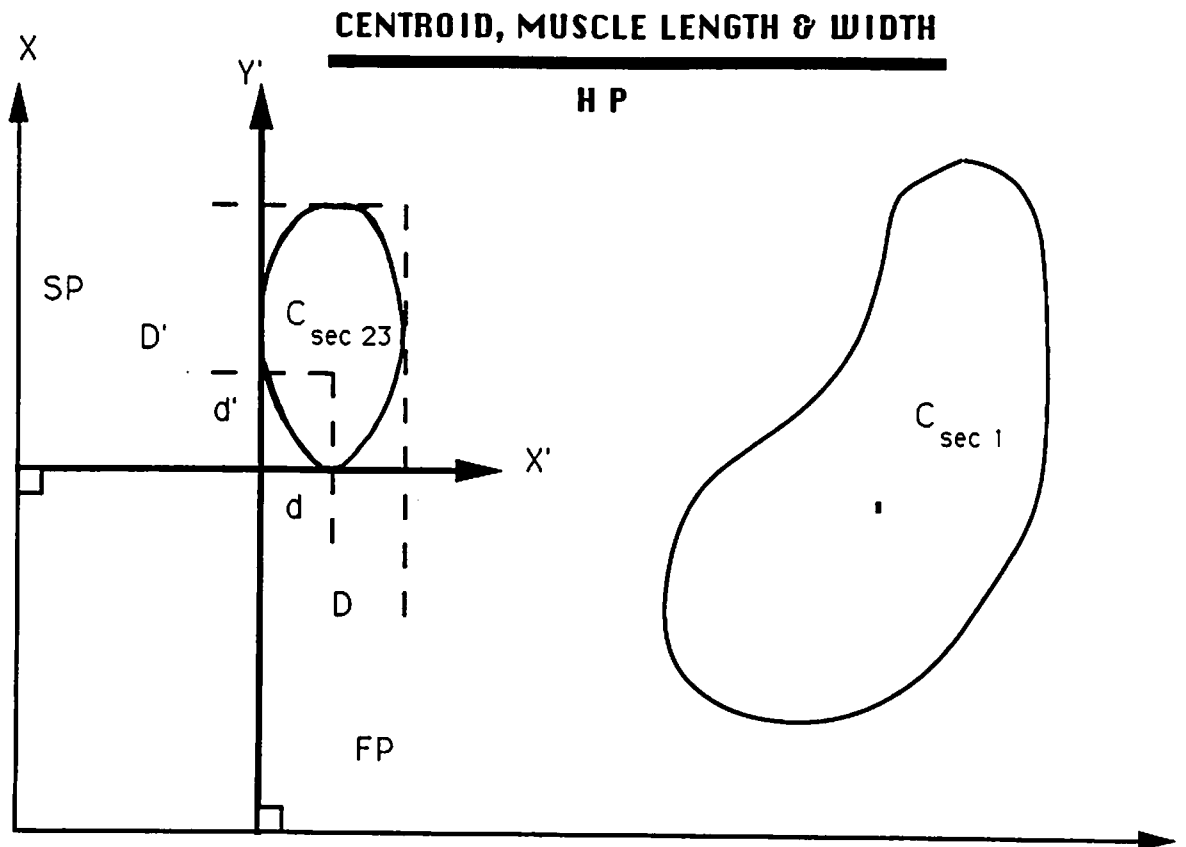
ZIDAS ---> C (X , Y)

X' -> FP
Y' -> SP

d : distance of the centroid of section 23
in the FP from M->L

D: width of the muscle of section 23 in
the FP from M->L

d': distance of the centroid of section 23
in the SP from A->P

D': length of the muscle of section 23 in
the SP from A->P
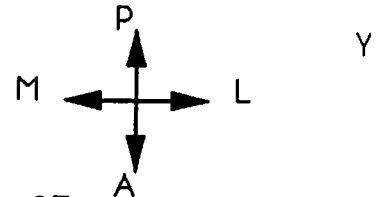
Figure 2. Schematic representation of centroid, muscle length and width determination in the horizontal plane. C(X,Y): coordinates of the centroid in the X and Y axes; Csec1: centroid of section 1; Csec23: centroid of section 23.

MAGNIFICATION CONVERSION FORMULAS

$$M(b) = \frac{D\ sec(n,n+1)\ M(b)}{D\ sec(n,n+1)\ M(1)} \quad ; \quad CF\ M(b\text{->}1) = \frac{M(1)}{M(b)}$$

$$5\ mm$$

$$L\ sec(n)\ M(1) = L\ sec(n)\ M(b)\ X\ CF(b\text{->}1)$$

$$M(a) = \frac{L\ sec(n)\ M(a)}{L\ sec(n)\ M(1)}$$

$$M(c) = \frac{D\ sec(n,n+1)\ M(c)}{D\ sec(n,n+1)\ M(1)} \quad ; \quad CF\ M(x\text{->}y) = \frac{M(y)}{M(x)}$$
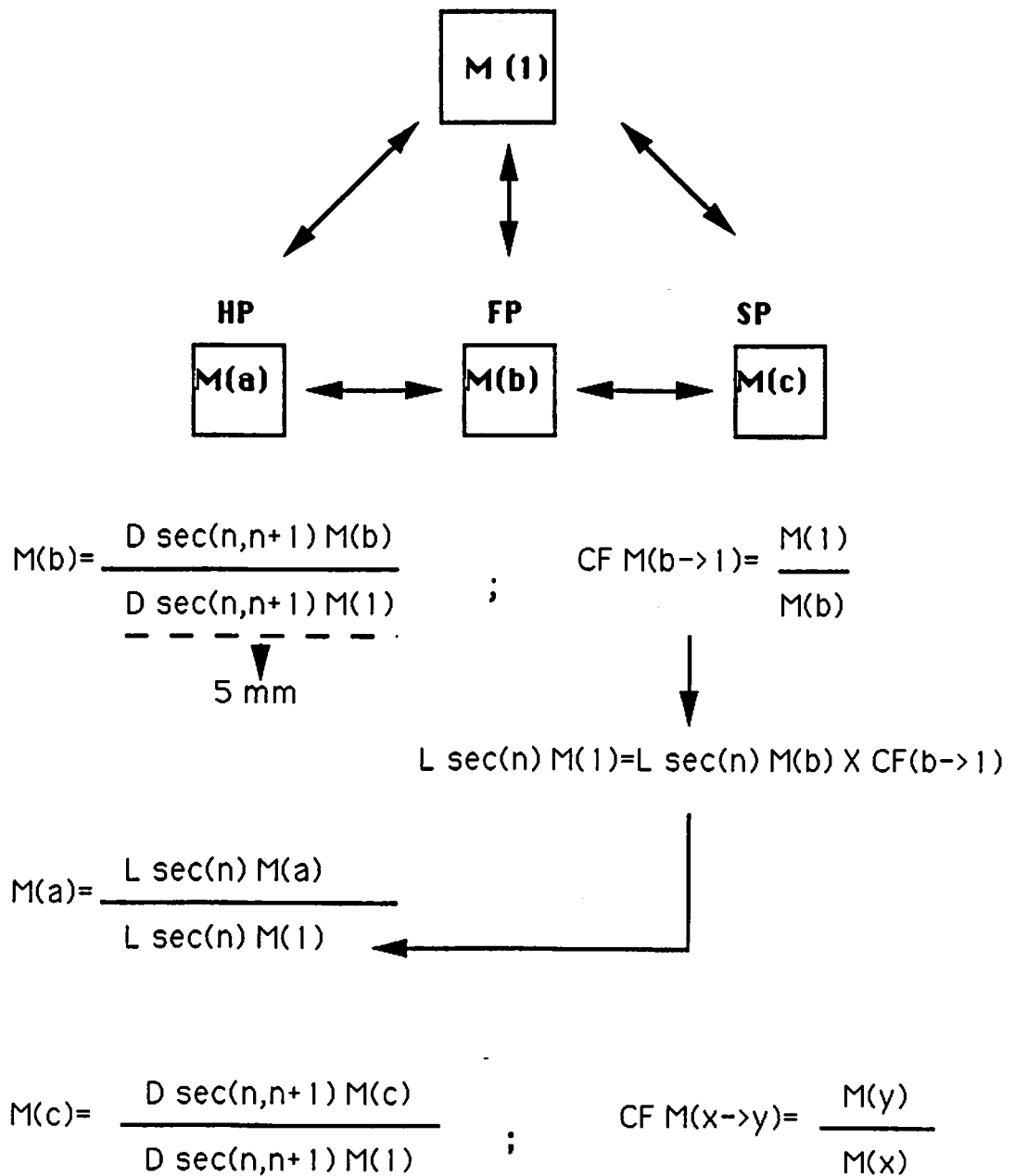
Figure 3. Schematic diagram on magnification conversion formulas. M(1): magnification 1 - normal size; M(a): magnification a; M(b): magnification b; M(c): magnification c; D sec(n,n+1) M(b): distance between sections n and n+1 in magnification b; CF M(c->1): conversion factor from magnification c to 1; L sec(n) M(1): length of section n in magnification 1.

VECTOR MEASUREMENT
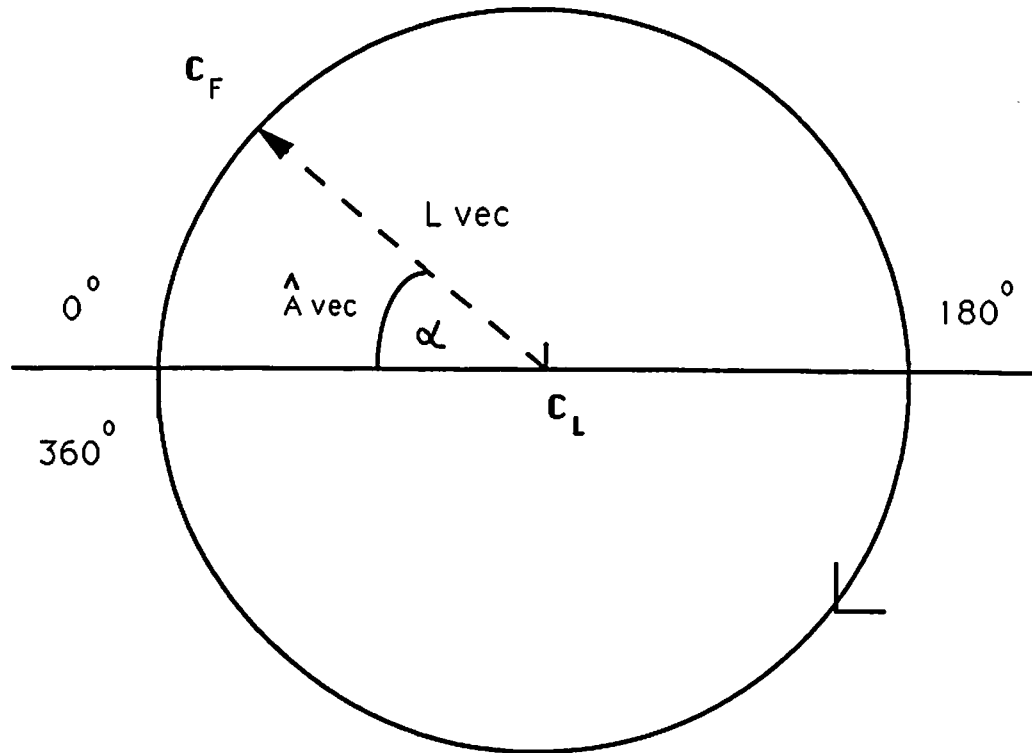
HP, FP, SP

MAGNIFICATION = a

$\hat{A} \text{ vec} = \alpha$

$L \text{ vec } M(1) = L \text{ vec } M(a) \times CF \ M(a\text{->}1)$

Figure 4. Schematic representation of vector measurement (angle and length). Cf: centroid of the first section; Cl: centroid of the last section; $\hat{A}$ vec: angle of the vector; L vec M(1): length of the vector in magnification 1; M(a): magnification a; M(1): magnification 1 - normal size; CF M(a->1): conversion factor from magnification a to 1; HP, FP, SP: horizontal, frontal and sagittal planes respectively

VECTOR LOCATION IN RELATION TO M1
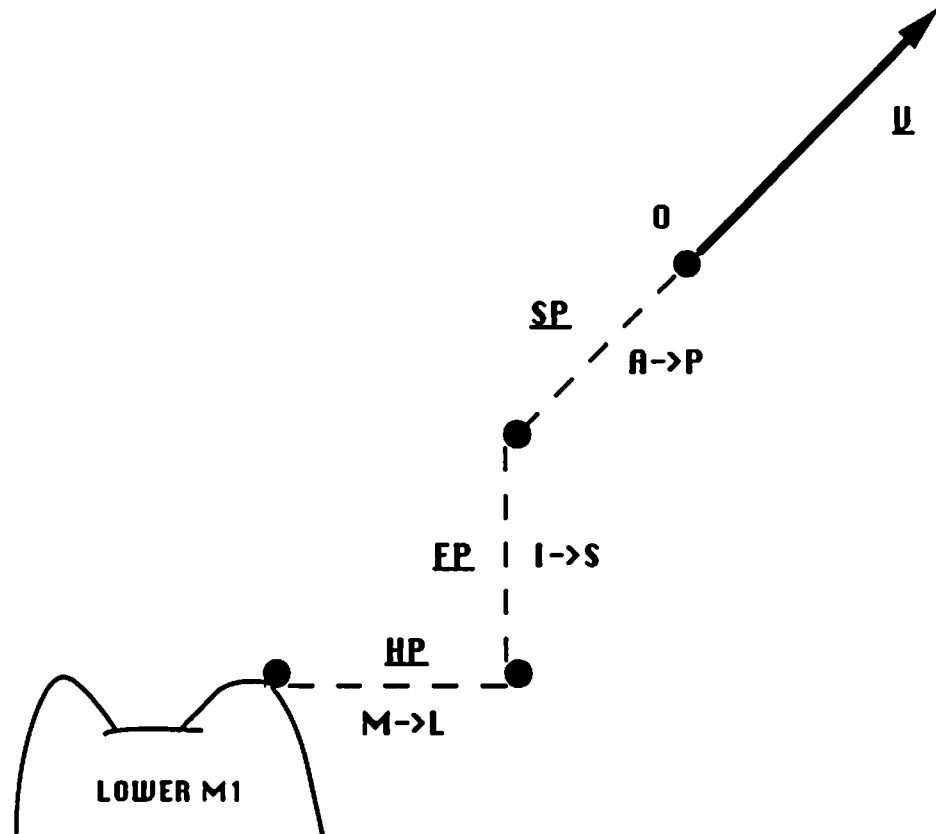
Figure 5. Schematic diagram on vector location in relation to the mesio-vestibular cusp of the lower first molar in the horizontal, frontal and sagittal planes. M1: lower first molar; HP: horizontal plane; FP: frontal plane; SP: sagittal plane; M->L: from medial to lateral; S->I: from inferior to superior; A->P: from anterior to posterior; O: vector origin; V: vector.

RESULTS

Alignment of Sections for 3-D Reconstruction

The aligned head and neck sections can be seen in Figures 6 - 9. The major structures in the head sections (Figure 6 and 7) such as the calvarium, the orbit, the zygomatic arch, the frontal nasal process, the mandible, the spine, the external carotid artery and the superficial temporal artery can be easily identified both in the frontal (Figure 6) and in the sagittal view (Figure 7). In the neck sections (Figure 8 and 9), the structures digitized such as the mandible, the hyoid bone, and internal jugular artery can also be easily identified in both frontal (Figure 8) and sagittal views (Figure 9).

Muscle Vector Direction and Relative Position in the Head

The results of vector measurements in length and in angulation in the horizontal, frontal and sagittal planes are shown in Tables 1-3, and in Figures 10-39. The anterior temporalis muscle vector was directed 185° in the horizontal plane, 94° in the frontal plane, and 94° in the sagittal plane. The vector respective length was 16.65 mm, 66 mm, and 61 mm. The overall muscle vector direction was slightly outward (horizontal plane), upward (frontal plane), and slightly backward (sagittal plane), as shown in Figures 10 - 12.

The medial temporalis muscle vector was directed 128° in the horizontal plane, 100° in the frontal plane, and 124° in the sagittal plane. Its length was 35.39 mm in the horizontal plane, 67 mm in the frontal plane, and 73 mm in the sagittal plane. The direction

of the muscle vector was outward (horizontal plane), upward (frontal plane), and backward (sagittal plane), as shown in Figures 10 - 12.

The posterior temporalis muscle vector angulation was 106° in the horizontal plane, 94° in the frontal plane, and 141° in the sagittal plane. The vector length in these three planes was 57.6 mm, 66 mm, and 97 mm respectively. The combined muscle vector direction was slightly outward (horizontal plane), upward (frontal plane), and pronouncedly backward (sagittal plane), as shown in Figures 10 - 12.

The superficial masseter muscle vector was directed 240° in the horizontal plane, 108° in the frontal plane, and 85° in the sagittal plane. The vector respective length was 22.71 mm, 76 mm, and 72.67 mm. The overall muscle vector direction was outward (horizontal plane), upward (frontal plane), and slightly forward (sagittal plane), as shown in Figures 13 - 15.

The deep masseter muscle vector was directed 243° in the horizontal plane, 104° in the frontal plane, and 92° in the sagittal plane. Its length was 16.33 mm in the horizontal plane, 74.67 mm in the frontal plane, and 72.33 mm in the sagittal plane. The general muscle vector direction was slightly outward (horizontal plane), upward (frontal plane), and almost in a straight line (sagittal plane), as shown in Figures 13 - 15.

The medial pterygoid muscle vector angulation was 316° in the horizontal plane, 73° in the frontal plane, and 76° in the sagittal plane. The vector length in these three planes was 28.47 mm, 64.54 mm, and 63.18 mm respectively. The combined muscle vector direction was inward (horizontal plane), upward (frontal plane), and forward (sagittal plane), as shown in Figures 16 - 18.

The lateral pterygoid muscle vector (superior head) was directed 308° in the horizontal plane, 7° in the frontal plane, and 6° in the sagittal plane. The vector respective length was 28.62 mm, 19.58 mm, and 24.28 mm. The general muscle vector direction was inward (horizontal plane), slightly upward (frontal plane), and pronouncedly forward (sagittal plane), as shown in Figures 19 - 21.

The lateral pterygoid muscle vector (inferior head) was directed 299° in the horizontal plane, 0° in the frontal plane, and 0° in the sagittal plane. Its length was 44.07 mm in the horizontal plane, 34.04 mm in the frontal plane, and 42.32 mm in the sagittal plane. The overall muscle vector direction was inward (horizontal plane), horizontal (frontal plane), and pronouncedly forward (sagittal plane), as shown in Figures 22 - 24.

The digastric muscle vector (anterior belly) angulation was 283° in the horizontal plane, 77° in the frontal plane, and 34° in the sagittal plane. The vector length in these three planes was 46.5 mm, 20.26 mm, and 34.37 mm respectively. The combined muscle vector direction was slightly inward (horizontal plane), upward (frontal plane), and pronouncedly forward (sagittal plane), as shown in Figures 25 - 27.

The digastric muscle vector (posterior belly) was directed 117° in the horizontal plane, 108° in the frontal plane, and 124° in the sagittal plane. Its length was 52.58 mm in the horizontal plane, 70 mm in the frontal plane, and 80 mm in the sagittal plane. The general muscle vector direction was slightly outward (horizontal plane), upward (frontal plane), and pronouncedly backward (sagittal plane), as shown in Figures 28 - 30.

The stylohyoid muscle vector was directed 123° in the horizontal plane, 104° in the frontal plane, and 113° in the sagittal plane. The vector respective length was 22.86 mm, 57.14 mm, and 60 mm. The overall muscle vector direction was outward (horizontal plane), upward (frontal plane), and pronouncedly backward (sagittal plane), as shown in Figures 31 - 33.

The mylohyoid muscle vector was directed 187.5° in the horizontal plane, 110° in the frontal plane, and 86° in the sagittal plane. Its length was 17.34 mm in the horizontal plane, 46.07 mm in the frontal plane, and 42.92 mm in the sagittal plane. The combined muscle vector direction was pronouncedly outward (horizontal plane), upward (frontal plane), slightly forward (sagittal plane), as shown in Figures 34 - 36.

The geniohyoid muscle vector angulation was 271° in the horizontal plane, 89.5° in the frontal plane, and 44.5° in the sagittal plane. The vector length in these three planes was 34 mm, 33.75 mm, and 46.67 mm respectively.The general muscle vector direction was vertical (horizontal plane), upward (frontal plane), and pronouncedly forward (sagittal plane), as shown in Figures 37 - 39.

The relative position in mm from the origin of each muscle vector described to the mesio-vestibular cusp of the left first lower molar in both the horizontal, frontal, and sagittal plane was shown in Table 4.

The list of all conversion factors and their applications was summarized in Table 11B. The section lengths and widths and the correct position of all centroids of all muscles can be seen in Tables 1B-10B (see Appendix B).

Statistical Analysis

In the results found in the statistical analysis, all measurements (intra- and interobserver) for vector length and angle gave a coefficient of reliability equal to 1 which is considered highly reliable. The variability of measurements never exceeded +-1 mm for vector lengths and +- 1 degree for vector angles as seen in Tables 1A-4A (see Appendix A).

The intraclass correlation coefficient of reliability for the conversion factors at 95% significance level for one factor Anova was like in the vector measurements equal to 1, also proving to be highly reliable. Changes from the original value were in average 1 to 2/100 mm for each conversion, exceeding 1/10 mm just in exceptional occasions as seen in Table 5A (see Appendix A1). The results have also proven to be highly reliable, being the intraclass coefficient of reliability equals to 1 for both single and all measurements undertaken at 95% of significance level for one factor ANOVA.

	ANGLE (degrees)	LENGTH M(1) mm
Temporalis (anterior portion)	185	16.65
Temporalis (medial portion)	128	35.39
Temporalis (posterior portion)	106	57.60
Masseter (superficial portion)	240	22.71
Masseter (deep portion)	243	16.33
Medial pterygoid	316	28.47
Lateral pterygoid (superior head)	308	28.62
Lateral pterygoid (inferior head)	299	44.07
Digastric (anterior belly)	283	46.5
Digastric (posterior belly)	117	52.58
Stylohyoid	123	22.86
Mylohyoid	187.5	17.34
Geniohyoid	271	34

Table 1. Length (mm) and angle (degrees) of all muscle vectors in the horizontal plane.

	ANGLE (degrees)	LENGTH M(1) mm
Temporalis (anterior portion)	94	66
Temporalis (medial portion)	100	67
Temporalis (posterior portion)	94	66
Masseter (superficial portion)	108	76
Masseter (deep portion)	104	74.67
Medial pterygoid	73	64.54
Lateral pterygoid (superior head)	7	19.58
Lateral pterygoid (inferior head)	0	34.04
Digastric (anterior belly)	77	20.26
Digastric (posterior belly)	108	70
Stylohyoid	104	57.14
Mylohyoid	110	46.07
Geniohyoid	89.5	33.75

Table 2. Length (mm) and angle (degrees) of all muscle vectors in the frontal plane.

	ANGLE (degrees)	LENGTH M(1) mm
Temporalis (anterior portion)	94	61
Temporalis (medial portion)	124	73
Temporalis (posterior portion)	141	97
Masseter (superficial portion)	85	72.67
Masseter (deep portion)	92	72.33
Medial pterygoid	76	63.18
Lateral pterygoid (superior head)	6	24.28
Lateral pterygoid (inferior head)	0	42.32
Digastric (anterior belly)	34	34.37
Digastric (posterior belly)	124	80
Stylohyoid	113	60
Mylohyoid	86	42.92
Geniohyoid	44.5	46.67

Table 3. Length (mm) and angle (degrees) of all muscle vectors in the sagittal plane.

MUSCLE	HORIZ PL (DIRECTION)	FRONTAL PL (DIRECTION)	SAGITTAL PL (DIRECTION)
Temporalis	34 mm (M-->L)	35 mm (I-->S)	35 mm (A-->P)
Masseter	22.7 mm (M-->L)	45 mm (S-->I)	43.3 mm (A-->P)
Medial pterygoid	15 mm (M-->L)	45 mm (S-->I)	53.7 mm (A-->P)
Lateral pterygoid (superior head)	28.9 mm (M-->L)	30 mm (I-->S)	64 mm (A-->P)
Lateral pterygoid (inferior head)	28.3 mm (M-->L)	17.5 mm (I-->S)	65 mm (A-->P)
Digastric (anterior belly)	7.8 mm (L-->M)	65 mm (S-->I)	29.5 mm (A-->P)
Digastric (posterior belly)	10.5 mm (M-->L)	55 mm (S-->I)	58 mm (A-->P)
Stylohyoid	1 mm (M-->L)	65 mm (S-->I)	51 mm (A-->P)
Mylohyoid	13.2 mm (L-->M)	65 mm (S-->I)	33 mm (A-->P)
Geniohyoid	15.7 mm (L-->M)	65 mm (S-->I)	36.5 mm (A-->P)

Table 4. Location of all muscle vectors in relation to the mesio-vestibular cusp of the lower first molar in the horizontal, frontal and sagittal planes. M: medial; L: lateral; S: superior; I: inferior; A: anterior; and P: posterior.
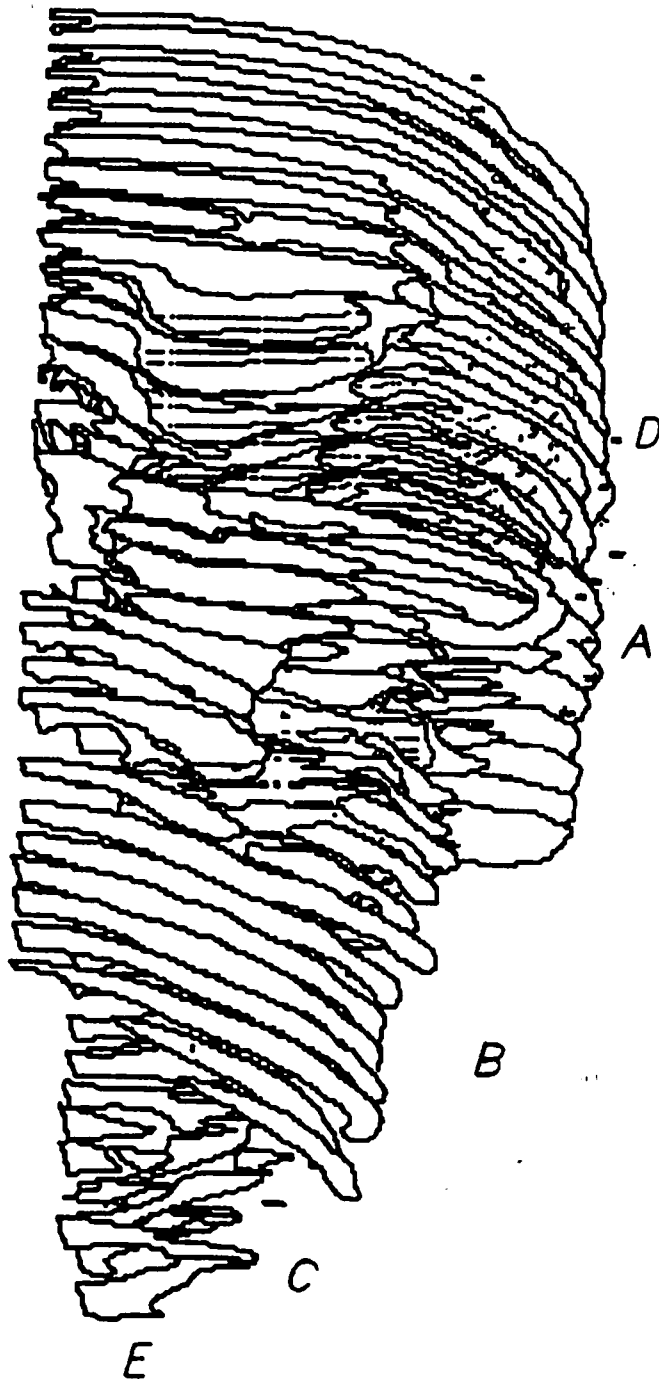
Figure 6. 3D reconstruction of the head sections in the frontal plane using the angulation: R(75X), R(-5Y); frontal inferior view. A: skull; B: mandible; C: external carotid artery; D: superficial temporal artery; and E: vertebrae (C1-C4).

**Figure 7.** 3D reconstruction of the head sections in the sagittal plane using the angulation: R(70X), R(-70Y); oblique lateral inferior view. A: skull; B: mandible; C: external carotid artery; D: superficial temporal artery; and E: vertebrae (C1-C4).
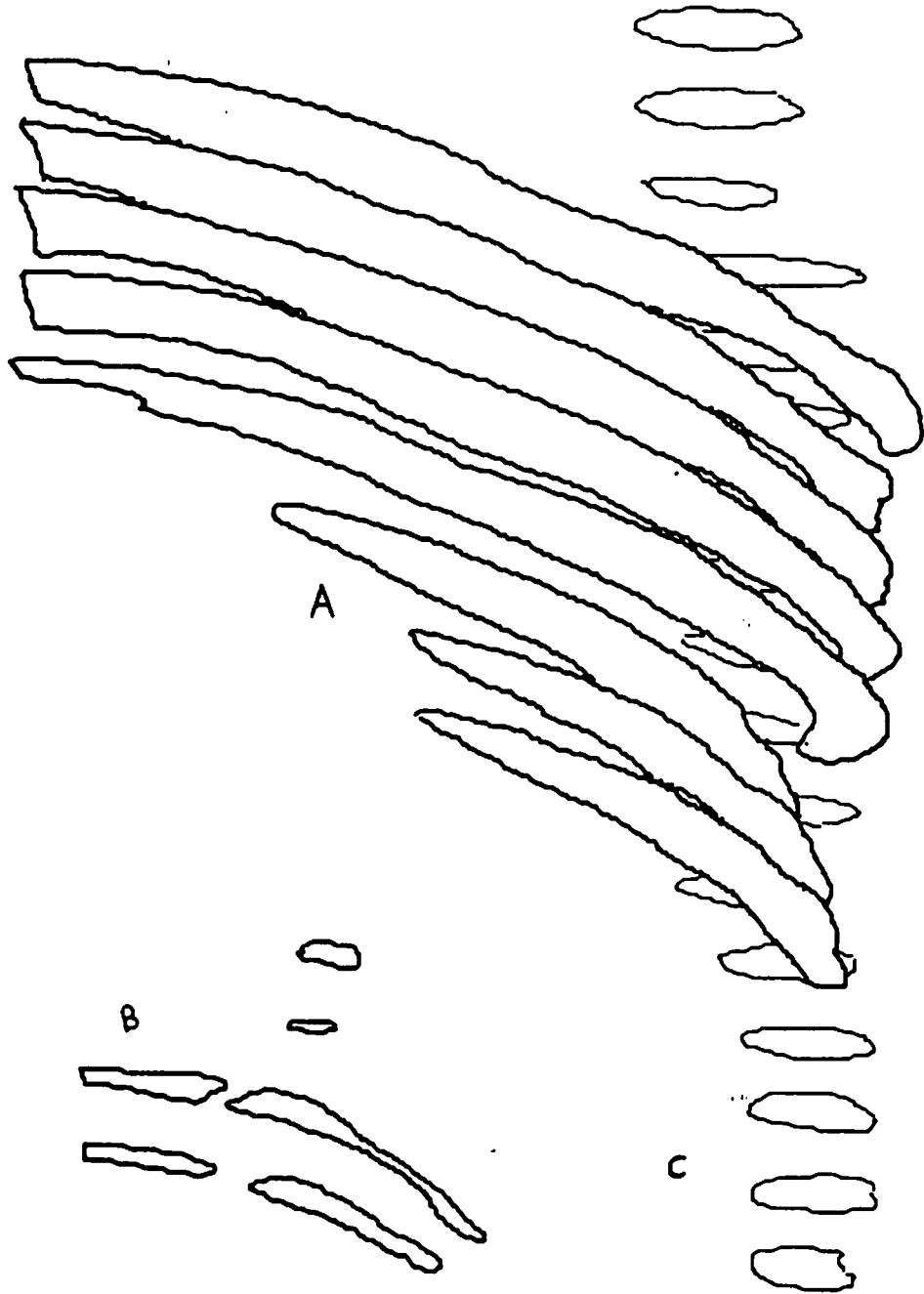
Figure 8. 3D reconstruction of the neck sections in the frontal plane using the angulation: R(75X), R(-5Y); frontal inferior view. A: mandible; B: hyoid bone; C: internal jugular vein.
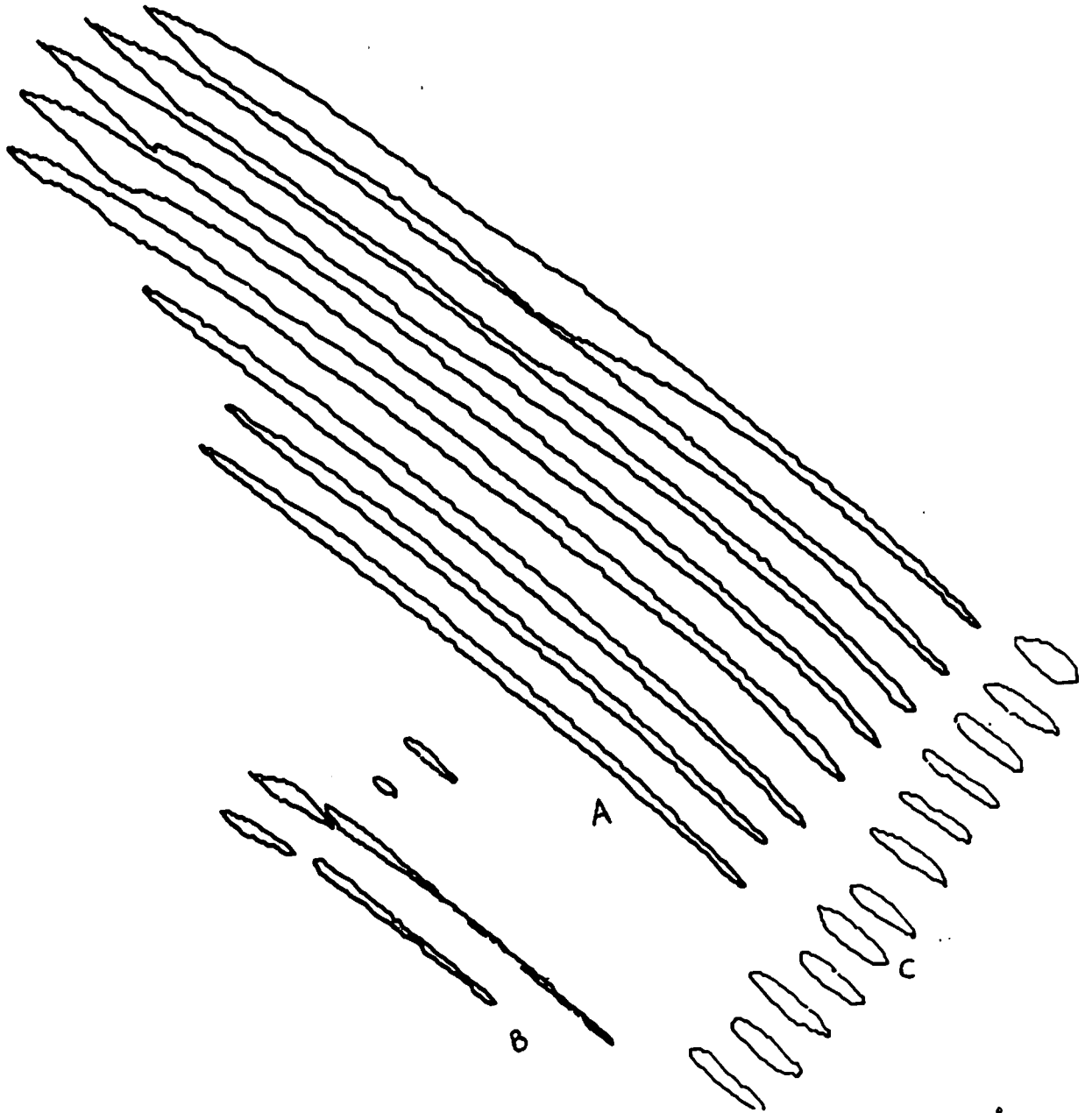
Figure 9. 3D reconstruction of the neck sections in the sagittal plane using the angulation: R(70X), R(-70Y); oblique lateral inferior view. A: mandible; B: hyoid bone; C: internal jugular vein.
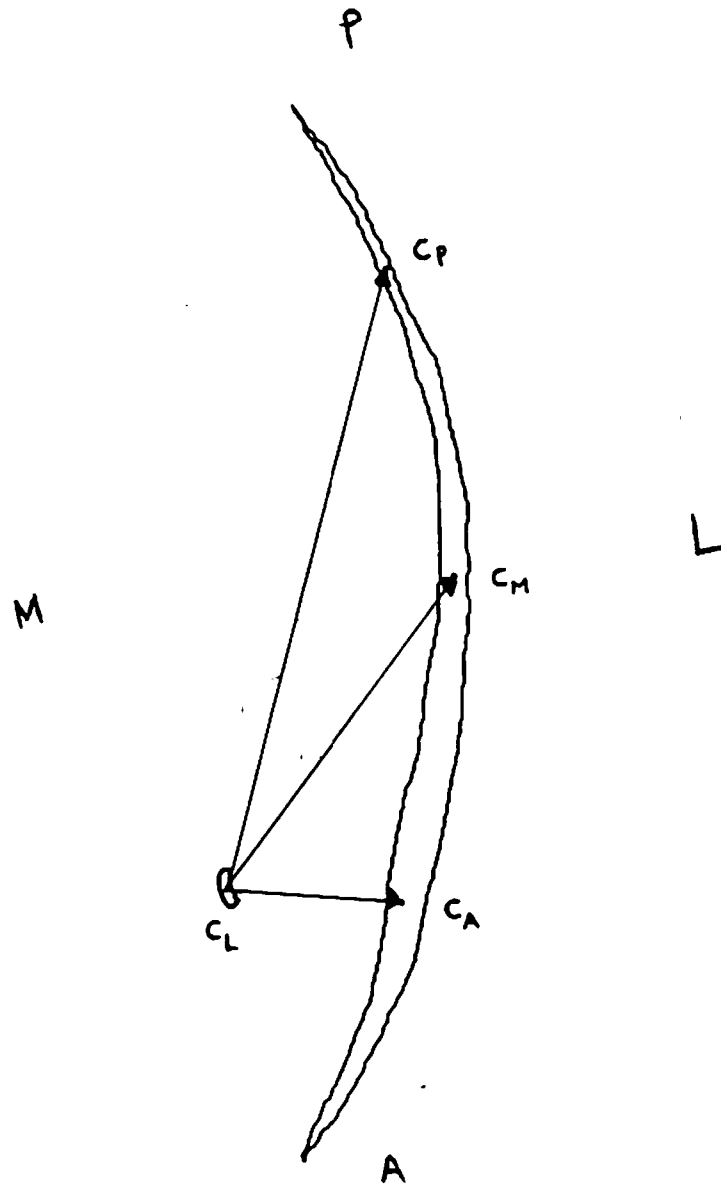
Figure 10. Projection of the vectors of the temporalis muscle in the horizontal plane using the angulation R(180X). Ca: centroid of the anterior temporalis; Cm: centroid of the medial temporalis; Cp: centroid of the posterior temporalis; Cl: centroid of the last section of the temporalis; M: medial; P: posterior; L: lateral; and A: anterior.
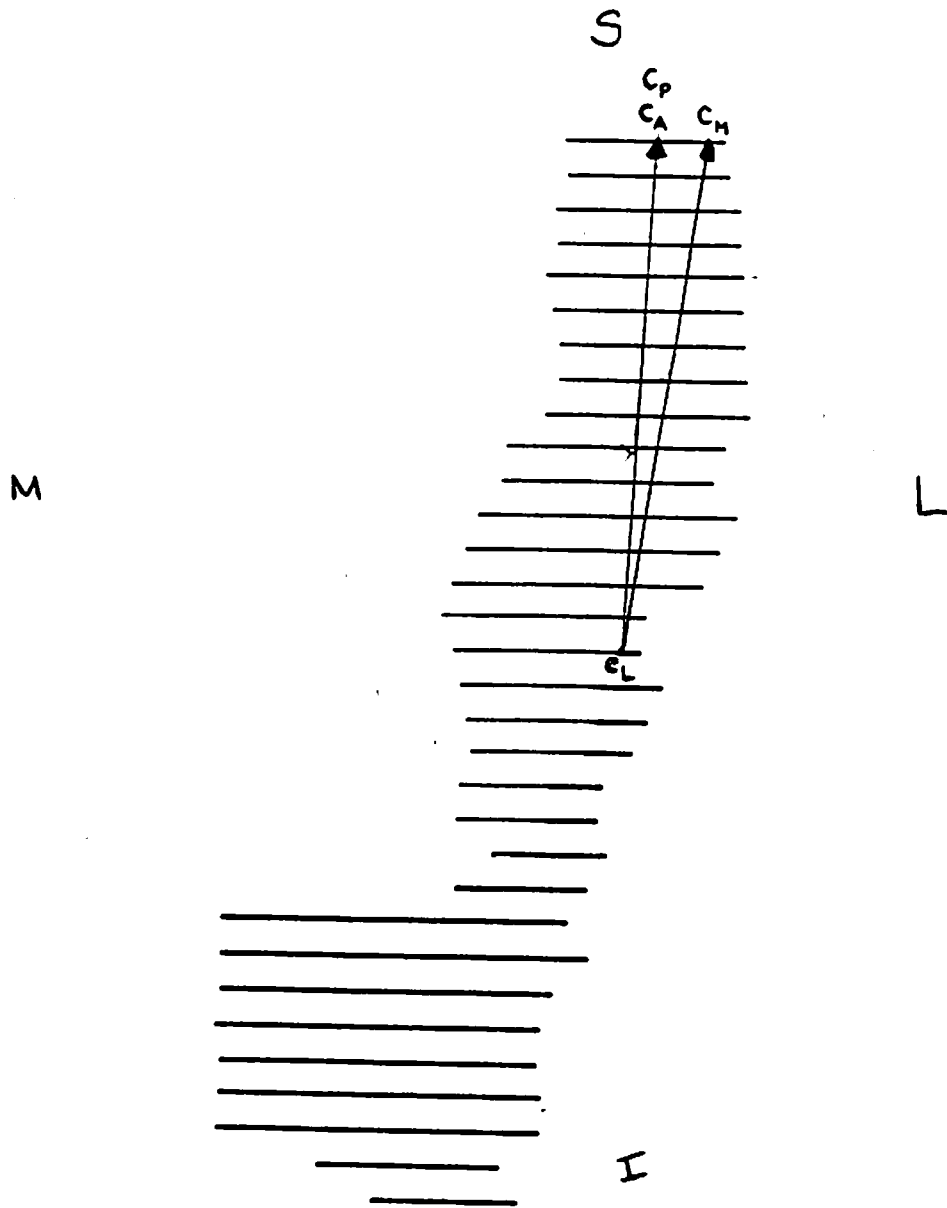
Figure 11. Projection of the vectors of the temporalis muscle in the frontal plane using the angulation R(90X). Ca: centroid of the anterior temporalis; Cm: centroid of the medial temporalis; Cp: centroid of the posterior temporalis; Cl: centroid of the last section of the temporalis; M: medial; L: lateral; S: superior; and I: inferior.
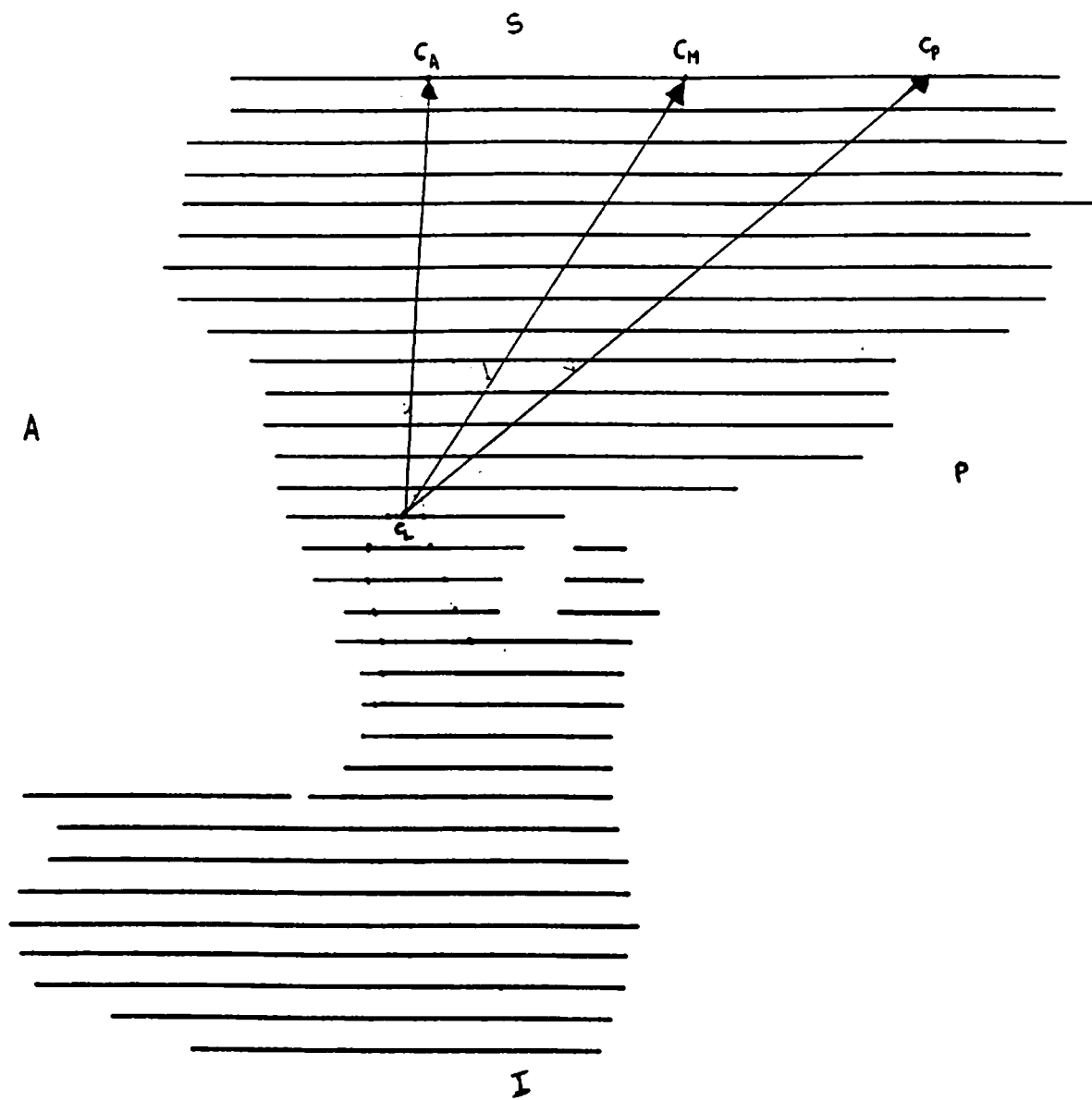
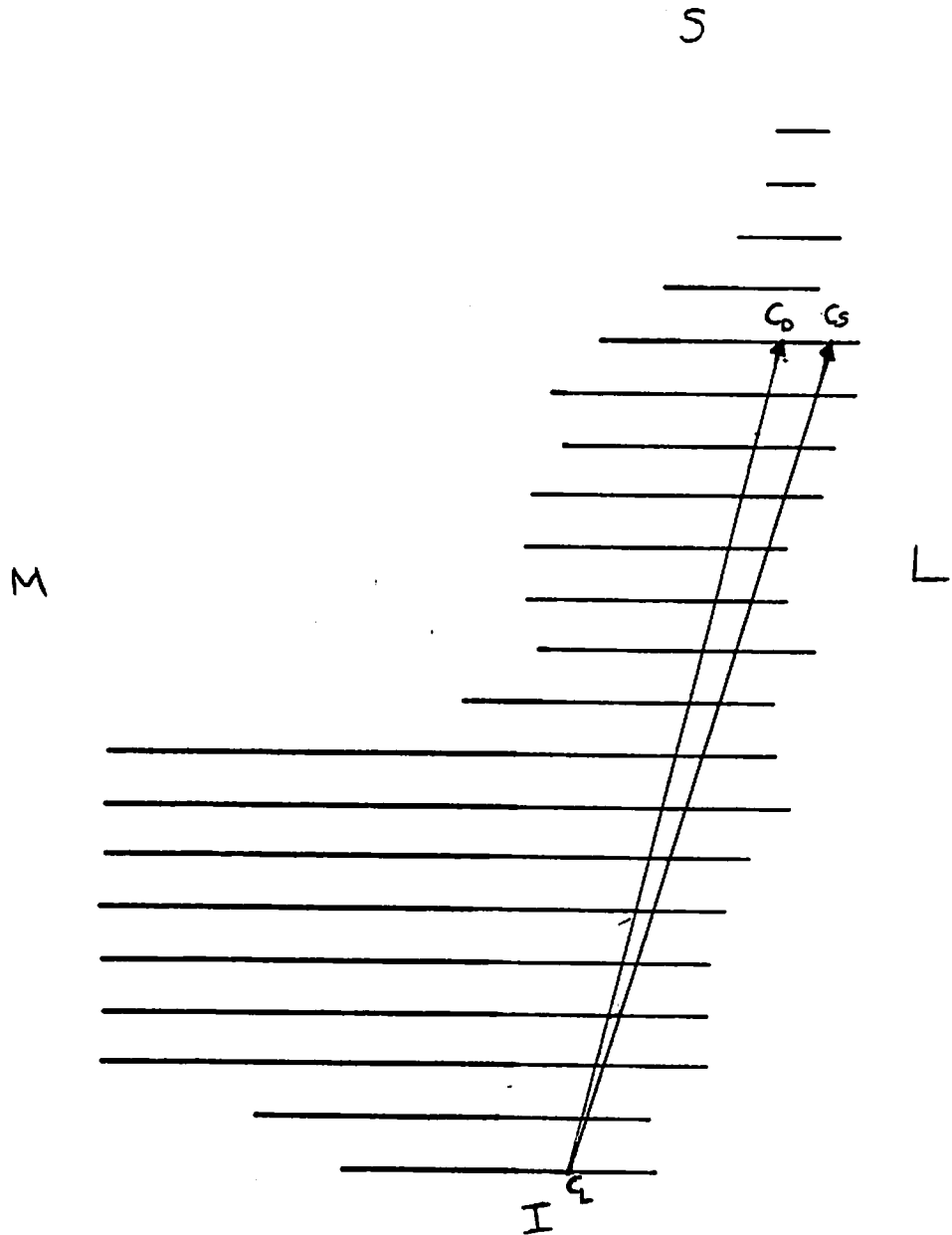**Figure 12.** Projection of the vectors of the temporalis muscle in the sagittal plane using the angulation R(90X), R(-90Y). Ca: centroid of the anterior temporalis; Cm: centroid of the medial temporalis; Cp: centroid of the posterior temporalis; Cl: centroid of the last section of the temporalis; S: superior; P: posterior; I: inferior; and A: anterior.
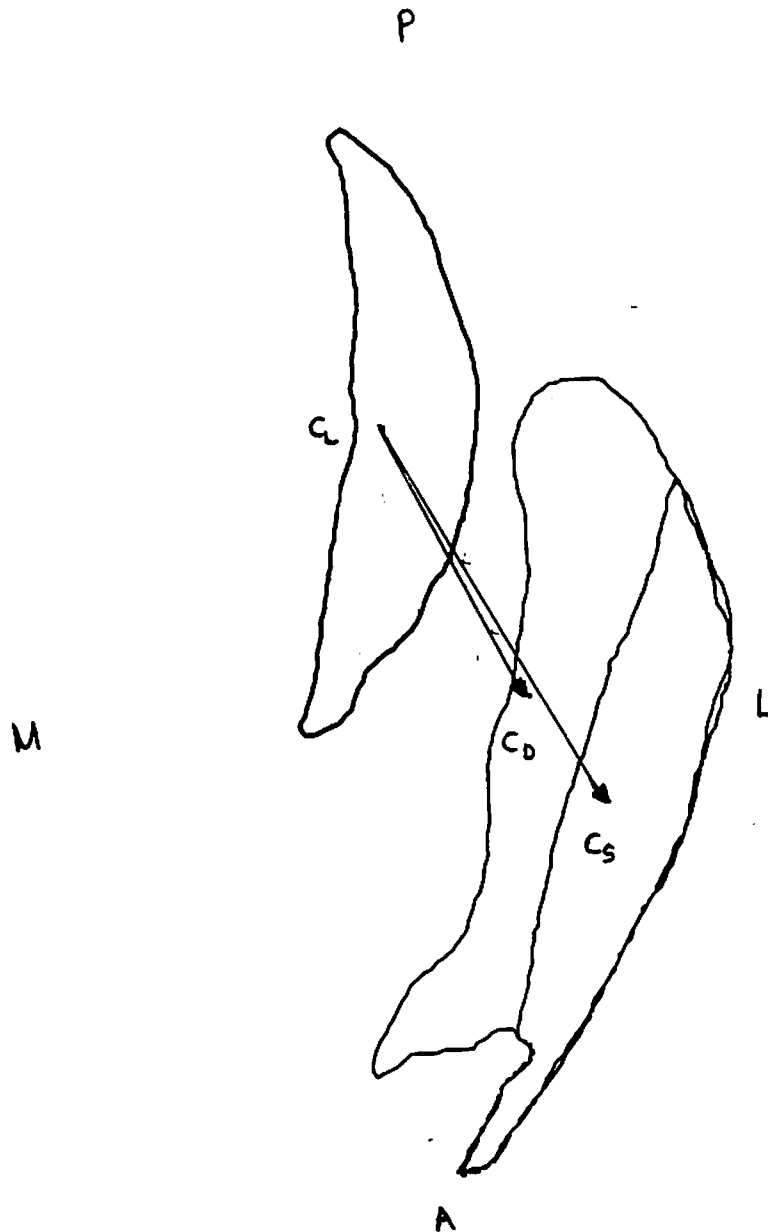
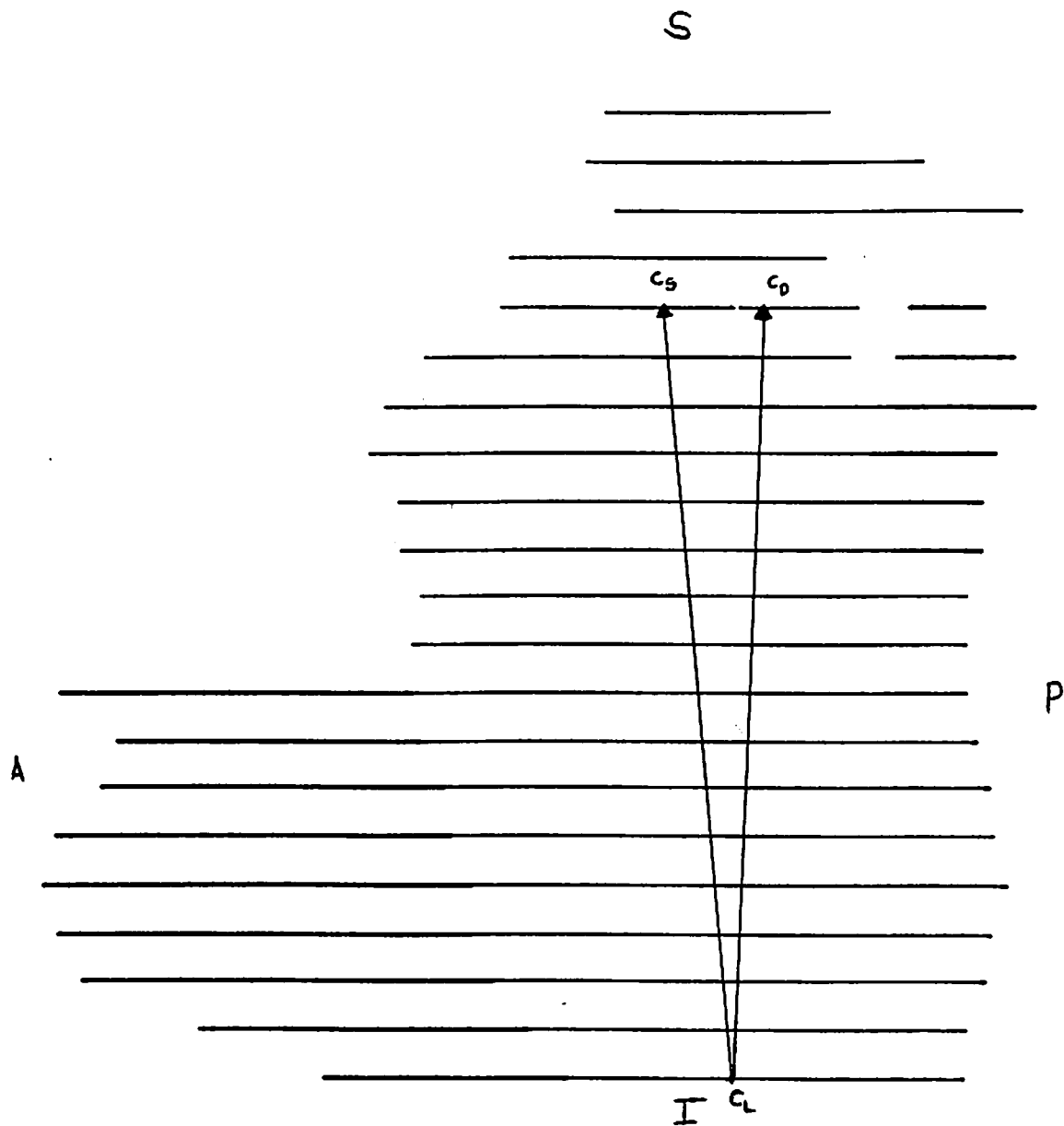**Figure 13.** Projection of the vectors of the masseter muscle in the horizontal plane using the angulation R(180X). Cs: centroid of the masseter (superior portion); Cd: centroid of the masseter (inferior portion); Cl: centroid of the last section of the masseter. M: medial; P: posterior; L: lateral; and A: anterior.
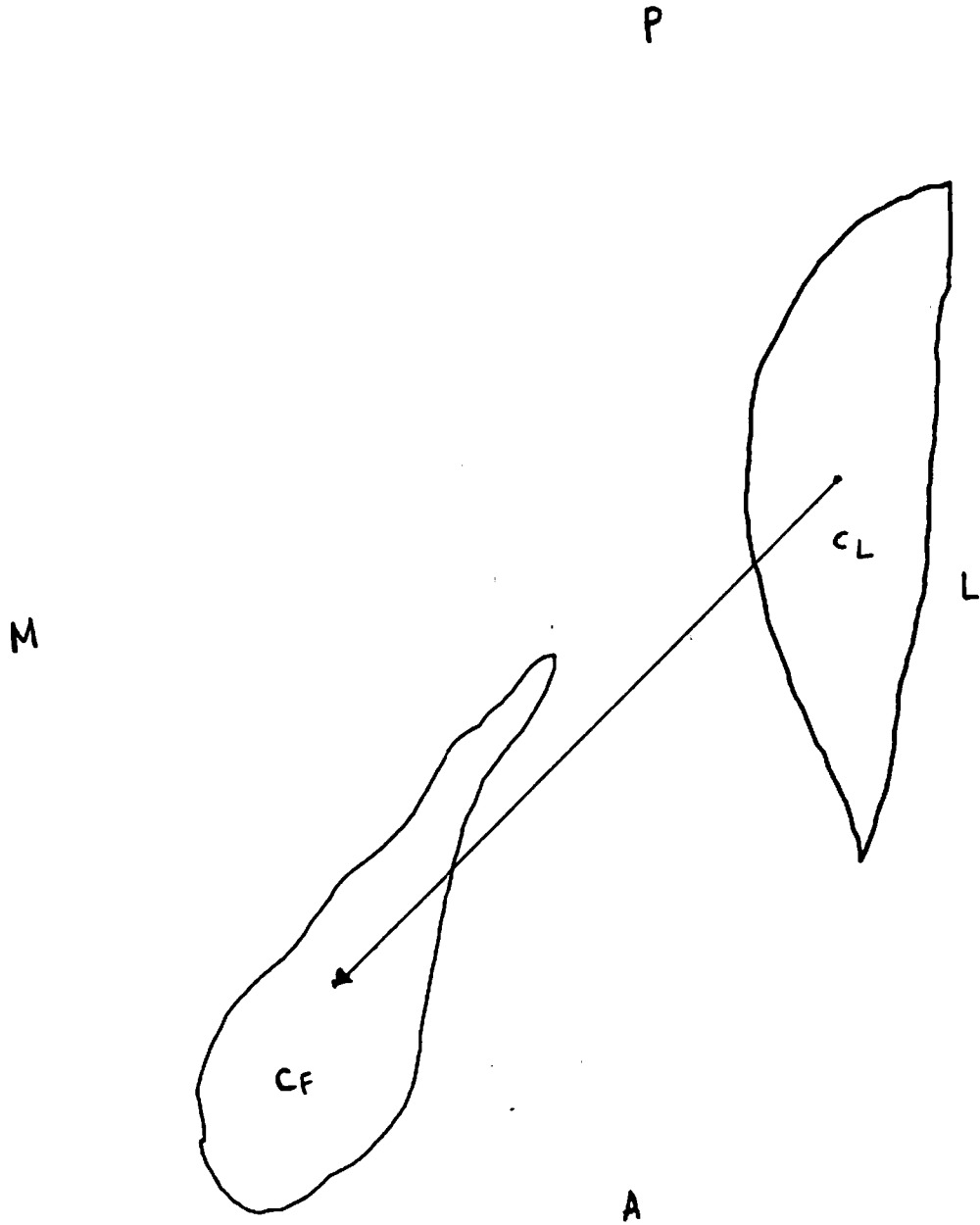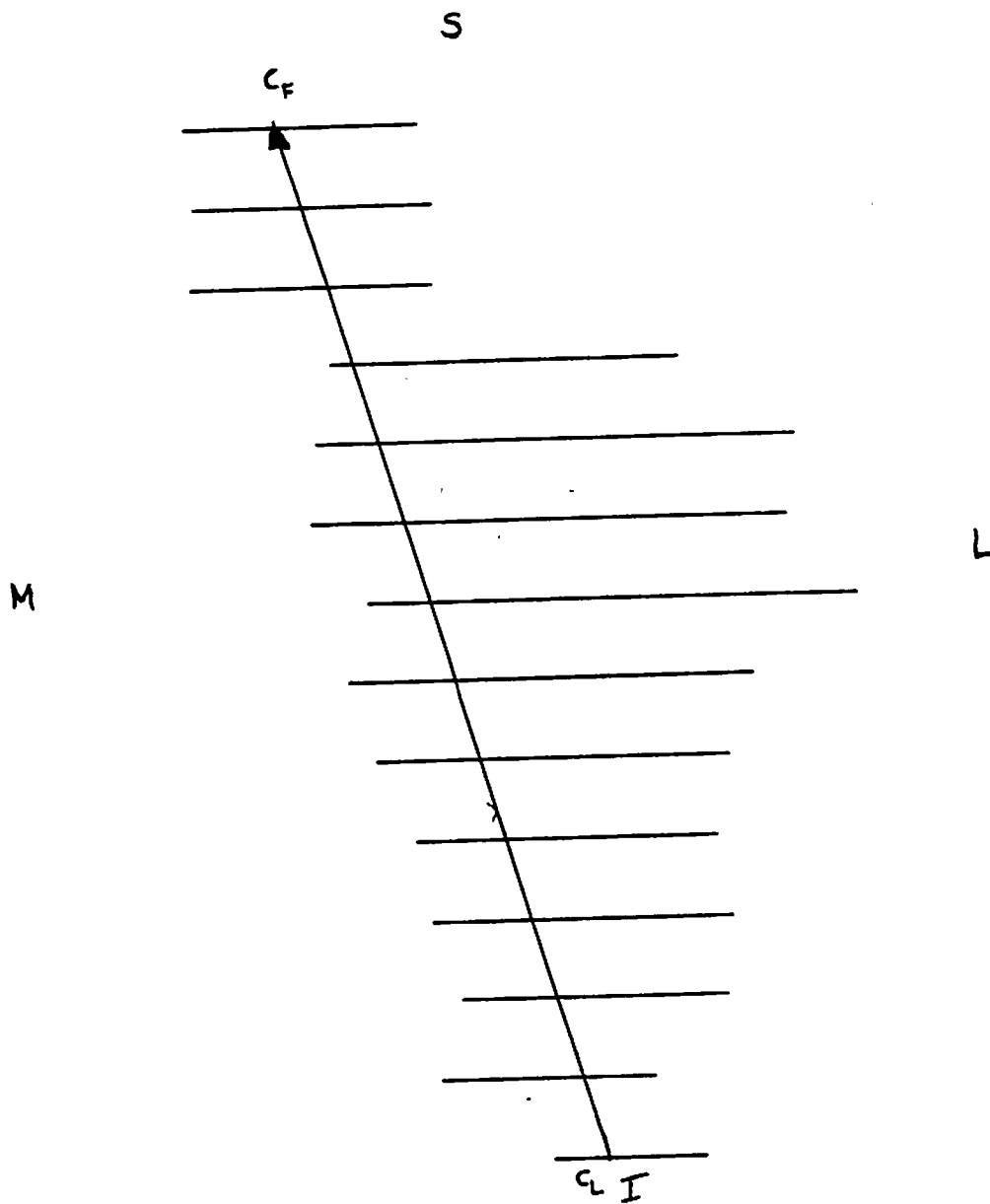
Figure 14. Projection of the vectors of the masseter muscle in the frontal plane using the angulation R(90X). Cs: centroid of the masseter (superior portion); Cd: centroid of the masseter (inferior portion); Cl: centroid of the last section of the masseter. M: medial; L: lateral; S: superior; and I: inferior .
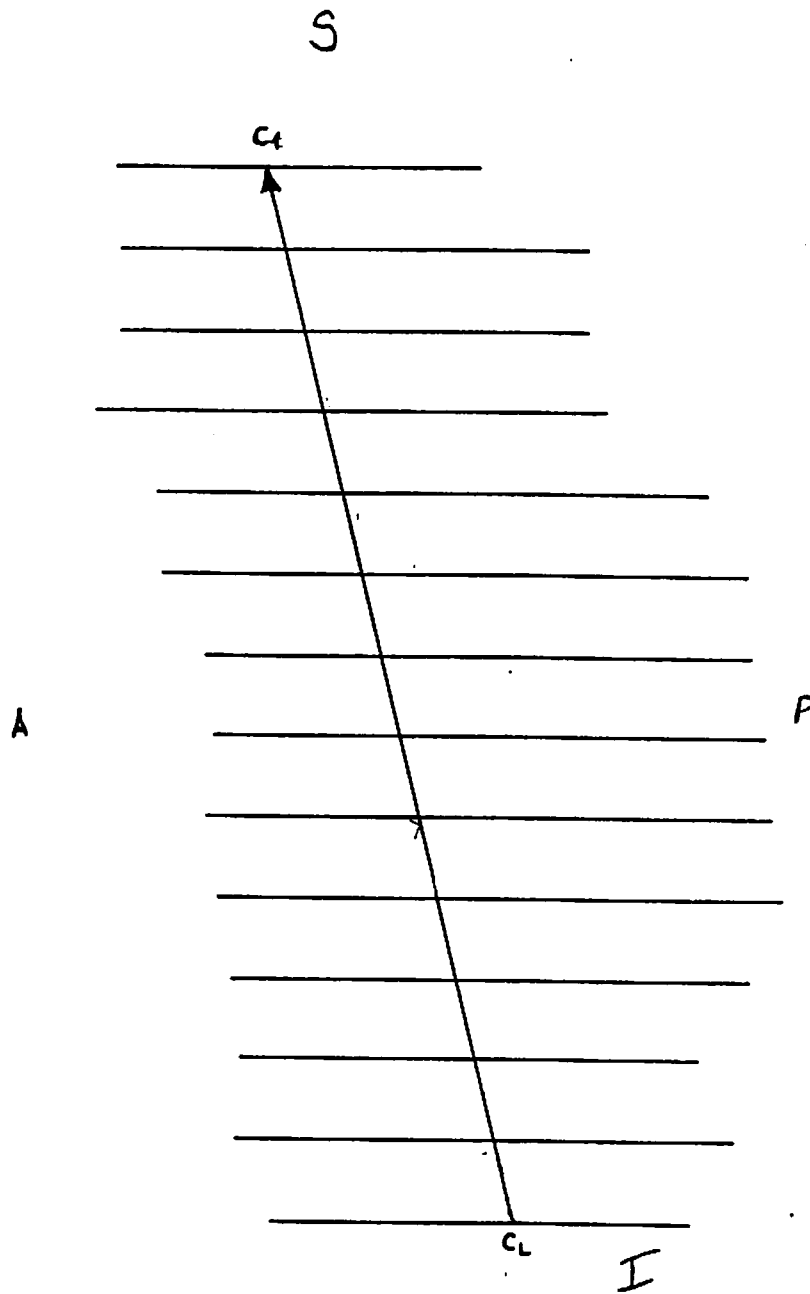
Figure 15. Projection of the vectors of the masseter muscle in the sagittal plane using the angulation R(90X), R(-90Y). Cs: centroid of the masseter (superior portion); Cd: centroid of the masseter (inferior portion); Cl: centroid of the last section of the masseter. P:posterior; A: anterior; S: superior; I: inferior.
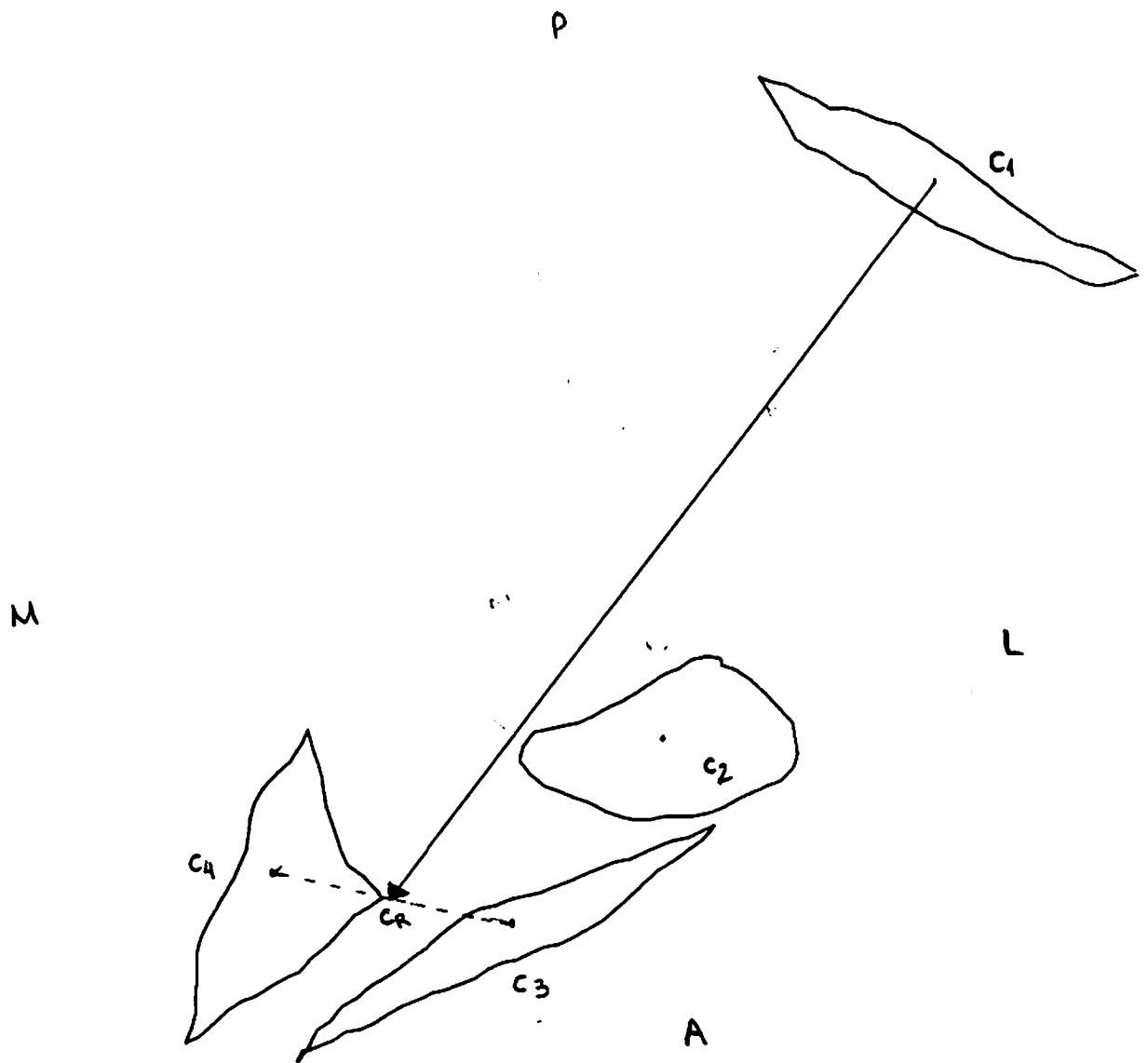
Figure 16. Projection of the vectors of the medial pterygoid muscle in the horizontal plane using the angulation R(180X). Cf: centroid of the first muscle section; Cl: centroid of the last muscle section. A: anterior; P: posterior; M: medial, L: lateral
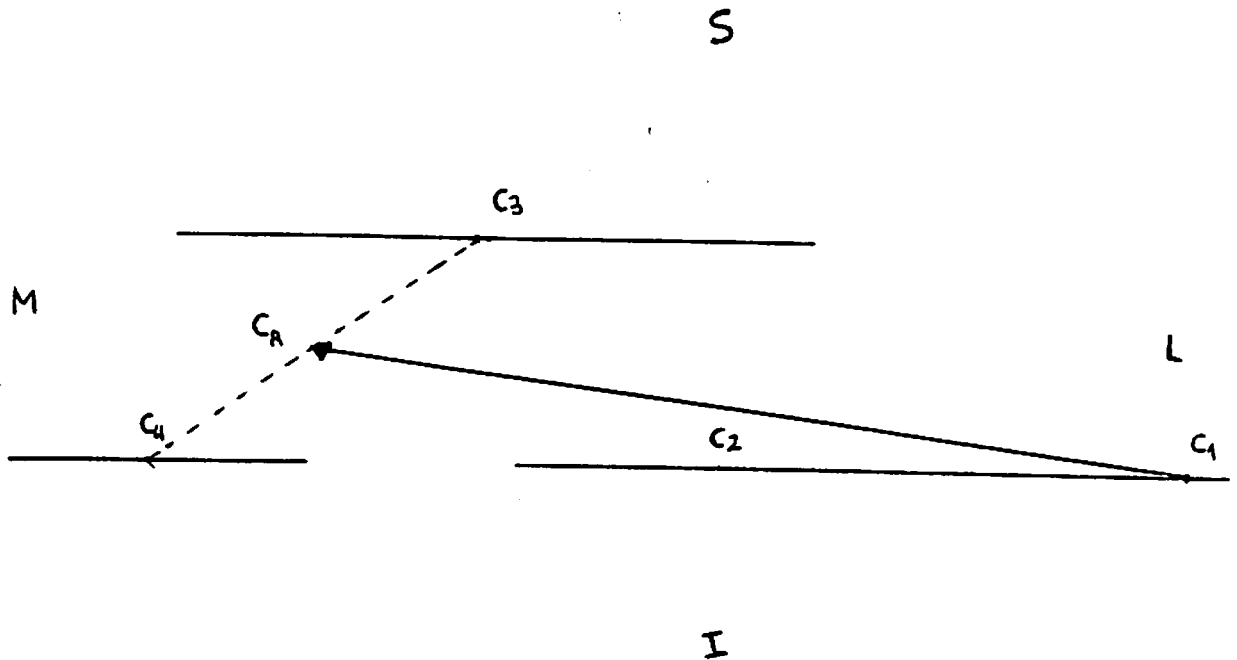
Figure 17. Projection of the vectors of the medial pterygoid muscle in the frontal plane using the angulation R(90X). Cf: centroid of the first muscle section; Cl: centroid of the last muscle section. M: medial; L: lateral; S: superior; and I: inferior.
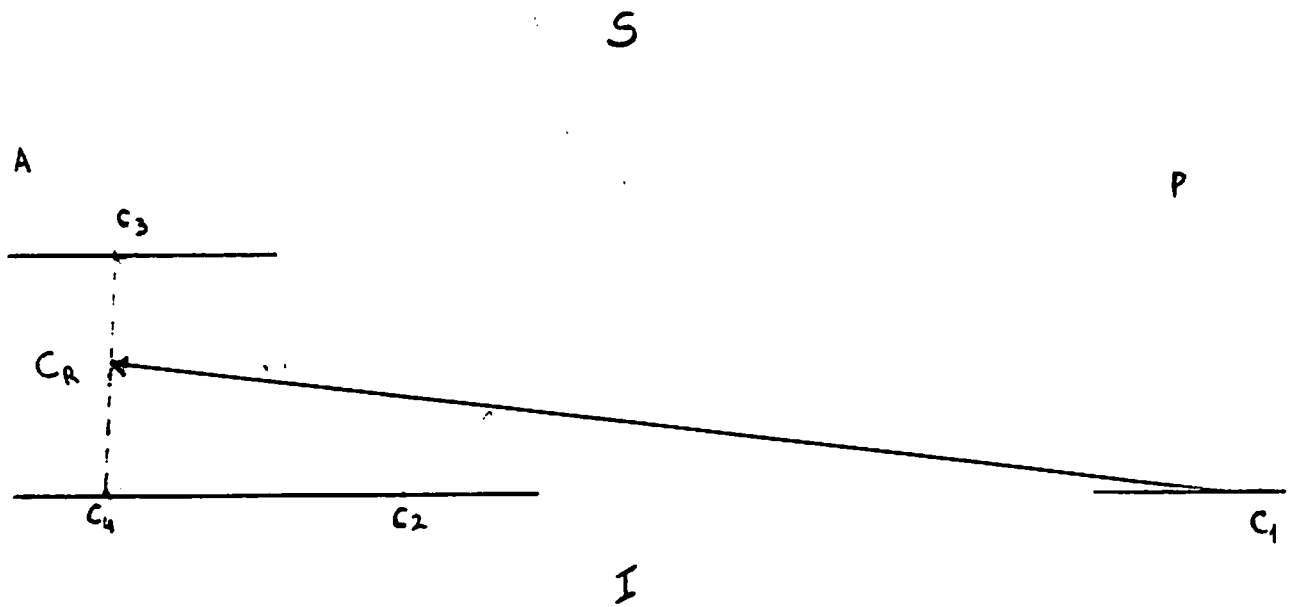
Figure 18. Projection of the vectors of the medial pterygoid muscle in the sagittal plane using the angulation R(90X), R(-90Y). Cf: centroid of the first muscle section; Cl: centroid of the last muscle section. A: anterior; P: posterior; S: superior; I: inferior.

Figure 19. Projection of the vectors of the lateral pterygoid muscle (superior head) in the horizontal plane using the angulation R(180X). C1: centroid of the first muscle section; C2: centroid of the second muscle section; C3: centroid of the third muscle section; C4: centroid of the fourth muscle section; and Cr: resultant centroid. A: anterior; P: posterior; M: medial, L: lateral.

Figure 20. Projection of the vectors of the lateral pterygoid muscle (superior head) in the frontal plane using the angulation R(90X). C1: centroid of the first muscle section; C2: centroid of the second muscle section; C3: centroid of the third muscle section; C4: centroid of the fourth muscle section; and Cr: resultant centroid. S: superior; I: inferior; M: medial, L: lateral.

Figure 21. Projection of the vectors of the lateral pterygoid muscle (superior head) in the sagittal plane using the angulation R(90X); R(-90Y). C1: centroid of the first muscle section; C2: centroid of the second muscle section; C3: centroid of the third muscle section; C4: centroid of the fourth muscle section; and Cr: resultant centroid. A: anterior; P: posterior; S: superior; I: inferior.

Figure 22. Projection of the vectors of the lateral pterygoid muscle (inferior head) in the horizontal plane using the angulation R(180X). C1: centroid of the first muscle section; Cl: centroid of the last muscle section; and Cr: resultant centroid. A: anterior; P: posterior; M: medial, L: lateral.
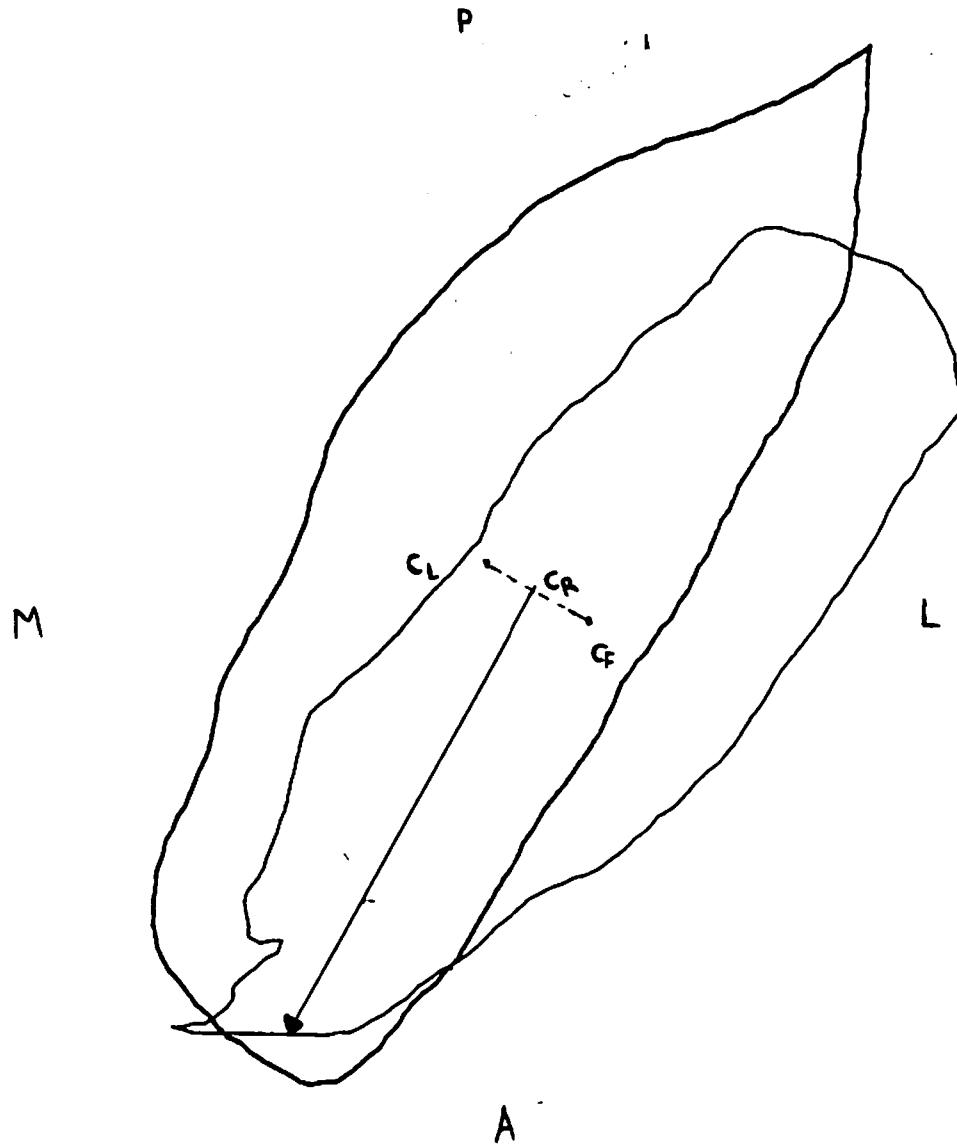
Figure 23. Projection of the vectors of the lateral pterygoid muscle (inferior head) in the frontal plane using the angulation R(90X). C1: centroid of the first muscle section; Cl: centroid of the last muscle section; and Cr: resultant centroid. S: superior; I: inferior; M: medial, L: lateral.
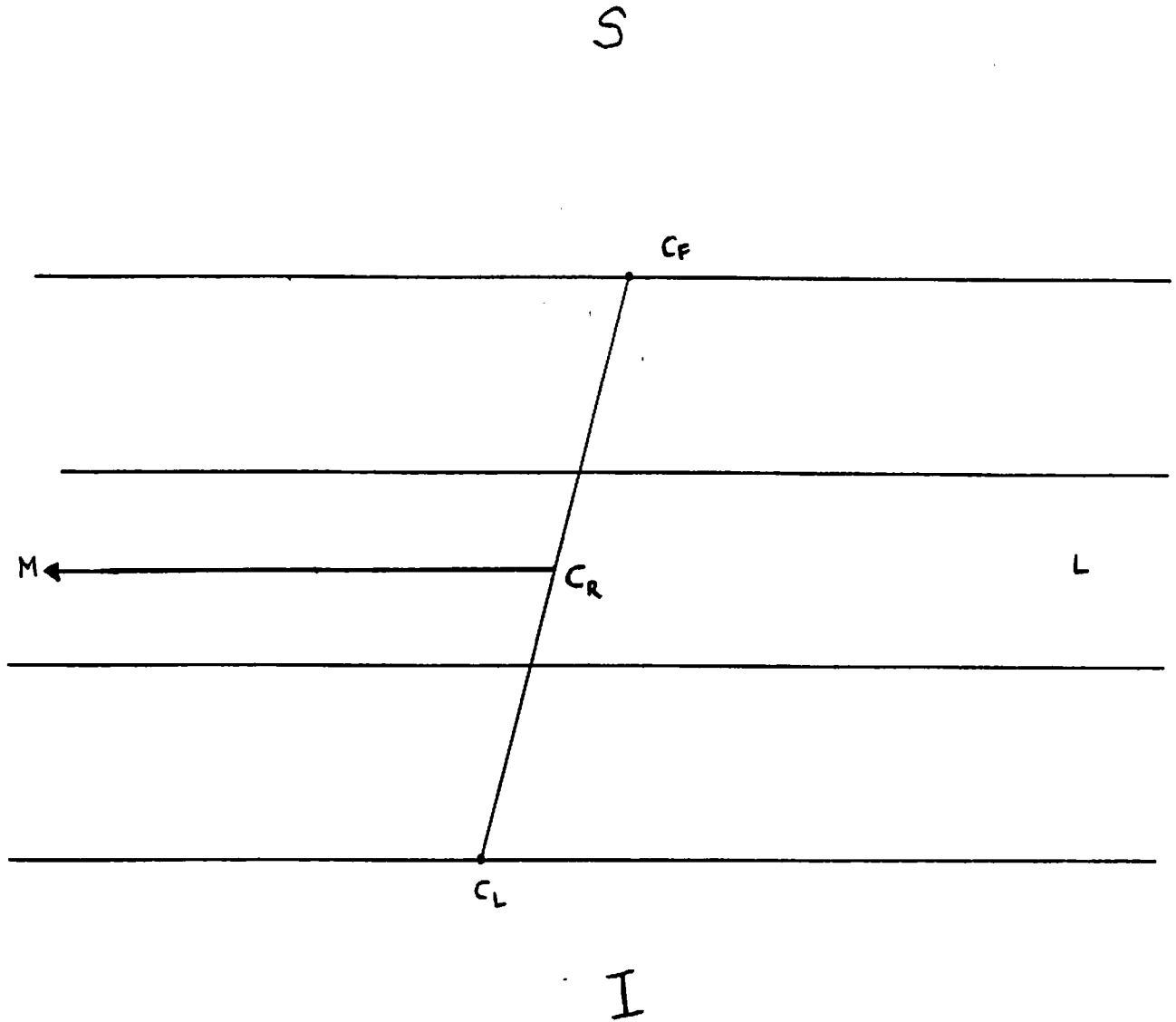
Figure 24. Projection of the vectors of the lateral pterygoid muscle (inferior head) in the sagittal plane using the angulation R(90X), R(-90Y). Cl: centroid of the first muscle section; Cl: centroid of the last muscle section; and Cr: resultant centroid. A: anterior; P: posterior; S: superior; I: inferior.
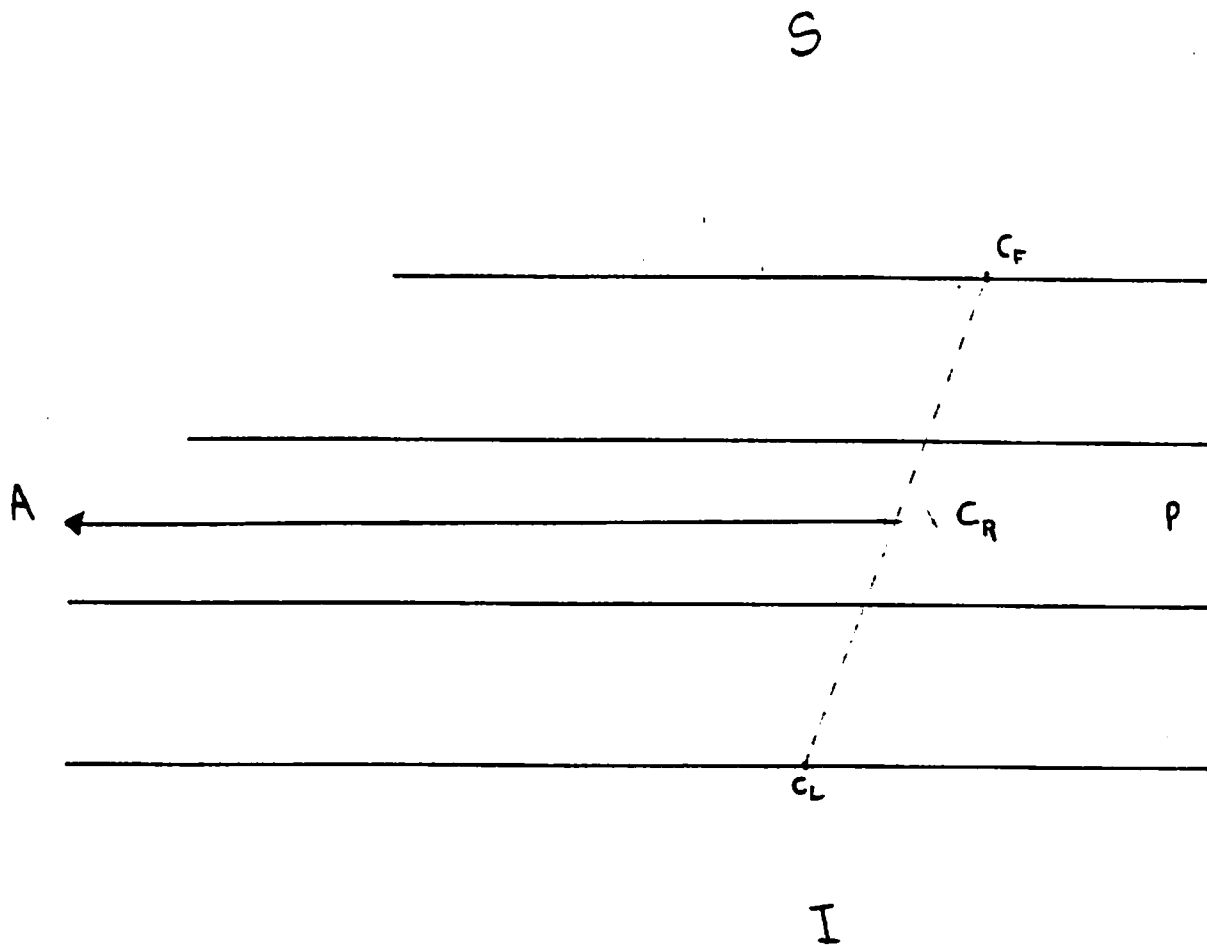
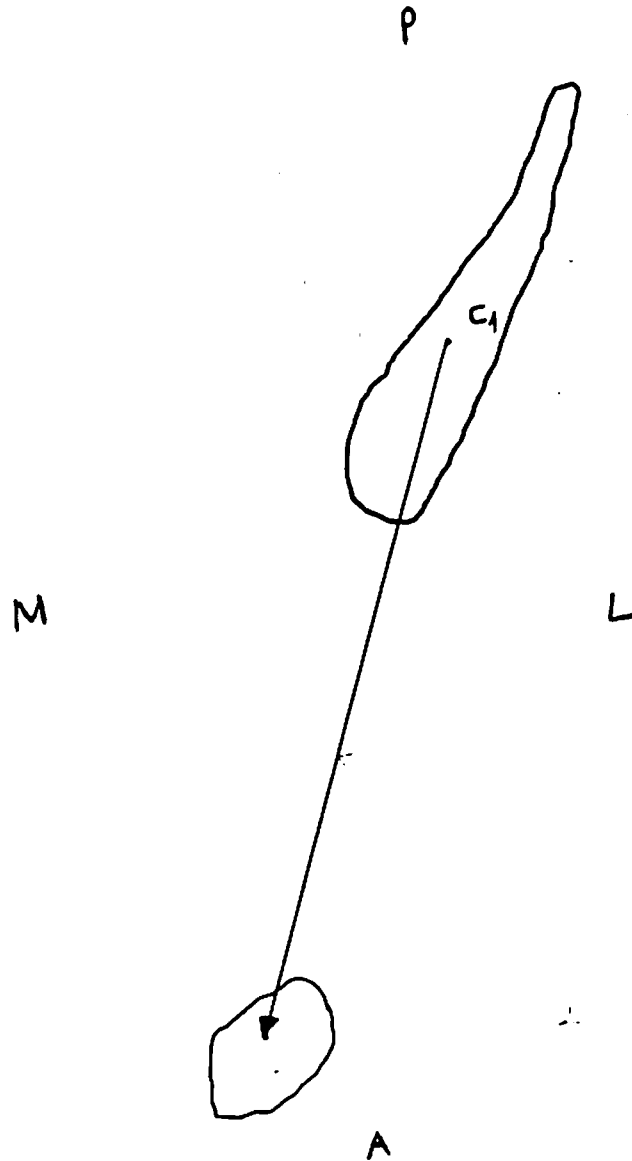**Figure 25.** Projection of the vectors of the digastric muscle (anterior belly) in the horizontal plane using the angulation R(180X). C1: centroid of the first muscle section; Cl: centroid of the last muscle section. A: anterior; P: posterior; M: medial, L: lateral.

Figure 26. Projection of the vectors of the digastric muscle (anterior belly) in the frontal plane using the angulation R(90X). C1: centroid of the first muscle section; Cl: centroid of the last muscle section. S: superior; I: inferior; M: medial, L: lateral.

Figure 27. Projection of the vectors of the digastric muscle (anterior belly) in the sagittal plane using the angulation R(90X), R(-90Y). C1: centroid of the first muscle section; Cl: centroid of the last muscle section. A: anterior; P: posterior; S: superior; I: inferior.

Figure 28. Projection of the vectors of the digastric muscle (posterior belly) in the horizontal plane using the angulation R(180X). C1: centroid of the first muscle section; Cl: centroid of the last muscle section. A: anterior; P: posterior; M: medial, L: lateral.
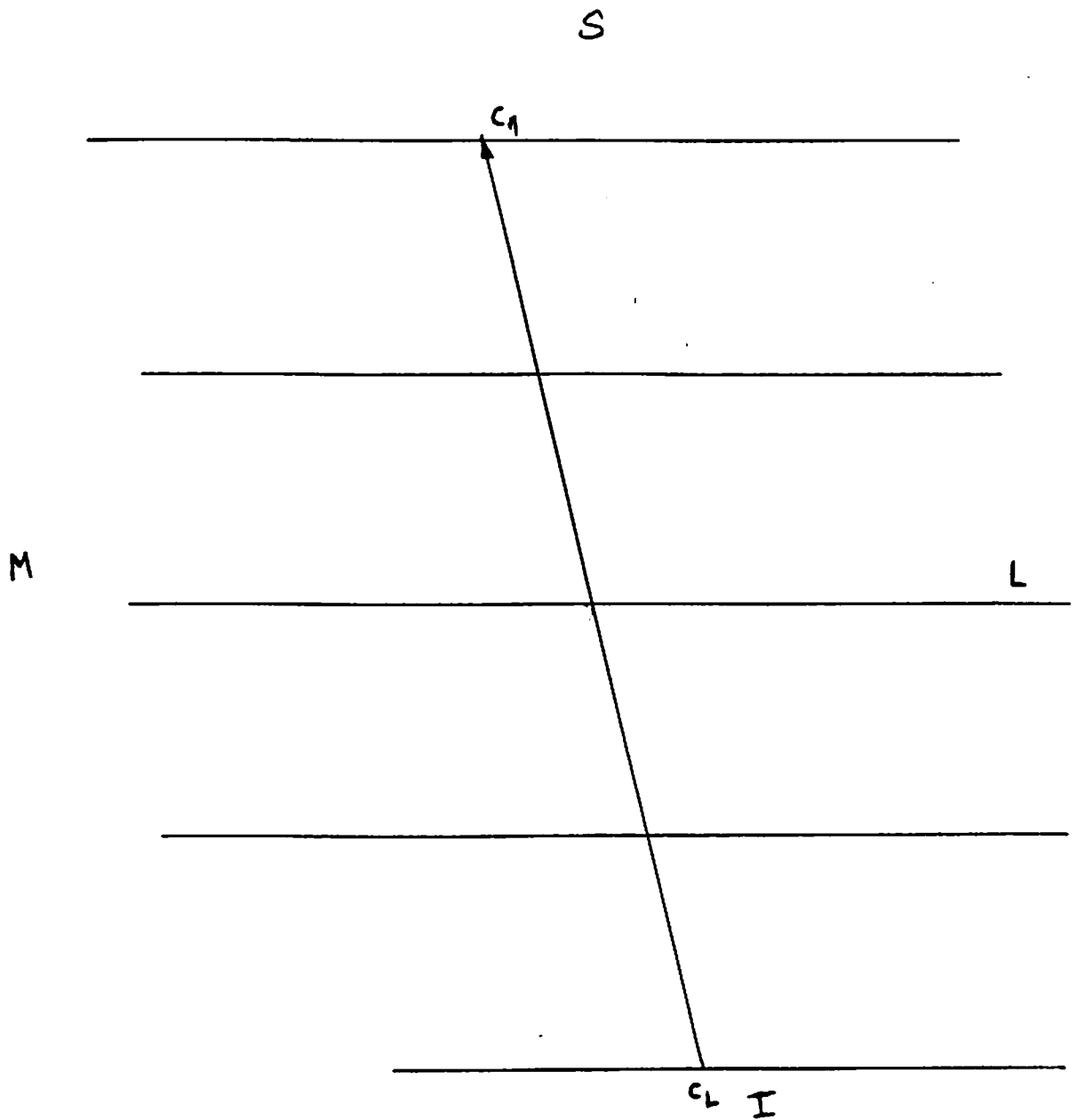
Figure 29. Projection of the vectors of the digastric muscle (posterior belly) in the frontal plane using the angulation R(90X). C1: centroid of the first muscle section; Cl: centroid of the last muscle section. S: superior; I: inferior; M: medial, L: lateral.
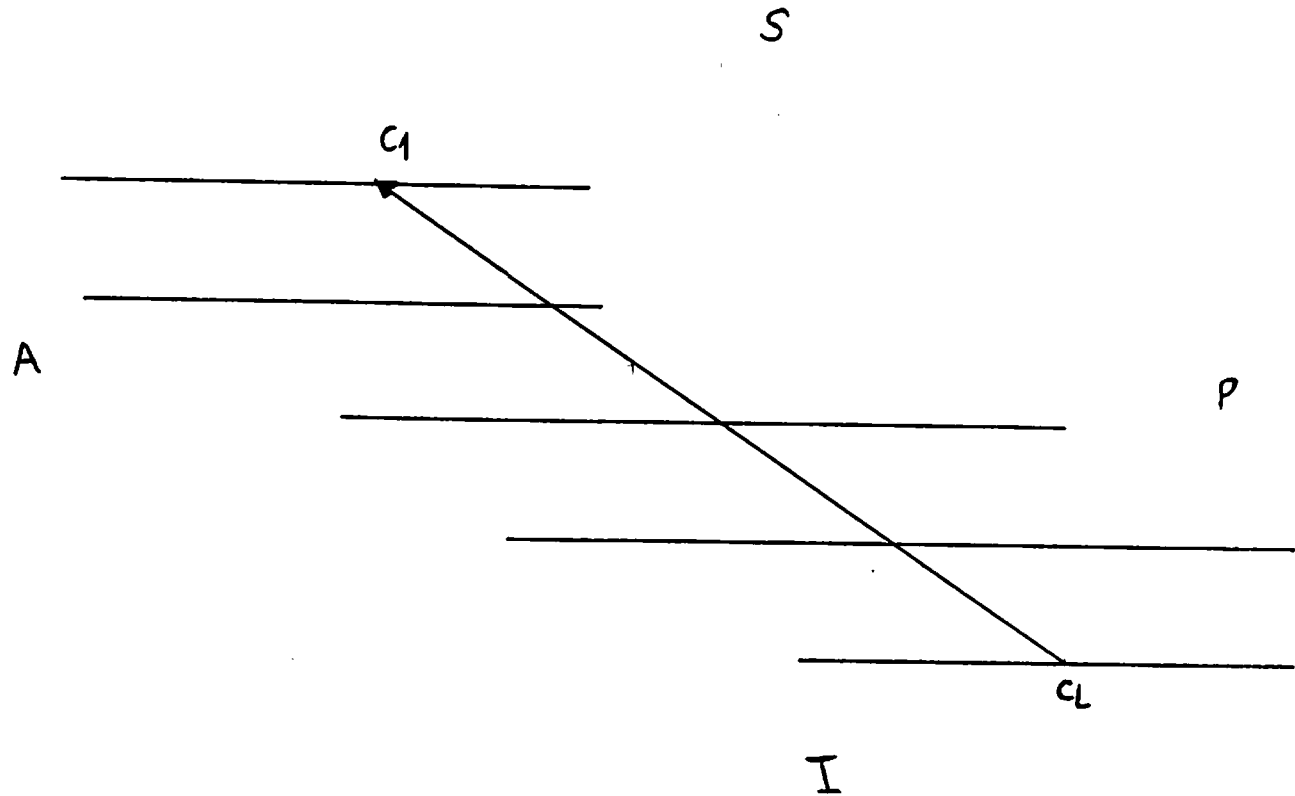
Figure 30. Projection of the vectors of the digastric muscle (posterior belly) in the sagittal plane using the angulation R(90X), R(-90Y). C1: centroid of the first muscle section; Cl: centroid of the last muscle section. A: anterior; P: posterior; S: superior; I: inferior.
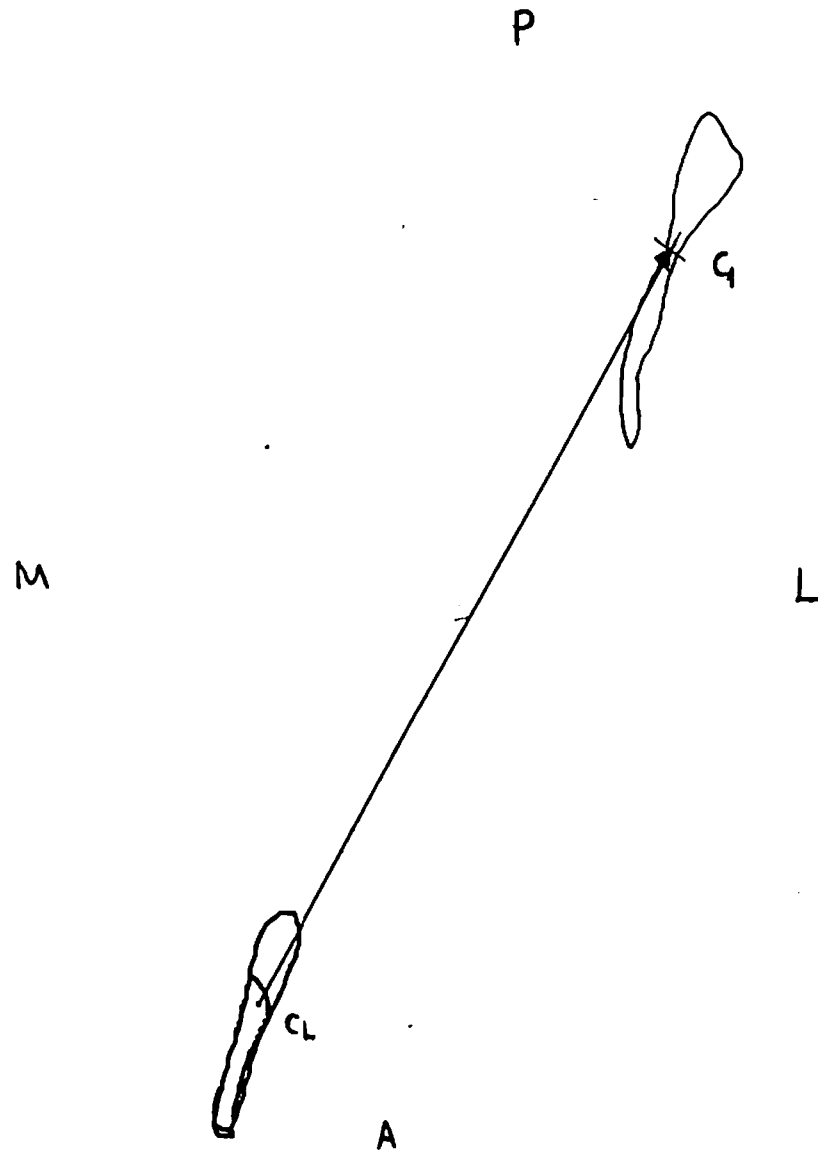
Figure 31. Projection of the vectors of the stylohyoid muscle in the horizontal plane using the angulation R(180X). C1: centroid of the first muscle section; Cl: centroid of the last muscle section. A: anterior; P: posterior; M: medial, L: lateral.
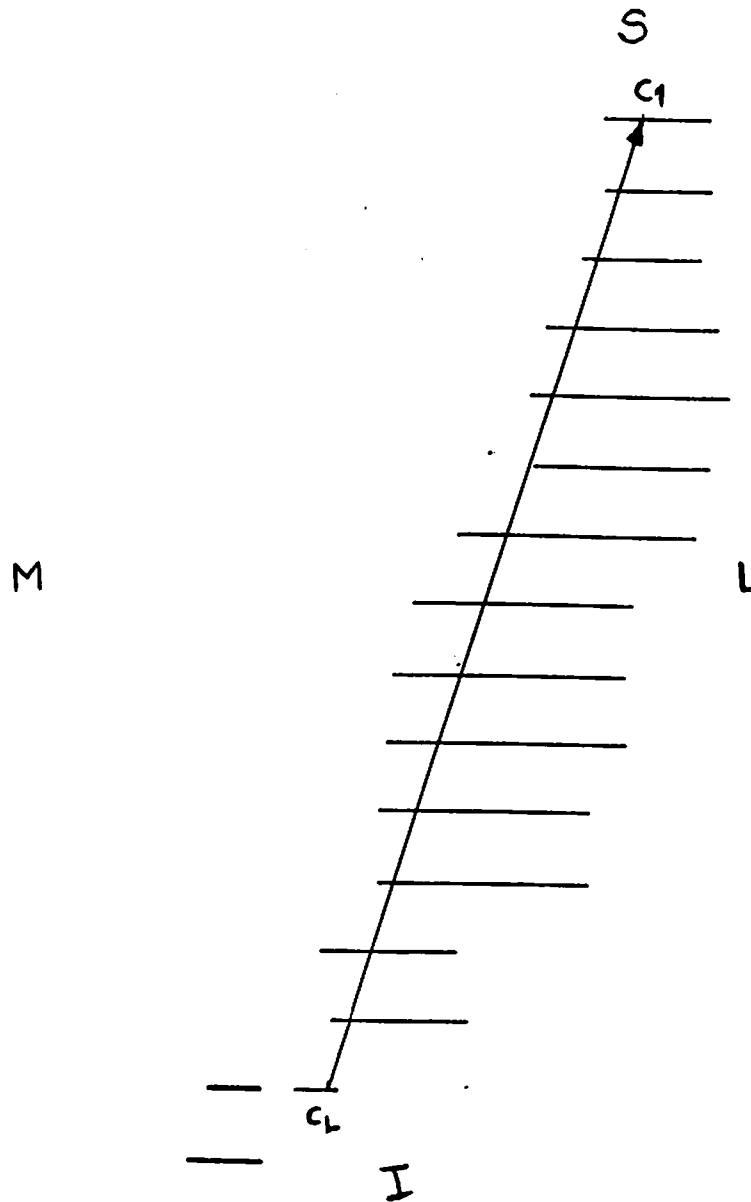
Figure 32. Projection of the vectors of the stylohyoid muscle in the frontal plane using the angulation R(90X). C1: centroid of the first muscle section; Cl: centroid of the last muscle section. S: superior; I: inferior ; M: medial, L: lateral.

Figure 33. Projection of the vectors of the stylohyoid muscle in the sagittal plane using the angulation R(90X), R(-90Y). Cl: centroid of the first muscle section; Cl: centroid of the last muscle section. A: anterior; P: posterior; S: superior; I: inferior.
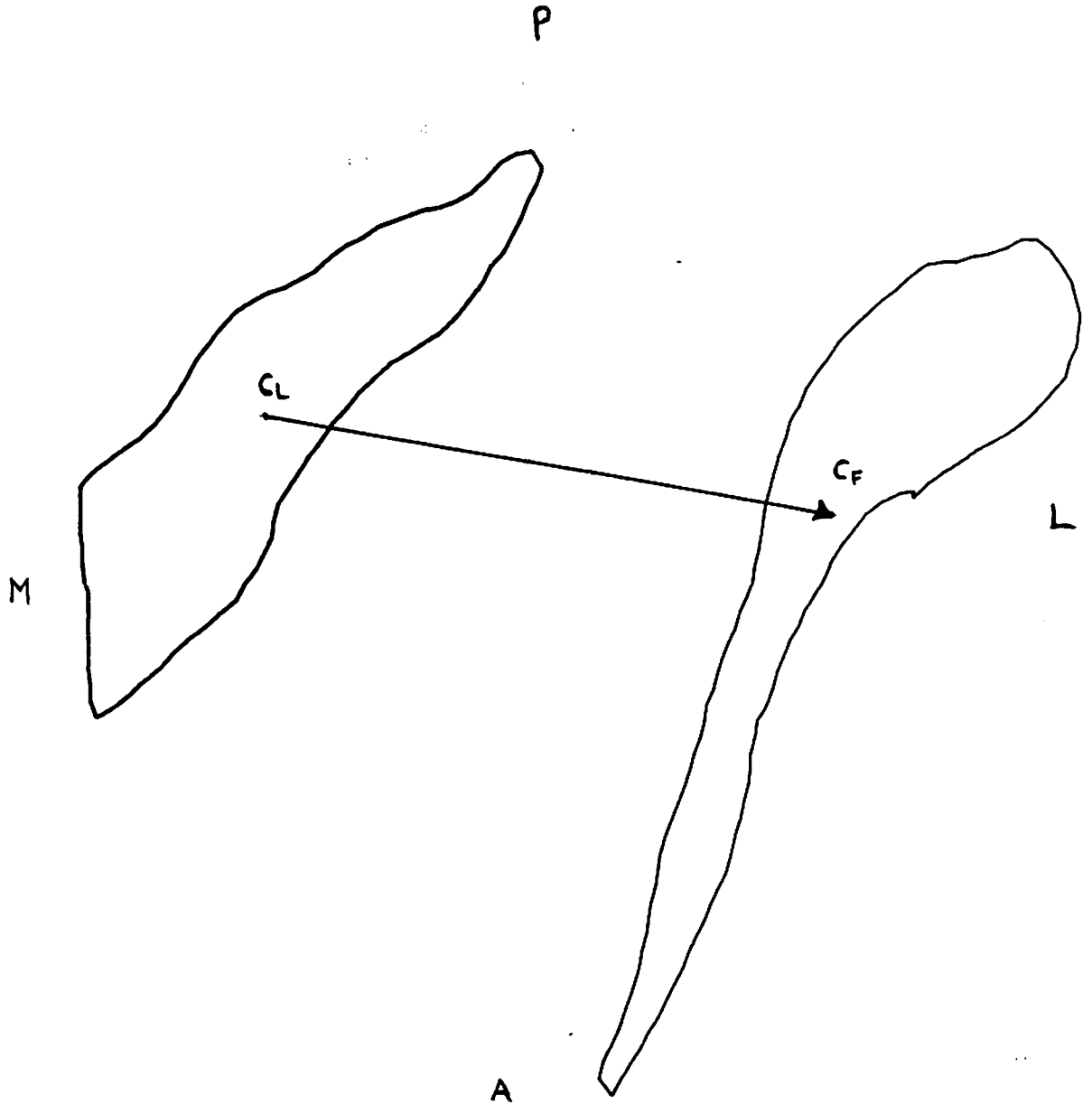
Figure 34. Projection of the vectors of the mylohyoid muscle in the horizontal plane using the angulation R(180X). Cl: centroid of the first muscle section; Cl: centroid of the last muscle section. A: anterior; P: posterior; M: medial, L: lateral.
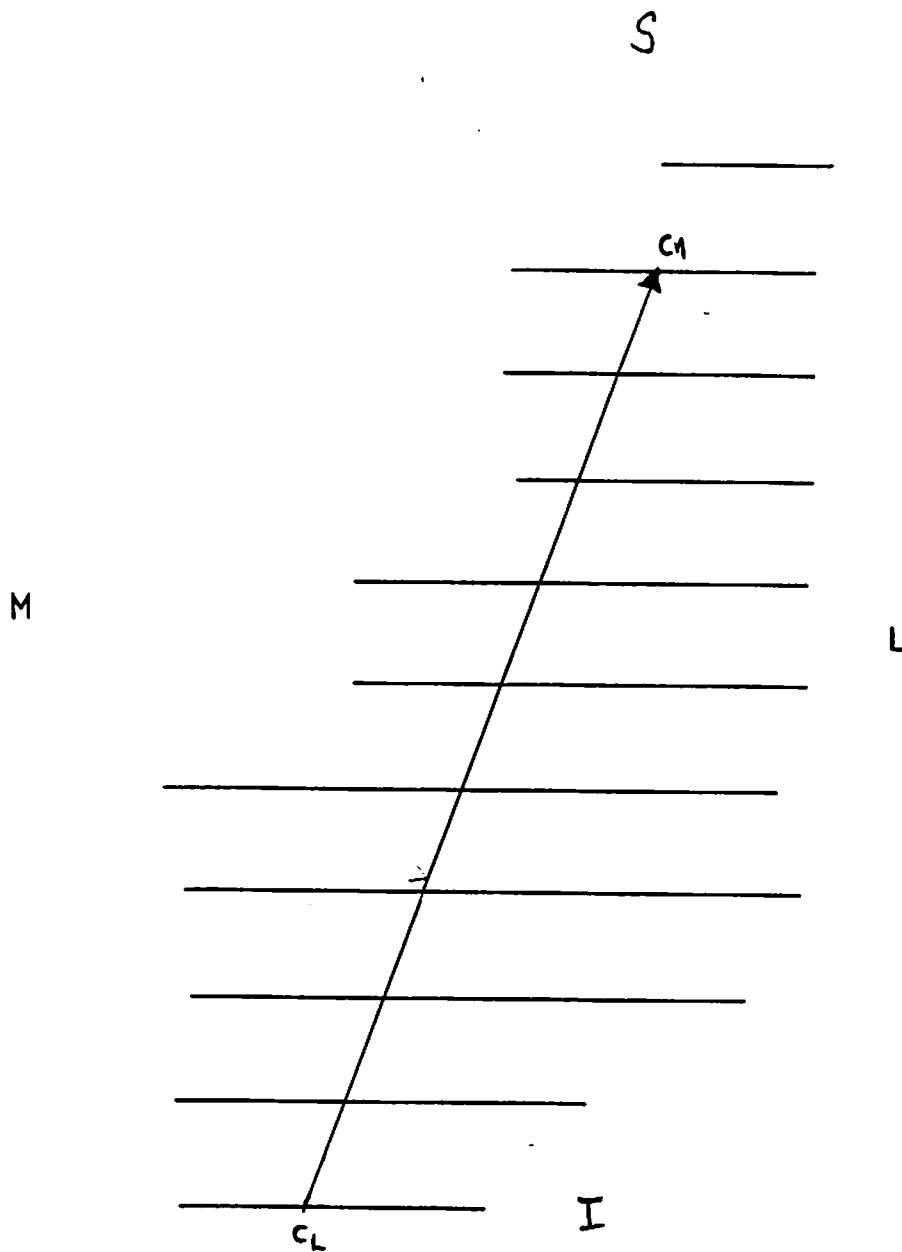
Figure 35. Projection of the vectors of the mylohyoid muscle in the frontal plane using the angulation R(90X). C1: centroid of the first muscle section; Cl: centroid of the last muscle section. S: superior; I: inferior; M: medial; L: lateral.
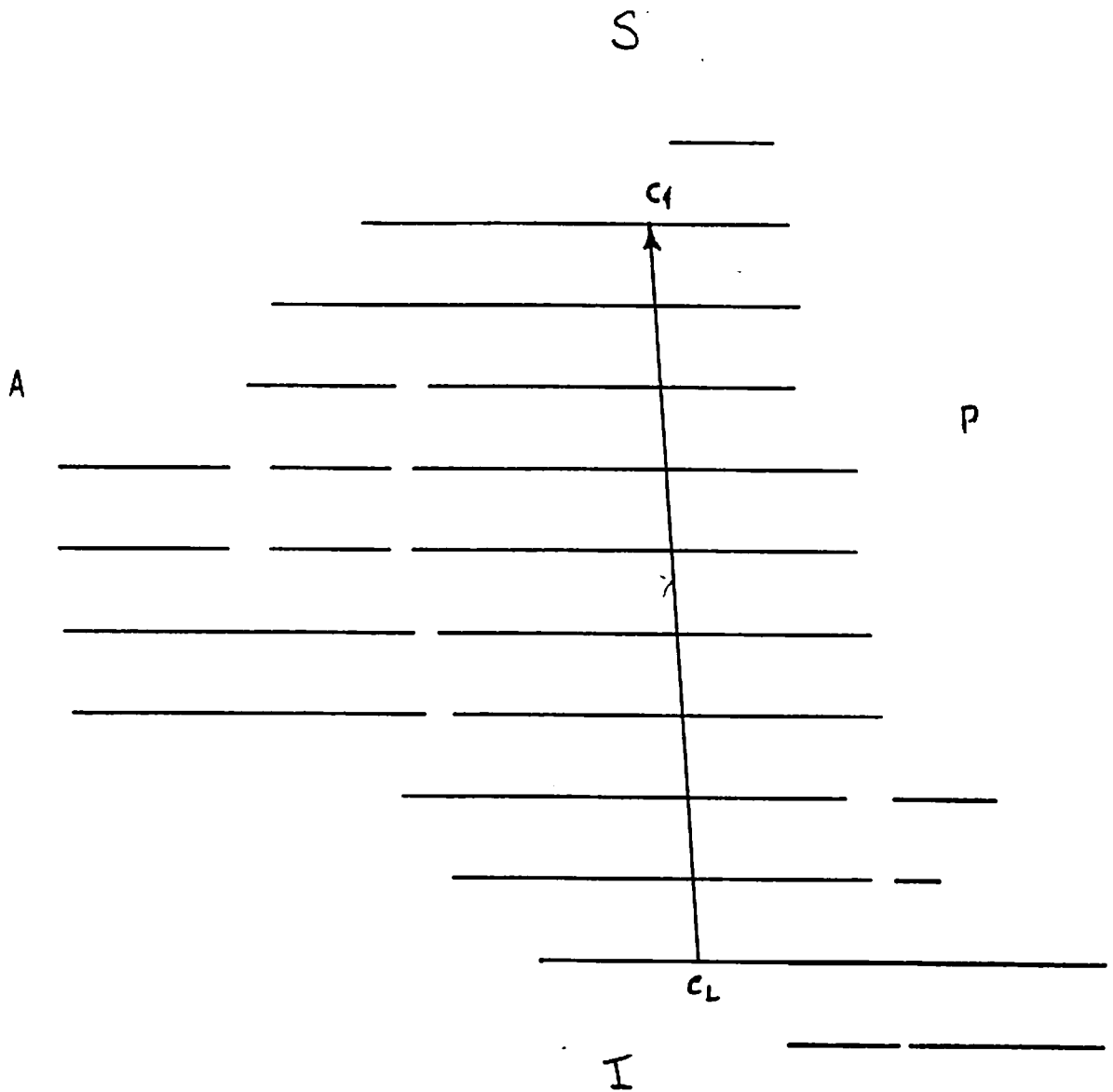
Figure 36. Projection of the vectors of the mylohyoid muscle in the sagittal plane using the angulation R(90X), R(-90Y). C1: centroid of the first muscle section; Cl: centroid of the last muscle section. A: anterior; P: posterior; S: superior; I: inferior.
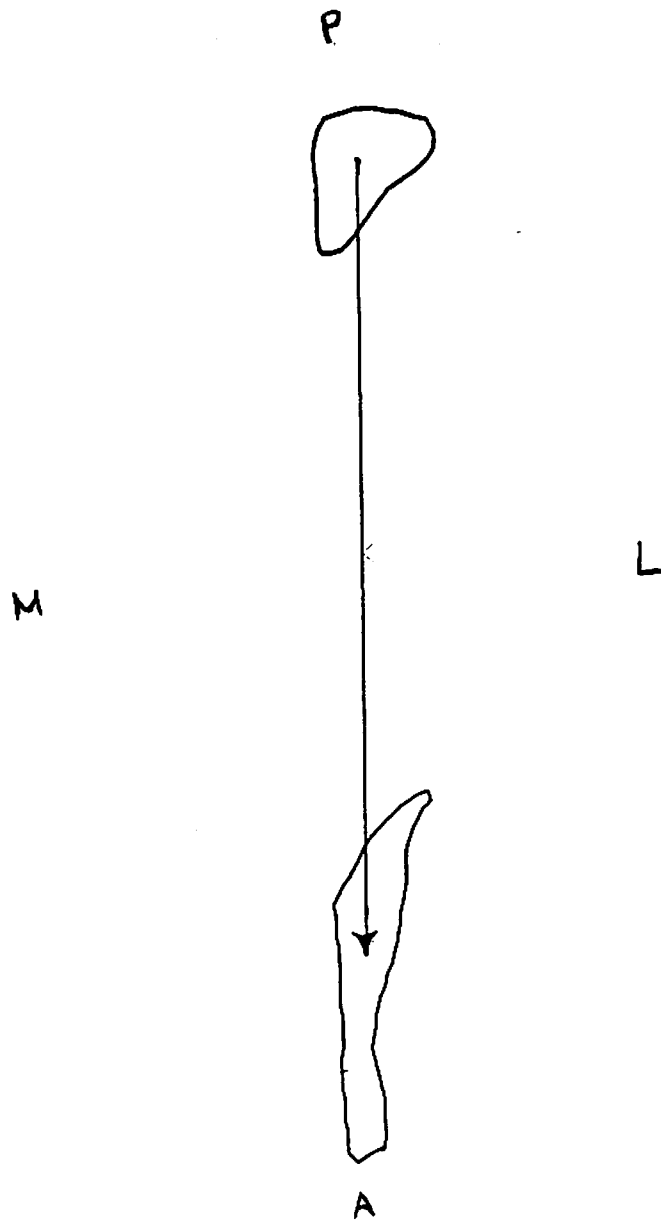
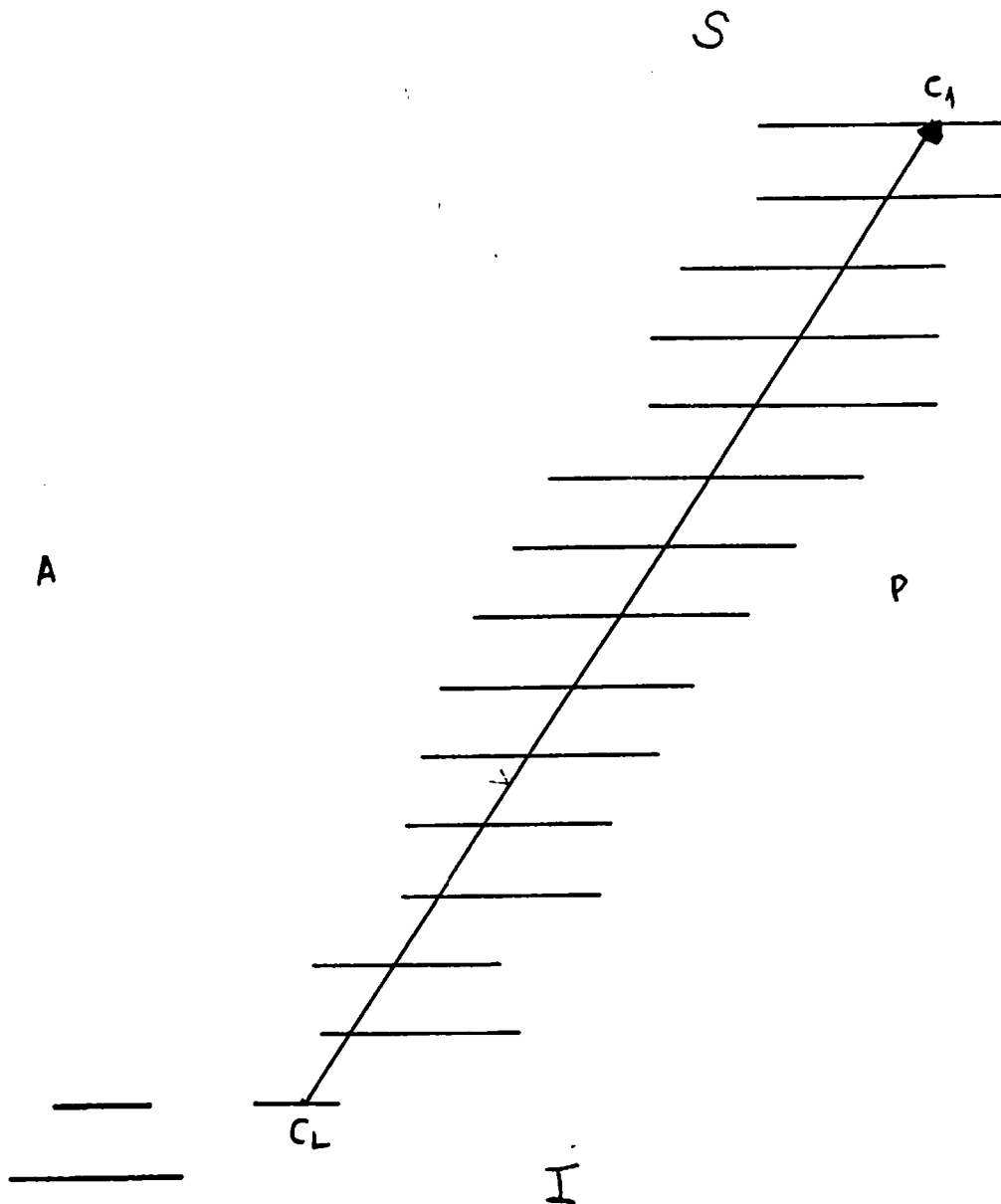**Figure 37.** Projection of the vectors of the geniohyoid muscle in the horizontal plane using the angulation R(180X). C1: centroid of the first muscle section; Cl: centroid of the last muscle section. A: anterior; P: posterior; M: medial, L: lateral.
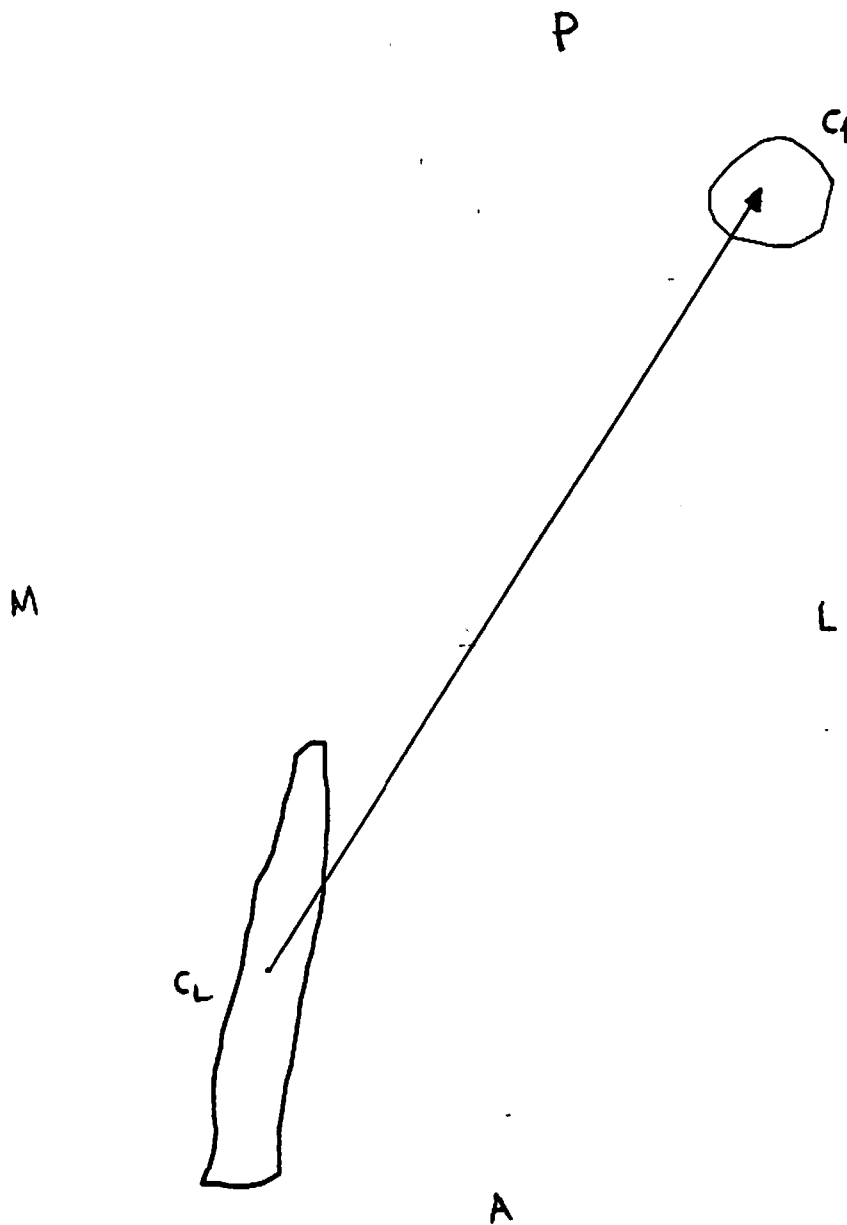
S

C_1

M   L

C_L I
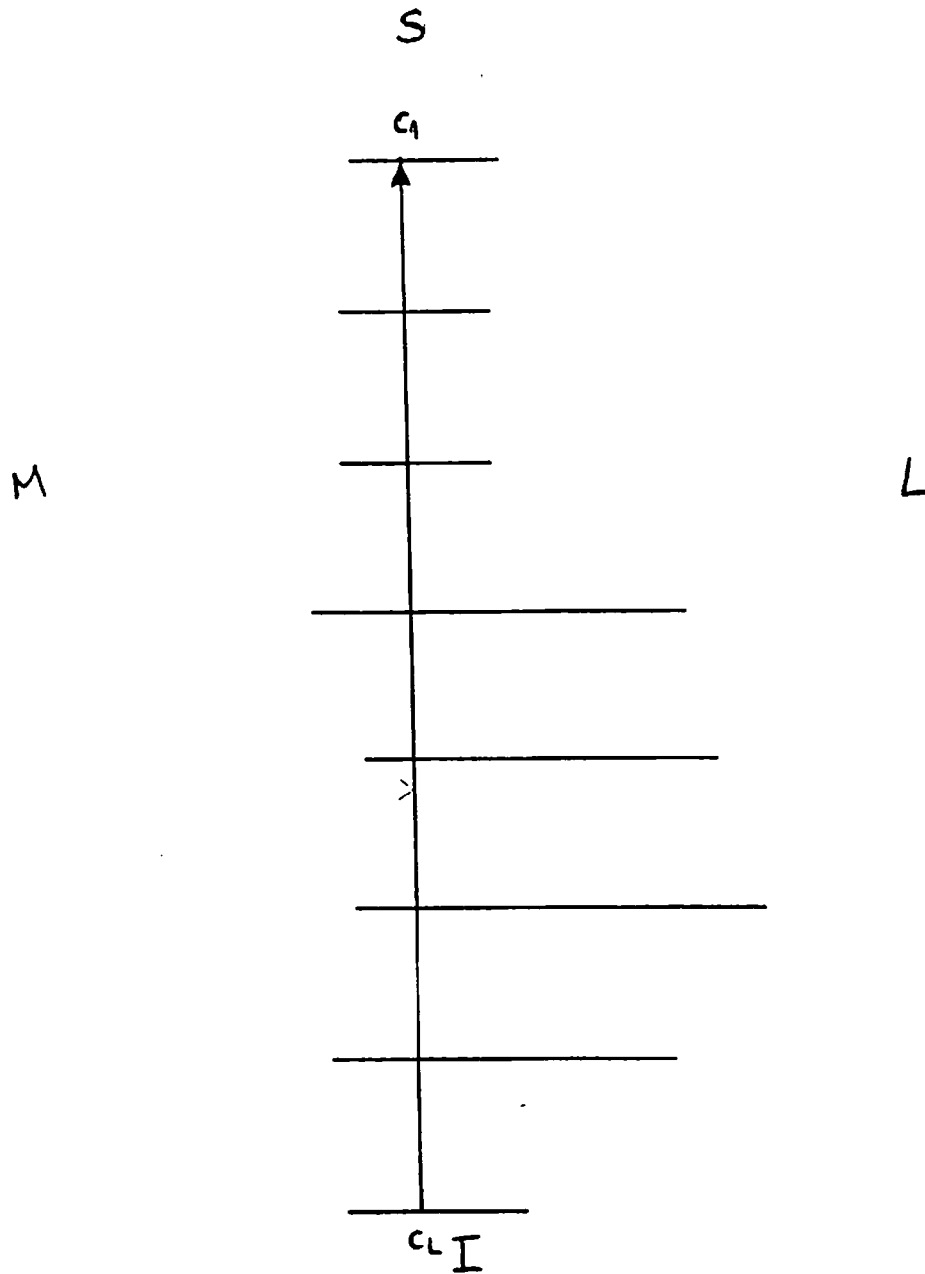
Figure 38. Projection of the vectors of the geniohyoid muscle in the frontal plane using the angulation R(90X). C1: centroid of the first muscle section; Cl: centroid of the last muscle section. S: superior; I: inferior; M: medial, L: lateral.
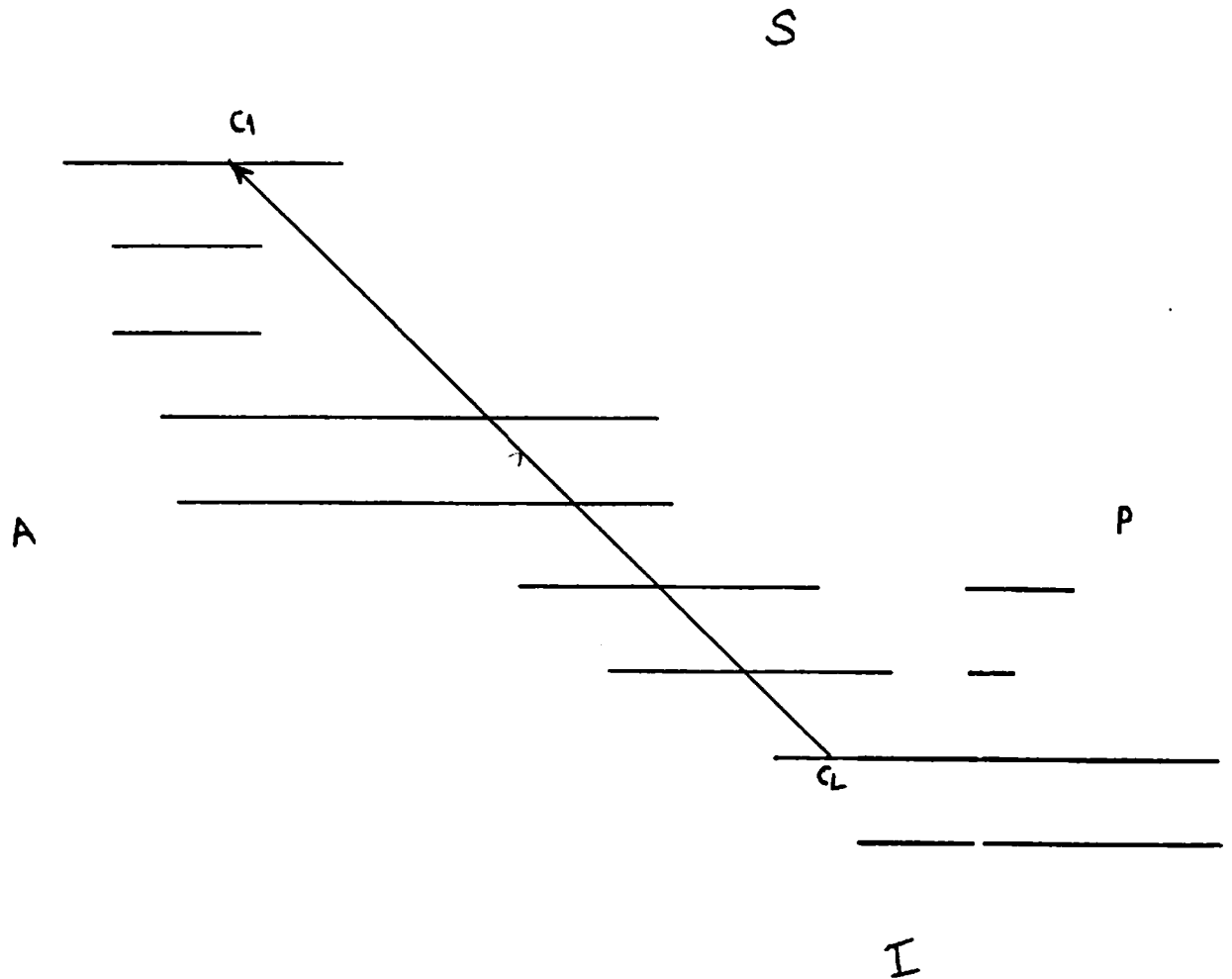
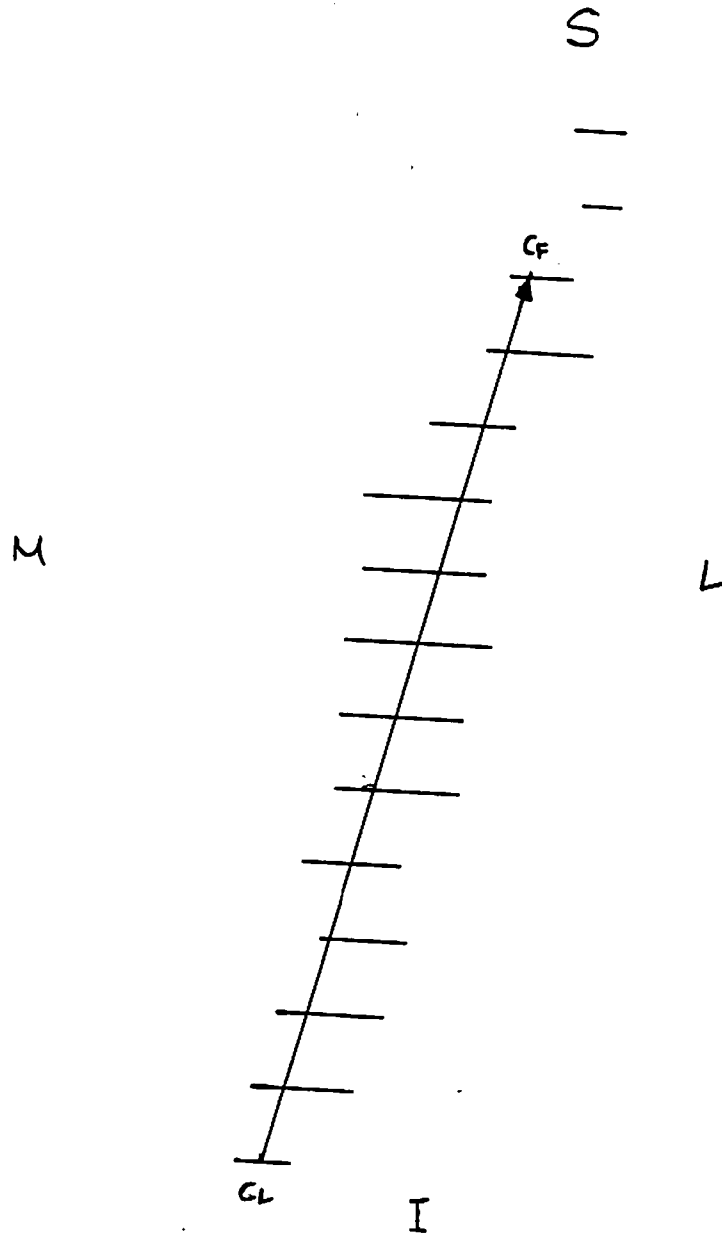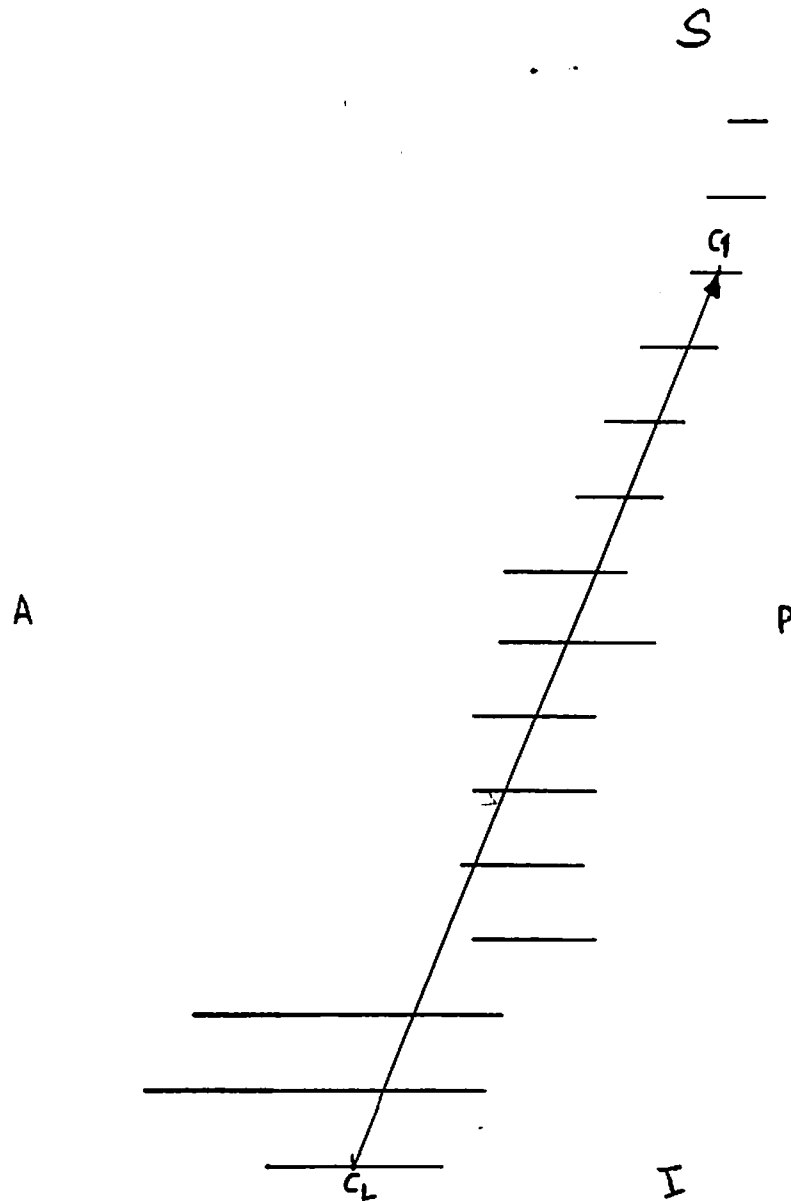**Figure 39.** Projection of the vectors of the geniohyoid muscle in the sagittal plane using the angulation R(90X), R(-90Y). C1: centroid of the first muscle section; Cl: centroid of the last muscle section. A: anterior; P: posterior; S: superior; I: inferior.

DISCUSSION

There are a number of variables which make it very difficult to determine the current accuracy of calculations of temporomandibular joint forces. First, the relationship between relative electromyographic activity of jaw muscles and relative muscle force during isometric bites has not been firmly established. Second, the range of possible directions of jaw muscle forces has not been experimentally measured. Therefore, the degree of correspondence between origin and insertion of jaw muscles and the direction of the force produced remains to be tested, particularly in those large complex muscles showing different levels of activity during different functions (Ahlgren et al, 1973; Carlsoo, 1952; Ingervall, Ridell and Thilander, 1979; Moller, 1966). Without knowing the directions of the muscle forces precisely, the lengths of the moment arms cannot be precisely known.

Accuracy

According to Throckmorton (1985), the major effect of muscle force direction is its influence on the length of the muscle force moment arm. The calculation of joint reaction force is much more sensitive to errors in muscle force direction than to muscle force magnitude. An error of 1° in muscle force could produce a 2° in the joint reaction force direction.

One could argue that it would be impossible to calculate the muscle lines of action (vectors), because these lines might vary with the different functions in which the muscle is involved. Nevertheless, when a muscle is working in its maximum force (e.g. clenching),

the muscle line of action (vector) could be considered almost as a single line, being closely related to the muscle general fiber direction (Koolstra, 1988).

Until the present time, there is little experimental evidence that magnitude, direction, and moment arm length of the muscle forces can be determined to the accuracy mentioned above. However, the data shown in this proposed model have proven to be highly reliable and precise enough not only in terms of measurement of vector length (+- 1mm), but also in terms of vector angulation (+- 1 degree). Besides this study, just one MRI study by Koolstra *et al.* (1990) measured the accuracy of its measurements. He determined the accuracy of his model by calculating the difference between the muscle action lines readings of the frontal sectional images (FSI) by the transversal section images (TSI). He found a reproducibility of about 5° which is not considered accurate enough according to Throckmorton (1985).

Comparison with Previous Models

The angulations found for the the masticatory muscles on the frontal and sagittal planes are compatible with previously reported studies (Table 5 and 6). Unfortunately, no single study has been reported for both the inframandibular muscle vector angulation and length in any of the three planes, making it impossible a comparison with the results found in this investigation. Additionally, previous studies haven't also reported the vector length for both inframandibular and masticatory muscles as well. The only comparison that could be made with previous studies was the vector angulation of masticatory muscles on the frontal plane in just one study (Table 5) and on the sagittal plane (Table 6).

One difference from this model to the previous ones was that this is three dimensional which increases the accuracy of the calculation of the muscle vector and the corresponding arm length. Both of these variables are indispensable for the determination of both direction and magnitude of temporomandibular joint reaction forces. Another

difference was that this model includes not only the masticatory muscles but also the inframandibular muscles. Since all these muscles take active participation in the act of chewing, the determination of their vectors also seems extremely important for the calculation of the temporomandibular reaction forces. Additionally, this model provides not only an accurate measurement of muscle vectors in length and angulation, but also the actual location the origin of the vectors in relation to the head as a whole (mesio-vestibular cusp of the lower first molar). Finally, the results found in this experiment are reproducible if the same data base and the same materials and method are used.

Error of Method

One of the possible errors in the method employed in this study is the fact that this u just utilized sections of the left side of the face. Asymmetries between the left and right side of the face could lead to major differences between the orientation of the muscle vectors from one side of the face to the other. Therefore, this could lead to major differences in the determination of the vector arm length and the total temporomandibular joint forces between the left and the right sides. However, the MRI study made by Koolstra *et al.* (1991) has shown that the averages between muscle vectors from the right to the left side were not dramatic. On the other hand, asymmetries between individuals might be sometimes large. According to the author, this difference might be due not only to real asymmetries between muscles, but also it could be caused by malpositioning of the subject in the MRI-apparatus.

Another source of error could be inaccuracies in tracings of the muscle contour. To facilitate identification of muscle contours, magnified copied (140%) were taken from the original horizontal illustrations; therefore, reducing the possibility of errors in tracing. In the model provided by Koolstra *et al.* (1991), one of the main problems faced was the poor reconstruction of muscle shape caused by tracing errors. This might be caused by the following factors: 1) MRI images don't have the necessary resolution making muscle

outlines not always clearly distinguishable, 2) minor movements of the subject's head during image acquisition, 2) the thickness of the imaged slice (5 mm for the frontal and 6.25 mm for the transversal sections), and/or 3) morphological ambiguities (e.g., the continuity of muscle fibers between masseter and temporalis muscle).

MUSCLE	Koolstra *et al.* (1990)	Grossi (1991)
Temporalis (anterior portion)	104.9	94
Temporalis (medial portion)	—	100
Temporalis (posterior portion)	109.5	94
Masseter (superficial portion)		108
Masseter (deep portion)	94.1	104
Medial pterygoid	63.5	73
Lateral pterygoid (superior head)	5	7
Lateral pterygoid (inferior head)	0	0
Digastric (anterior belly)	—	77
Digastric (posterior belly)	—	108
Stylohyoid	—	104
Mylohyoid	—	110
Geniohyoid	—	89.5

Table 5. Reported directions for vector angulations (degrees) for masticatory and inframandibular muscles in the frontal plane.

	Carlsoo (1952)	Schumacher (1961)	Baron and Debussy (1979)	Pruim et al. (1980)	Throckmorton (1985)	Koolstra et al. (1990)	Grossi (1991)
Temporalis (anterior portion)	120	90 - 170	90	99.5	112	80.4	94
Temporalis (medial portion)	–		–	–	–	–	124
Temporalis (posterior portion)	156		155	139.8	–	125.2	141
Masseter (superficial portion)	90	75	59	64.1	66	77.7	85
Masseter (deep portion)	–	–	–	–	–		92
Medial pterygoid	82	80	60 or 80	70.3	–	72.6	76
Lateral pterygoid (superior head)	–	20	7	0.0	–	19	6
Lateral pterygoid (inferior head)	–	340	350	–	–	2.3	0.0
Digastric (anterior belly)	–	–	–	–	–	–	34
Digastric (posterior belly)	–	–	–	–	–	–	124
Stylohyoid	–	–	–	–	–	–	113
Mylohyoid	–	–	–	–	–	–	86
Geniohyoid	–	–	–	–	–	–	44.5

Table 6. Reported directions for vector angulations (degrees) for masticatory and inframandibular muscles in the sagittal plane.

SUMMARY AND CONCLUSIONS

The purpose of this study was to determine both the length and angulation of muscle vectors (muscle force direction) in a three-dimensional ten-muscle model. The position of the vector origin in relation to a fixed point in skull (mesio-vestibular cusp of the lower first molar) was also determined.

The material used for this study was 50 horizontal head and neck sections of the left side of an adult male caucasian cadaver. They were digitized using with a 3-D computer software: PC3D (Jandel Scientific Co.) . Possible error of method might be in section alignment and tracing. According to a previously reported study, error in symmetry seemed to be negligible (Koolstra *et al.*, 1990).

The results found for both vector angle and length measurements had proven to be very precise (+- 1mm, +- 1 degree) and highly reliable (intraclass correlation coefficient of reliability = 1, at 95% significance level for one factor ANOVA). Comparison with previously reported muscle vector angulation could just be made for the masticatory muscles on the frontal plane (in one study) and on the sagittal plane. Since no previous data have been reported, comparison could not be made either for the vector angulation on the horizontal plane or the vector length on all three planes of the masticatory muscles .The present data couldn't also be compared with both the muscle vector angulation and length of the inframandibular muscles in either of the three planes.

It could be concluded that this model seems to have positive peculiarities in comparison with previously reported models. First, it was a three dimensional model and; therefore, much more accurate in determining the direction of the muscle force. Second, it was a ten-muscle model including the masticatory and inframandibular muscles of the left side of the face, being much more comprehensive than previous studies. Third, errors in symmetry, alignment and tracing could be considered minimal. Finally, it reported not only the vector length and angulation for all masticatory and inframandibular muscles in all three planes, but also its position in relation to the head as a whole (mesio-vestibular cusp of the lower first molar).

BIBLIOGRAPHY

Ahlgren JG, Ingervall BF and Thilander BL (1973): Muscle activity in normal and postnormal occlusion; Am J Orthod, 64: 445-456.

Atkinson HF, Shepherd RW (1967): Masticatory movements and the resulting force; Arch Oral Biol, 12:195-202.

Barbenel JC (1972): The biomechanics of the temporomandibular joint: a theorical study; J Biomechanics, 5: 251-256.

Barbenel JC (1974): The mechanics of the temporomandibular joint: a theoretical and electromyographic study. J Oral Rehabil, 1:19-27.

Baron P (1975): Contribution a l'etude des muscles masticateurs humains: etude des faisceaux musculaires et de leur projections sur lex trois plans orthogonaux de reference. L'Inform Dent ,18: 21-24.

Baron P and Debussy T (1979): A biomechanical functional analysis of the masticatory muscles in man; Archs Oral Biol, 24: 547-553.

Bigland B, Lippold OCJ (1954): The relation between force, velocity and integrated electrical activity in human muscles; J Physiol, 123:214-224.

Boyd RL, Gibbs CH, Mahan PE, Richmond AF and Laskin JL (1990): Temporomandibular joint forces measured at the condyle of Macaca arctoides; Am J Orthod Dentofacial Orthop, 97(6): 472-479.

Brehnan K, Boyd RL, Laskin J, Gibbs CH and Mahan P (1981): Direct measurements of loads at the temporomandibular joint in *Macaca arctoides*; J Dent Res, 60: 1820-1824.

Brudevold F (1951): a basic study of the chewing forces of a denture wearer; J Am Dent Assoc, 43:45-51.

Carlsoo S (1952): Nervous coordination and mechanical function of the mandibular elevators: an electromyographic study of the activity and anatomic analysis of the mechanics of muscles; Acta Odontologica Scan, 10 (Suppl 11): 1-129.

Carlsson GE (1974): Bite force and chewing efficiency, in Kawamura Y (ed). Frontiers of Oral Physiology, vol 1, Basel, Karger, pp 265-292.

De Boever JA, McCall WD, Holden S, et al (1978): Functional occlusal forces: An investigation by telemetry; J Prosthet Dent, 40:325-333.

Devlin H, Wastell DG (1985): Bite force and masseter muscle electromyographic activity during onset of an isometric clench in man; Archs Oral Biol, 30:213-215.

Ebert H (1938/39): Morphologische und funktionelle Analyse des Musculus masseter; Atschr. f. Anat. u. Entwckingsgesch, 109:790.

Floystrand F, Kleven E, Oilo G (1982): A novel miniature bite force recorder and its clinical application; Acta Odontol Scand, 40:209-214.

Freisfel H (1927): Uber die Kaumuskeln des menschl. Neugeborenen; Vierteljahrschr. fur Zahnheilkunde, 43:552.

Gaspard M, Laison F and Mailland M (1973a): Organisation architecturale et texture du muscle masseter chez les Primates et l'Homme; J Biol Buccale, 1:7-20.

Gaspard M, Laison F and Mailland M (1973b): Organisation architecturale et texture du muscle temporal et des fisceaux transition du complexe temporo-masseterin chez les Primates et l'Homme; J Biol Buccale, 1:171-196.

Gaspard M, Laison F and Mailland M (1973c) Organisation architecturale et texture des muscle pterygoidiens chez l'Homme; J Bio Buccale, 1: 353-366.

Gibbs CH, Mahan PE, Lundeen HC, et al (1981a): Occlusal forces during chewing and swallowing as measured by sound transmission; J Prosthet Dent, 46:443-449.

Gibbs CH, Mahan PE, Lundeen HC, et al (1981b): Occlusal forces during chewing - Influences of biting strength and food consistency; J Prosthet Dent, 46:561-567.

Gibbs CH, Mahan PE, Mauderli A, et al (1986): Limits of human bite strength; J Prosthet Dent, 56:226-229.

Gingerich PD (1971): Functional significance of mandibular translation in vertebrate jaw mechanics; Postilla, 152: 1-10.

Gysi A (1921): Studies on the leverage problem of the mandible; Dental Digest, 27: 74-84, 144-150, 203-208.

Hagberg C (1986a): The amplitude distribution of electromyographic activity of masticatory muscles during unilateral chewing; J Oral Rehabil, 13:567-574.

Hagberg C (1986b): Electromyography and bite force studies of muscular function and dysfunction in masticatory muscles. (thesis). Umea: University of Umea; Swed Dent J (suppl 37): 1-64.

Hagberg C, Agerberg G, Hagberg M (1986): Discomfort and bite force in painful masseter muscles after intramuscular injections of local anesthetics and saline solution; J Prosthet Dent, 56:354-358.

Hagberg C (1987): The amplitude distribution of electromyographic activity in painful masseter muscles during unilateral chewing; J Oral Rehabil.

Hannam AG (1976): The regulation of the jaw bite force in man; Arch Oral Biol, 21:641-664.

Haraldson T, Carlsson GE, Ingervall B (1979): Functional state, bite force and postural muscle activity in patients with osseointegrated oral implant bridges; Acta Odontol Scand, 37:195-206.

Haraldson T, Carlsson GE, Dahlstrom L, et al. (1985): Relationship between myoelectric activity on masticatory muscles and bite force; Scand J Dent Res, 93:539-545.

Helkimo E, Ingervall B(1978): Bite force and functional state of the masticatory system in young men; Swed Dent J, 2:167-175.

Hohl TH and Tucek WH (1982): Measurement of condylar loading forces by instrumented prosthesis in the baboon; J Max Fac Surg, 10: 1-7.

Hylander WL (1975): The human mandible, lever or link?; Am J Phys Anthrop, 43: 277-243.

Hylander WL (1978): Incisal bite force direction in humans and the functional significance of mammalian mandibular translation; Am J Phys Anthropol, 48: 1-8.

Hylander WL (1979): An experimental analysis of temporomandibular joint reaction force in macaques. Am J Phys Anthrop, 51: 433-456.

Hylander WL and Bays R (1979): An *in vivo* strain-gauge analysis of the squamosal-density joint reaction force during mastication and incisal biting in *Macaca mulatta* and *Macaca fascicularis;* Archs Oral Biol, 24: 689-697.

Ingervall B, Ridell A and Thilander B (1979): Changes in activity of the temporal and masseter and lip muscles after surgical correction of mandibular prognathism; Int J Oral Surg, 8: 290-300.

Kang QS, Updike DP and Salathe EP (1990): Theoretical prediction of muscle forces on the mandible during bite; J Biomech Eng, 112(4): 432-436.

Koolstra JH, Van Eijden TM, Weijs WA and Naeije M (1988): A three-dimensional mathematical model of the human masticatory system predicting maximum possible bite forces; J Biomech, 21(7):563-576.

Koolstra JH, Van Eijden TM, Van Spronsen PH, Weijs WA and Valk J (1990): Computer-assisted estimation of lines of action of human masticatory muscles reconstructed in vivo by means of magnetic resonance imaging of parallel sections; Archs Oral Biol, 35(7):549-556.

Korioth TW and Hannam AG (1990): Effect of bilateral asymmetric tooth clenching on load distribution at the mandibular condyles; J Prosthet Dent, 64(1):62-73.

Laurell L (1985): Occlusal forces and chewing ability in dentitions with cross-arch bridges (thesis); Swed Dent J (suppl 26).

Linderholm H, Wennstrom A (1970): Isometric bite force and its relation to general muscle force and body build; Acta Odontol Scand, 28:679-689.

Mainland D and Hiltz JE (1934): Forces exerted on the human mandible by the muscles of mastication; J Dent Res, 14: 107-124.

Manns A, Miralles R, Palazzi C (1979): EMG, bite force and elongation of the masseter muscle under isometric voluntary contraction and variations of vertical dimension; J Prosthet Dent, 42:674-682.

Moller E (1966): The chewing apparatus; Acta Physiol Scand, 69 (Suppl 280): 1-229.

Moller E, Sheikholeslam A, Lous I (1984): Response of elevator activity during mastication to treatment of functional disorders; Scand J Dent Res, 92:64-83.

Oyen OJ and Tsay TP (1991): A biomechanical analysis of craniofacial form and bite force; Am J Orthod Dentofacial Orthop, 99(4): 298-309.

Pruim GJ, Ten Bosch JT and De Jongh HJ (1978): Jaw muscle EMG activity and static loading of the mandible; J Biomechanics, 11: 389-395.

Pruim GJ, De Jongh HJ and Ten Bosch JT (1980): Forces acting on the mandible during bilateral static bites at different bite force levels; J Biomechanics, 13: 755-763.

Roberts D (1974): The etiology of the temporomandibular joint dysfunction syndrome; Am J Orthod, 66: 498-515.

Roberts D and Tattersall I (1974): Skull form and the mechanics of mandibular evolution in mammals; Am Mus Novit, 2536: 1-9.

Roth TE, Boldberg JS and Behrents RG (1984): Synovial fluid pressure determination in the temporomandibular joint; Oral Surg Oral Med Oral Pathol, 57: 583-588.

Schnabel G (1933): Uber das Verhaltnis des mittleren Querschnitts und der mittleren Langen der eizelnen kaumuskeln zu einander an sieben menschlichen Schadeln. Dissertation. Gebruder Memminger, Wurzburg.

Smith RJ (1978): Mandibular biomechanics and temporomandibular joint function in primates; Am J Phys Anthropol, 49: 341-350.

Throckmorton GS, Finn RA and Bell WH (1980): Biomechanics of differences in lower facial height; Am J Orthod, 77: 410-420.

Throckmorton GS (1985): Quantitative calculations of temporomandibular joint reaction forces - II. The importance of the direction of the jaw muscle forces; J Biomech, 18(6):453-461.

Throckmorton GS and Throckmorton LS (1985): Quantitative calculations of temporomandibular joint reaction forces - I. The importance of the magnitude of the jaw muscle forces; J Biomech, 18(6):445-452.

Throckmorton GS, Groshan GJ and Boyd SB (1990): Muscle activity patterns and control of temporomandibular joint loads; J Prosthet Dent, 64(1):62-73.

Van Eijden TM, Klok EM, Weijs WA and Koolstra JH (1988): Mechanical capabilities of the human jaw muscles studied with a mathematical model; Archs Oral Biol, 33: 819-826.

Van Ruijven LJ and Weijs WA (1990): A new model for calculating muscle forces from electromyograms; Eur J Appl Physiol, 61(5-6):479-485.

Weber EF (1851): Ueber die Langenverhaltnisse der Fleishfasern der Muskeln im Allgemeinen. Berichte uber die Verhandlungen der koniglich sachsischen Gesellschaft der Wissenschaften zu Leipzig. Mathematisch-Physische Classe II: 63.

Wennstrom A (1971a): Psychophysical investigation of bite force. Part I. Bite force in healthy adult women; Swed Dent J, 64:807-819.

Wennstrom A (1971b): Psychophysical investigation of bite force. Part II. Studies in individuals with full dentures; Swed Dent J, 64:821-827.

Wennstrom A (1972a): Psychophysical investigation of bite force. Part III. Perceived and physically recorded bite force; Swed Dent J, 65:177-184.

Wennstrom A (1972b): Psychophysical investigation of bite force. Part IV. A clinical assessment of bite force in patients with full dentures; Swed Dent J, 65:185-190.

Wennstrom A, Marklun G, Eriksson PO (1972): A clinical investigation of bite force and chewing habits in patients with total maxillary denture and partial mandibular denture; Swed Dent J, 65:279-284.

Williams WN, Levin BDS, LaPointe LL, et al (1985): Bite force discrimination by individuals with complete dentures; J Prothet Dent, 54:146-150.

Yurkstas A, Curby WA (1953): Force analysis of prosthetic appliance during function; J Prosthet Dent, 3:82-87.

APPENDIX A

	TIME 1	TIME 2	TIME 3	TIME 4	TIME 5
Temporalis (anterior portion)	24	24	23	23.5	24
Temporalis (medial portion)	51	50	50.5	51.5	51
Temporalis (posterior portion)	83	82.5	83.5	83	83
Masseter (superficial portion)	56.5	57	56	56.5	56
Masseter (deep portion)	40	40.5	40	41	40
Medial pterygoid	95	94.5	95	95.5	94.5
Lateral pterygoid (superior head)	126	125.5	126	126	125
Lateral pterygoid (inferior head)	132	132.5	133	132	132
Digastric (anterior belly)	93	92.5	92	93	93.5
Digastric (posterior belly)	113	112	112.5	113	112
Stylohyoid	120	119.5	120	121	120.5
Mylohyoid	84	83.5	83	84	84
Geniohyoid	102	101	102	101	101

Reliability Estimates for- All measurements: 1   Single measurement: 1   (Intraclass correlation coefficient of reliability),
Multi-comparison significance level for one factor ANOVA: 95%.

Table 1A. Intraobserver measurement reliability: Vector length (mm) in the horizontal plane.

	TIME 1	TIME 2	TIME 3	TIME 4	TIME 5
Temporalis (anterior portion)	185.5	185.5	186	185.5	186
Temporalis (medial portion)	128	128	128	128.5	128
Temporalis (posterior portion)	116.5	116	116	116.5	116
Masseter (superficial portion)	240	240	240.5	240	240
Masseter (deep portion)	243	243.5	243	243.5	243
Medial pterygoid	316	316	316	316	316
Lateral pterygoid (superior head)	308	308.5	308.5	308	308.5
Lateral pterygoid (inferior head)	298.5	299	298	298.5	299
Digastric (anterior belly)	283	283.5	283	283	283
Digastric (posterior belly)	117	117.5	117.5	118	117
Stylohyoid	122.5	123	123	122	123
Mylohyoid	187.5	187	188	188	188
Geniohyoid	271	271	271	271	271

* Reliability Estimates for- All measurements: 1   Single measurement: 1   (Intraclass correlation coefficient of reliability), Multi-comparison significance level for one factor ANOVA: 95%.

Table 2A. Intraobserver measurement reliability: Vector angle (degrees) in the horizontal plane.

	OBSERVER 1	OBSERVER 2	OBSERVER 3	OBSERVER 4	OBSERVER 5
Temporalis (anterior portion)	24	24.5	23	23	24
Temporalis (medial portion)	51	50	50.5	51	51
Temporalis (posterior portion)	83	82.5	83.5	83	82
Masseter (superficial portion)	56.5	56	57	56	56.5
Masseter (deep portion)	40	41	40	40.5	40
Medial pterygoid	95	95.5	96	95	95
Lateral pterygoid (superior head)	126	125	125.5	126	125
Lateral pterygoid (inferior head)	132	131	131.5	132.5	132
Digastric (anterior belly)	93	93	92	92.5	92
Digastric (posterior belly)	113	112	113	113	112.5
Stylohyoid	120	119	120.5	121	120
Mylohyoid	84	84	83	83.5	84
Geniohyoid	102	101.5	102	102	101

Reliability Estimates for- All measurements: 1   Single measurement: 1   (Intraclass correlation coefficient of reliability), Multi-comparison significance level for one factor ANOVA: 95%.

Table 3A. Interobserver measurement reliability: Vector length (mm) in the horizontal plane.

	OBSERVER 1	OBSERVER 2	OBSERVER 3	OBSERVER 4	OBSERVER 5
Temporalis (anterior portion)	185.5	186	185	186	185.5
Temporalis (medial portion)	128	129	128.5	129	128
Temporalis (posterior portion)	116.5	116	117	116.5	116
Masseter (superficial portion)	240	241	239.5	240.5	240
Masseter (deep portion)	243	242	242.5	243	242.5
Medial pterygoid	316	315	316	315.5	316
Lateral pterygoid (superior head)	308	307.5	308	307	307.5
Lateral pterygoid (inferior head)	298.5	298	298.5	299	298
Digastric (anterior belly)	283	282	282	283	282.5
Digastric (posterior belly)	117	116	116.5	117	116
Stylohyoid	122.5	123	122	122	123
Mylohyoid	187.5	187	188	187	187.5
Geniohyoid	271	272	271	272	271.5

** Reliability Estimates for- All measurements: 1   Single measurement: 1   (Intraclass correlation   coefficient of reliability),
Multi-comparison significance level for one factor ANOVA: 95%.*

Table 4A. Interobserver measurement reliability: Vector angle (degrees) in the horizontal plane

	ORIGINAL LENGTH	FIRST CONVERSION	SECOND CONVERSION	THIRD CONVERSION	FOURTH CONVERSION
Temporalis (anterior portion)	24	23.99	23.97	23.96	23.94
Temporalis (medial portion)	51	50.99	50.98	50.96	50.95
Temporalis (posterior portion)	83	82.98	82.97	82.95	82.94
Masseter (superficial portion)	56.5	56.47	56.45	56.42	56.4
Masseter (deep portion)	40	39.98	39.95	39.93	39.9
Medial pterygoid	96	95.97	95.94	95.91	95.87
Lateral pterygoid (superior head)	126	125.98	125.94	125.89	125.85
Lateral pterygoid (inferior head)	132	131.99	131.96	131.93	131.9
Digastric (anterior belly)	93	93	93	93	93
Digastric (posterior belly)	113	112.98	112.96	112.94	112.91
Stylohyoid	120	119.96	119.9	119.85	119.8
Mylohyoid	84	83.99	83.94	83.89	83.84
Geniohyoid	102	101.99	101.96	101.93	101.9

* Reliability Estimates for- All conversions: 1   Single conversion: 1   (Intraclass correlation coefficient of reliability), Multi-comparison significance level for one factor ANOVA: 95%.

Table 5A. Conversion factor reliability: Vector length (mm) in the horizontal plane.

APPENDIX B

Plane and Direction	HP(M->L) m. width	HP(A->P) m. length	FP(M->L) m. width	SP(A->P) m. length
Magnification	1.1441	1.1441	1	1
First section of the temporalis muscle	24.50	135.00	21.413	117.99
Centroid of the anterior temporalis	14.50	33.00	12.673	28.842
Centroid of the medial temporalis	21.50	74.50	18.791	65.113
Centroid of the posterior temporalis	14.50	114.00	12.673	99.636
Last section of the temporalis muscle	4.00	6.00	3.496	5.244
Centroid of the last section	1.00	2.00	0.874	1.748

Table 1B. Muscle lengths and widths (mm) and the correct position of the centroids (mm) of the temporalis muscle in the original and converted magnifications. HP(M->L): horizontal plane, from medial to lateral; HP(A->P): horizontal plane, from anterior to posterior; FP(M->P): frontal plane from medial to lateral; and SP(A->P): sagittal plane from anterior to posterior.

Plane and Direction	HP(M->L) m. width	HP(A->P) m. length	FP(M->L) m. width	SP(A->P) m. length
Magnification	2.4880	2.4880	1.5	1.5
First section of the masseter muscle	49.00	102.00	29.54	61.50
Centroid of the superficial portion	32.00	55.00	19.29	33.16
Centroid of the deep portion	22.00	41.00	13.26	24.72
Last section of the masseter muscle	25.00	78.50	15.07	47.33
Centroid of the last section	11.50	39.00	6.93	23.51

Table 2B. Muscle lengths and widths (mm) and the correct position of the centroids (mm) of the masseter muscle in the original and converted magnifications. HP(M->L): horizontal plane, from medial to lateral; HP(A->P): horizontal plane, from anterior to posterior; FP(M->P): frontal plane from medial to lateral; and SP(A->P): sagittal plane from anterior to posterior.

Plane and Direction	HP(M->L) m. width	HP(A->P) m. length	FP(M->L) m. width	SP(A->P) m. length
Magnification	3.3724	3.3724	2.2	2.2
First section of the medial pterygoid	49.50	74.80	32.29	48.79
Centroid of the fist section	*19.50*	*31.20*	*12.72*	*20.35*
Last section of the medial pterygoid	28.00	90.00	18.26	58.71
Centroid of the last section	*12.00*	*50.50*	*7.83*	*32.94*

Table 3B. Muscle lengths and widths (mm) and the correct position of the centroids (mm) of the medial pterygoid muscle in the original and converted magnifications. HP(M->L): horizontal plane, from medial to lateral; HP(A->P): horizontal plane, from anterior to posterior; FP(M->P): frontal plane from medial to lateral; and SP(A->P): sagittal plane from anterior to posterior.

Plane and Direction	HP(M->L) m. width	HP(A->P) m. length	FP(M->L) m. width	SP(A->P) m. length
Magnification	4.4020	4.4020	6.0	6.3
Lateral pterygoid superior head (portion 1)	52.90	29.90	72.10	42.79
Centroid of the first portion	*24.50*	*15.80*	*33.39*	*22.61*
Lateral pterygoid superior head (portion 2)	39.30	23.50	53.57	33.63
Centroid of the second portion	*19.80*	*12.00*	*26.99*	*17.17*
Lateral pterygoid superior head (portion 3)	58.10	30.50	79.19	43.65
Centroid of the third portion	*29.20*	*17.00*	*39.80*	*24.33*
Lateral pterygoid superior head (portion 4)	28.90	43.70	39.39	62.54
Centroid of the fourth portion	*13.30*	*23.50*	*18.13*	*33.63*

Table 4B. Muscle lengths and widths (mm) and the correct position of the centroids (mm) of the lateral pterygoid muscle - superior head in the original and converted magnifications. HP(M->L): horizontal plane, from medial to lateral; HP(A->P): horizontal plane, from anterior to posterior; FP(M->P): frontal plane from medial to lateral; and SP(A->P): sagittal plane from anterior to posterior.

Plane and Direction	HP(M->L) m. width	HP(A->P) m. length	FP(M->L) m. width	SP(A->P) m. length
Magnification	2.9951	2.9951	4.7	4.3
lateral pterygoid Inferior head (first section)	103.20	105.50	161.94	151.47
Centroid of the first section	*54.90*	*54.40*	*86.15*	*78.10*
lateral pterygoid Inferior head (last section)	93.20	134.50	146.25	193.10
Centroid of the last section	*44.20*	*68.00*	*69.36*	*97.63*

Table 5B. Muscle lengths and widths (mm) and the correct position of the centroids (mm) of the lateral pterygoid muscle - inferior head in the original and converted magnifications. HP(M->L): horizontal plane, from medial to lateral; HP(A->P): horizontal plane, from anterior to posterior; FP(M->P): frontal plane from medial to lateral; and SP(A->P): sagittal plane from anterior to posterior.

Plane and Direction	HP(M->L) m. width	HP(A->P) m. length	FP(M->L) m. width	SP(A->P) m. length
Magnification	0.8835	0.8835	6.86	3.2
Digastric anterior belly (first section)	17.00	19.30	132.00	69.90
Centroid of the first section	*7.60*	*11.50*	*59.01*	*41.65*
Digastric anterior belly (last section)	28.50	57.90	221.29	209.71
Centroid of the last section	*13.00*	*24.00*	*100.94*	*86.93*

Table 6B. Muscle lengths and widths (mm) and the correct position of the centroids (mm) of the digastric - anterior belly in the original and converted magnifications. HP(M->L): horizontal plane, from medial to lateral; HP(A->P): horizontal plane, from anterior to posterior; FP(M->P): frontal plane from medial to lateral; and SP(A->P): sagittal plane from anterior to posterior.

Plane and Direction	HP(M->L) m. width	HP(A->P) m. length	FP(M->L) m. width	SP(A->P) m. length
Magnification	2.1492	2.1492	1.9	1.9
Digastric posterior belly (first section)	14.70	44.00	12.99	38.90
Centroid of the first section	*5.90*	*27.00*	*5.22*	*23.87*
Digastric posterior belly (last section)	11.60	30.00	10.25	26.52
Centroid of the last section	*6.50*	*18.40*	*5.75*	*16.27*

Table 7B. Muscle lengths and widths (mm) and the correct position of the centroids (mm) of the digastric - posterior belly in the original and converted magnifications. HP(M->L): horizontal plane, from medial to lateral; HP(A->P): horizontal plane, from anterior to posterior; FP(M->P): frontal plane from medial to lateral; and SP(A->P): sagittal plane from anterior to posterior.

Plane and Direction	HP(M->L) m. width	HP(A->P) m. length	FP(M->L) m. width	SP(A->P) m. length
Magnitude	5.2499	5.2499	2.1	2.1
Stylohyoid (first section)	16.30	15.00	6.52	6.00
Centroid of the first section	*6.20*	*8.60*	*2.48*	*3.44*
Stylohyoid (last section)	17.50	58.00	7.00	23.20
Centroid of the last section	*9.20*	*29.00*	*3.68*	*11.60*

Table 8B. Muscle lengths and widths (mm) and the correct position of the centroids (mm) of the stylohyoid in the original and converted magnifications. HP(M->L): horizontal plane, from medial to lateral; HP(A->P): horizontal plane, from anterior to posterior; FP(M->P): frontal plane from medial to lateral; and SP(A->P): sagittal plane from anterior to posterior.

Plane and Direction	HP(M->L) m. width	HP(A->P) m. length	FP(M->L) m. width	SP(A->P) m. length
Magnification	4.8440	4.8440	2.8	2.4
Mylohyoid (first section)	70.50	123.10	40.75	60.98
Centroid of the first section	*34.10*	*83.50*	*19.71*	*41.37*
Mylohyoid (last section)	67.50	82.10	39.02	40.67
Centroid of the last section	*27.00*	*43.70*	*15.61*	*21.65*

Table 9B. Muscle lengths and widths (mm) and the correct position of the centroids (mm) of the mylohyoid in the original and converted magnifications. HP(M->L): horizontal plane, from medial to lateral; HP(A->P): horizontal plane, from anterior to posterior; FP(M->P): frontal plane from medial to lateral; and SP(A->P): sagittal plane from anterior to posterior.

Plane and Direction	HP(M->L) m. width	HP(A->P) m. length	FP(M->L) m. width	SP(A->P) m. length
Magnification	2.9998	2.9998	4	2.4
Geniohyoid (first section)	14.00	47.50	18.67	38.00
Centroid of the first section	*4.90*	*27.80*	*6.53*	*22.24*
Geniohyoid (last section)	16.50	18.80	22.00	15.04
Centroid of the last section	*6.90*	*12.10*	*9.20*	*9.68*

Table 10B. Muscle lengths and widths (mm) and the correct position of the centroids (mm) of the geniohyoid in the original and converted magnifications. HP(M->L): horizontal plane, from medial to lateral; HP(A->P): horizontal plane, from anterior to posterior; FP(M->P): frontal plane from medial to lateral; and SP(A->P): sagittal plane from anterior to posterior.

MUSCLE	CONVERSION	FACTOR	APPLICATION
TEMPORALIS	1.441 -> 1	0.6939	*CENTROID FP,SP* *VECTOR LENGTH HP*
MASSETER	2.488->1.5 2.4880->1 1.5->1	0.6029 0.4019 0.6666	*CENTROID FP, SP* *VECTOR LENGTH HP* *VECTOR LENGTH FP,SP*
MEDIAL PTER	3.3724->2.2 3.3724->1 2.2->1	0.6523 0.2965 0.4545	*CENTROID FP, SP* *VECTOR LENGTH HP* *VECTOR LENGTH FP,SP*
LAT PT SUP HEAD	4.4020->6 4.4020->6.3 4.4020->1 6->1 6.3->1	1.3630 1.4312 0.2272 1.6666 0.1587	*CENTROID FP* *CENTROID SP* *VECTOR LENGTH HP* *VECTOR LENGTH FP* *VECTOR LENGTH SP*
LAT PT INF HEAD	2.9951->4.7 2.9951->4.3 2.9951->1 4.7->1 4.3->1	1.5692 1.4357 0.3339 0.2128 0.2325	*CENTROID FP* *CENTROID SP* *VECTOR LENGTH HP* *VECTOR LENGTH FP* *VECTOR LENGTH SP*
DIG ANT BELLY	0.8835->6.86 0.8835->3.2 0.8835->1 6.86->1 3.2->1	7.7646 3.6219 1.1319 0.1458 0.3125	*CENTROID FP* *CENTROID SP* *VECTOR LENGTH HP* *VECTOR LENGTH FP* *VECTOR LENGTH SP*
DIG POST BELLY	2.1492->1.9 2.1492->1 1.9->1	0.8840 0.4653 0.5263	*CENTROID FP,SP* *VECTOR LENGTH HP* *VECTOR LENGTH FP,SP*
STYLOHYOID	5.2499->2.1 5.2499->1 2.1->1	0.4 0.1905 0.4762	*CENTROID FP,SP* *VECTOR LENGTH HP* *VECTOR LENGTH FP,SP*
MYLOHYOID	4.844->2.8 4.8440->2.4 4.844->1 2.8->1 2.4->1	0.578 0.4954 0.2064 0.3571 0.4167	*CENTROID FP* *CENTROID SP* *VECTOR LENGTH HP* *VECTOR LENGTH FP* *VECTOR LENGTH SP*
GENIOHYOID	2.9998->4 2.9998->2.4 2.998->1 4->1 2.4->1	1.3334 0.8 0.3333 0.25 0.4167	*CENTROID FP* *CENTROID SP* *VECTOR LENGTH HP* *VECTOR LENGTH FP* *VECTOR LENGTH SP*

Table 11B. List of all conversion factors used for all muscles and their application